2001

Development of a knowledge-based system for the control of 319-aluminum melt quality and prediction of casting characteristics.

Graciela. Pelayo Chagoya
University of Windsor

INFORMATION TO USERS

This manuscript has been reproduced from the microfilm master. UMI films the text directly from the original or copy submitted. Thus, some thesis and dissertation copies are in typewriter face, while others may be from any type of computer printer.

The quality of this reproduction is dependent upon the quality of the copy submitted. Broken or indistinct print, colored or poor quality illustrations and photographs, print bleedthrough, substandard margins, and improper alignment can adversely affect reproduction.

In the unlikely event that the author did not send UMI a complete manuscript and there are missing pages, these will be noted. Also, if unauthorized copyright material had to be removed, a note will indicate the deletion.

Oversize materials (e.g., maps, drawings, charts) are reproduced by sectioning the original, beginning at the upper left-hand corner and continuing from left to right in equal sections with small overlaps.

Photographs included in the original manuscript have been reproduced xerographically in this copy. Higher quality 6" x 9" black and white photographic prints are available for any photographs or illustrations appearing in this copy for an additional charge. Contact UMI directly to order.

ProQuest Information and Learning
300 North Zeeb Road, Ann Arbor, MI 48106-1346 USA
800-521-0600

DEVELOPMENT OF A KNOWLEDGE BASED SYSTEM FOR THE CONTROL OF 319-Al MELT QUALITY AND PREDICTION OF CASTING CHARACTERISTICS

by

GRACIELA PELAYO CHAGOYA

A Thesis Submitted to the
Faculty of Graduate Studies and Research
Through the Department of
Industrial Engineering in Partial Fulfillment
of the Requirements for the Degree of Master
of Applied Science at
the University of Windsor

Windsor, Ontario, Canada
2001

928753

ABSTRACT

Knowledge Based Systems are computer programs used in situations where the use of heuristic knowledge and reasoning offers the only possibility of a solution mainly because the problem being studied is too complex to be represented in an algorithmic form. In general terms, such systems address and solve knowledge-intensive problems that can have many acceptable answers. The interpretation of Thermal Analysis results is a suitable task for artificial intelligence technology since it is a knowledge intensive activity in which several factors interact and modify the characteristics of the cooling curves.

In the present work, an Aluminum Thermal Analysis System (AlTAS) developed at the University of Windsor was implemented at a casting plant and after verification of its performance in an industrial scenario a Case-Based Reasoning System coupled with a Statistical Process Control module were developed to upgrade the capabilities of the AlTAS. The system will be used to control, on-line and prior to casting, the quality of the W319-Al melt used to produce aluminum engine blocks under the Cosworth casting process, and predict their tensile properties and microstructure.

DEDICATION

To my Parents, Grandparents and my Aunt Marcela.

ACKNOWLEDGEMENTS

I would like to thank my supervisor Dr. Jerry Sokolowski for accepting me as a graduate student and supporting me through the grants and contributions provided to the Industrial Research Chair (IRC) by the Natural Sciences and Engineering Research Council of Canada (NSERC), Ford Motor Company and the University of Windsor. Thanks to the Foundry Educational Foundation for the support and professional opportunities with which I was provided.

I would like to thank my supervisor Dr. Reza Lashkari for his invaluable guidance during my studies. Thanks are extended to Dr. S Dutta for his continuous advice and to Dr. M. Ahmadi for serving as an external examiner to the dissertation committee.

I wish to express my appreciation to Ellen Moosberger for her invaluable support during my studies. Thanks are also extended to all the IRC members for their support and the excellent working environment that we created.

I would like to thank Rose Torielli, Buzz Brosnan, W. Evans, B. Barth, John Burford, Azita Ariapour, Fulton Gillis, Bill Booker, Nelson Vorges and all the people at Ford's Windsor Aluminum Plant who made possible the completion of this work. Thanks to Warren Mackinnon and Ron Hasenbusch from the Casting Process Development and the Technical Support Centre at the University of Windsor.

Thanks to Emma Mares for her invaluable help in the development of the user interfaces and software integration needed in this project and to Chris Price from the University of Aberystwyth for his help and for allowing me to use the shell Caspian.

Thanks to my family and friends whose love, support and guidance allowed me to reach this goal.

NOMENCLATURE

AITAS – Aluminum Thermal Analysis System

CBR – Case-Based Reasoning

IRC – NSERC/ Ford/ University of Windsor Industrial Research Chair in Light Metals Casting Technology.

KBS – Knowledge-Based System

R&R – Gauge Repeatability and Reproducibility Study

SPC – Statistical Process Control

WAP –Windsor Aluminum Plant

TABLE OF CONTENTS

LIST OF FIGURES

LIST OF TABLES

LIST OF EQUATIONS

CHAPTER 1

INTRODUCTION

The motivation of artificial intelligence technologies is to understand the human reasoning process and then use these concepts to build systems that help solve technical problems. These technologies have been successfully integrated into several industrial applications including metal casting operations. Techniques such as expert systems, fuzzy logic, neural networks or genetic algorithms offer solutions that have been applied to areas like material and process selection, defect classification, process monitoring and control, or production planning and scheduling.

In this project Case-Based Reasoning, which is one of the emerging paradigms for designing intelligent systems, was used to build a knowledge-based system for interpretation of thermal analysis results.

Thermal Analysis is a technique based on the analysis of a temperature-time plot (cooling curve) that is obtained during the solidification of a sample of metal or alloy. Extensive research has been carried out to relate the characteristics of the cooling curve to the microstructural features and mechanical properties of the alloy after solidification. For many years thermal analysis has been used in the cast iron industry to evaluate the quality of the molten metal prior to casting and more recently, due to the increasing use of aluminum castings, this technique was incorporated to the quality control of aluminum alloys.

The case-based reasoning system developed in this project will use the cooling curves of W319-Al alloy generated by a novel thermal analysis system developed at the University of Windsor to evaluate several characteristics of the semisolid melt prior to casting in order to predict the microstructure and mechanical properties of the critical sections of aluminum engine blocks.

This Knowledge-Based Thermal Analysis System aims to provide the aluminum casting industry with a tool that helps to control liquid metal processing, which is one of the critical steps towards the production of good quality castings.

1.1 Knowledge-Based Systems

Knowledge Based Systems are nonprocedural computer systems aimed to solve complex problems for which no algorithmic solution exists and reasoning offers the only possibility of solution. By their nature, expert systems address and solve knowledge-intensive problems (those that involve large information sets) that can have multiple correct or acceptable answers.

Such systems differ considerably from conventional programs. Knowledge based systems present an explicit separation between the control mechanism (inference engine) and the data structures. This makes them easier to modify and expand than procedural programs; solutions are achieved by making use of algorithms when they are available, but also make use of heuristics where knowledge can not be made precise and certain. They are based on intense search routines and are often designed to deal with uncertainty since their inputs may be incorrect or incomplete[1].
Rule-Based Systems are the most popular types of knowledge-based systems. More specifically, they are called Expert Systems if they are intended to emulate the thinking process followed by a human expert for the solution of problems using activities such as reasoning and inference. They are formed by a knowledge base, a user interface and an inference engine. Expert systems make use of automated reasoning, that is, using the existing axioms in their knowledge base (represented as a set of IF-THEN rules and facts), they can logically derive new truths.

An alternative paradigm for developing intelligent systems is Case Based Reasoning. This technique, which is characterized by the explicit use of past experience, offers the capability to recognize different contexts in which certain knowledge can be applicable and determine which information is transferable from a given scenario to another. It has been compared to rule-based reasoning[2], showing considerable improvements in development effort, validation and maintainability, while keeping the accuracy of the results. Case Based Reasoning is also considered as a better method to link data and knowledge in intelligent systems[3] since data is included within the case base, while knowledge about the problem domain is included in adaptation rules and the case itself. These advantages will be further explained in the following sections.

1.2 Case-Based Reasoning (CBR)

Case-Based Reasoning emulates the way human reasoning works by looking into past experience and applying previous solutions towards the solution of current problems. The cycle followed by CBR systems consists of four stages. First, this problem-solving technique works by *searching* into a database of previously solved problems, or case base, for one or more cases whose main features closely resemble the current problem. Once a case is selected, its solution is *retrieved* and applied to the current problem. If the historical case is not sufficiently similar to the current problem, the CBR system modifies the old solution to fit the current case. This *adaptation* is a function of the difference between the cases. When the solution for the new case is considered successful it can be *appended* to the case base to increase its robustness.

1.3 Aluminum-Silicon Alloys

As a result of the constraints set by government regulations on the Corporate Average Fuel Economy (CAFE) that is to be achieved by commercial vehicles, aluminum alloys have achieved large penetration in the automotive market. Due to the advantage offered by aluminum in terms of their strength to weight ratio, the transportation sector already accounts for more than one quarter of the total consumption of this metal and is expected to increase in the future[4]. To date, the major applications of aluminum in the automotive market have been in the form of castings, such as engine blocks, cylinder heads, brake and suspension components. In the production of engine blocks and cylinder heads, the alloy families 319 (Al-Si-Cu) and 356 (Al-Si-Mg) are the most commonly used.

The present work will focus on the treatment and control of W319 Al alloy, which is a grade of 319-Al alloy (7.5%Si hypoeutectic alloy).

1.3.1 Treatment of the 319 Aluminum Silicon Alloy

In order to ensure that the cast components for automotive applications achieve the required mechanical properties (fatigue and tensile properties) the melt composition, melt cleanliness and hydrogen content must be carefully controlled. Similarly, the control over the characteristics of

the as-cast microstructures (prior to heat treatment) is a critical factor. For this purpose, the addition of grain refiners and modifiers to the 319-Al melt in the form of master alloys is a common practice. Grain refiners improve mass feeding conditions during solidification resulting in smaller and improved distribution of porosity and secondary phase constituents[5]. This increase in casting integrity results in improved mechanical properties. Modifiers are added to alter the morphology of silicon particles, changing them from needle-like to globular with a consequent improvement of ductility and machinability.

These factors coupled with the cooling rate of the cast sections and the presence of impurity elements determine the feeding conditions that will prevail during the solidification process of the alloy and will determine the microstructure and properties of the casting.

1.3.2 Thermal Analysis

Thermal analysis, in general terms, is the study of the heat released or lost during the solidification process of a metal or alloy. During the solidification of a small sample of metal, a thermocouple placed within the sample measures temperature variations. Using a data acquisition system and adequate plotting software a cooling curve is obtained. Each metal and alloy has a characteristic cooling curve in which the metallurgical reactions are manifested by features such as inflection points and slope changes. This curve, along with its time derivatives can yield useful information about the characteristics of the solidification process, which can be related to the composition of the melt and to the casting structure. It is a common foundry practice to use this method to quantify the degree of grain refinement and the level of silicon modification.

The thermal analysis system developed at the University of Windsor (Aluminum Thermal Analysis System –AlTAS[6]) goes beyond these traditional applications and calculates parameters that quantify the feeding conditions giving information about the risk of development of shrinkage porosity.

These applications make this technique essential for the proactive, on-line control of metal quality in the foundry today.

1.3.3 Overview of the Present Work

This work is divided into ten chapters. Chapter 2 provides a general introduction to Case-Based Reasoning Systems. Chapter 3 includes a literature review of the metallurgical background pertaining to this work. It gives an introduction to 319-Al alloy, its solidification process and treatment. It also discusses the thermal analysis parameters used to evaluate melt quality prior to casting.

Chapter 4 consists of a literature review of Knowledge-Based Systems that have been developed for the interpretation of thermal analysis results.

Chapter 5 contains a description of the AlTAS system and the process in which it was incorporated as a quality control tool. Since the system had only been used in a research environment it was necessary to carry out a Gauge Repeatability and Reproducibility Study. The results of this study are presented.

Once the effects of different operators on the measurements of the AlTAS system were understood, thermal analysis and casting data were collected in order to populate the case base of the Case-Based Reasoning System. The experimental procedure followed to obtain and analyze these samples is presented in Chapter 6.

Chapter 7 describes the Statistical Process Control module that was developed in order to complement the capabilities of the AlTAS as a process control tool.

Chapter 8 describes the development of the CBR system. The validation procedure is described in Chapter 9.

Finally, Chapter 10 outlines the conclusions of this work and suggests future directions for the continuation of this project.

CHAPTER 2

CASE BASED REASONING SYSTEMS

2.1 Introduction

The principle behind Case Based Reasoning (CBR) is solving new problems by adapting solutions that worked for similar problems in the past.

In a general and simplified manner, the CBR process can be defined as a cycle composed of four main activities (Figure 1):

a) Matching a new case with a case stored in the case-base

b) Retrieving the solution for the historical case

c) Adapting the solution according to the differences between the new and old cases

d) Retention of the new case and its solution.

In this chapter, a detailed explanation of the activities involved in each step will be provided.

2.2 Organization of Case-Based Reasoning Systems

Similar to other types of knowledge based systems, CBR systems are formed by a knowledge base, an inference engine and a user interface. The knowledge base is formed by indexed cases and rules that are employed during retrieval and solution transformation. The inference engine is responsible for matching cases, applying adaptation rules and adding cases to the case base.

2.3 The Structure of Cases

A crucial component of CBR systems is the built-in set of cases within their case-base. Each of these cases represents a contextualized and relevant piece of knowledge, which links solutions with problems that will help in the future to give answers and warn about the possibility of unforeseen problems.

The usefulness of a CBR system is largely determined by the robustness of its case base; therefore, the cases must be selected carefully to cover the problem domain avoiding unnecessary

or misleading cases. The case set should cover as many different scenarios of the knowledge domain as possible providing good indexing. For completeness not only positive outcomes should be included, but also failures.

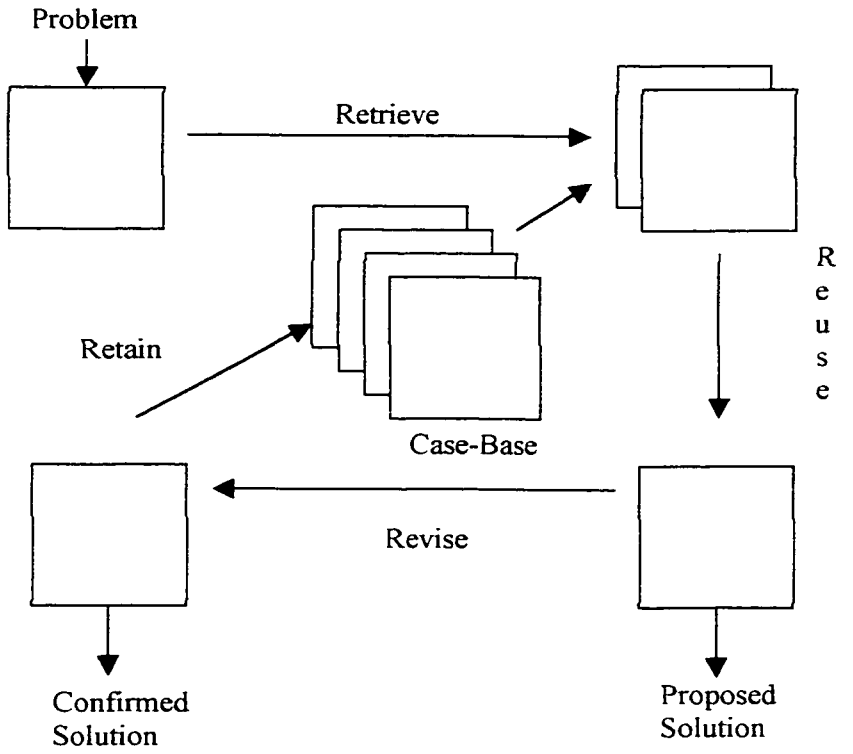

Figure 1 – The Case-Based Reasoning Cycle[3]

Cases are formed by the following three parts[2] (or at least the first two):

a) Description of the problem or situation: set of relevant parameters that define the situation that needs to be matched as well as the parameters that will be used as indexes. An index is a parameter that serves as indicator of the context in which a case is applicable and allows a more efficient search of the case-base.
b) Solution: parameters that describe the derived solution to the problem or situation.
c) Outcome: resulting state when the solution was carried out.

Both cases and solutions must be represented in data structures such as attribute – value vectors or frames.

2.4 Case Matching and Retrieval

CBR is considered as a pattern recognition method that is flexible to large pattern deviations. This inexact matching is possible due to the concept of similarity. In commercial systems similarity is usually formalized by the nearest neighbour concept. In nearest-neighbour matching the similarity between the new case and a source case is calculated for each attribute, usually as a distance function (*sim* in Equation 1). Qualitative comparisons are carried out when qualitative attributes are available and quantitative evaluations take place when numerical attributes are compared. This measure may be multiplied by a weighting factor and the products are added up to obtain an aggregate measure of the similarity of all attributes. Several functions for calculating similarity have been developed up to this date and have been summarized by Liao and Zhang[7]. The aggregate similarity is usually normalized to be within a range of 0 and 1 or as a percentage with 100% being an exact match[2, 8].

Equation 1 –General Nearest Neighbour Numerical Evaluation Function of Similarity[2]

$$AggregateSimilarity = \frac{\sum_{i=1}^{n} w_i \times sim\left(f_i^I, f_i^R\right)}{\sum_{i=1}^{n} w_i}$$

Where

w_i is the weight assigned to each attribute i, i = 1,2,.., n

sim is the similarity function

f_i^I and f_i^R are the values for attribute f_i in the input and retrieved cases respectively.

Normally two approaches are used for the purpose of case retrieval: one is the distance-based approach (nearest neighbour) and the second one is the indexing approach. In the latter approach, cases are connected by indexing structures which are explored to determine the similar case. A combination of these two approaches is also commonly used: the indices are used to separate a

subset of suitable cases for which a similarity measure is then calculated, and the case with the highest measure is retrieved.

2.5 Adaptation

When the most similar case in the case library has been retrieved, it is still possible for it to be significantly different from the current problem. In this situation it may be required to modify the solution to fit the current problem.

Adaptation requires additional background knowledge which can be represented in the form of rules as in rule-based systems. In the conclusion of the rules new attribute values for the solution case can be specified. Several other techniques such as null adaptation, parameterized solutions, abstraction and specialization[9] or even case-based adaptation[2] have been developed.

2.6 Learning

Once a historical case has been successfully retrieved and adapted, it can be integrated into the case library. If the added cases are carefully revised, this has the effect of continuously improving the CBR system.

CHAPTER 3

PROPERTIES AND THERMAL ANALYSIS OF THE 319-Al ALLOY

3.1 Introduction

Thermal Analysis is a non-destructive technique that is widely employed in foundries to assess the solidification of a small sample of metal. A temperature-time plot is recorded from the liquid state until the alloy has reached the solid state, and this information gives an insight into the characteristics of the microstructure that will develop during the solidification of the cast parts. The characteristics of the microstructure dictate the mechanical properties of the material and the performance of the cast parts during service.

This chapter provides an explanation of the solidification process of 319-Al alloy and the treatment used on the foundry floor to control the characteristics of the microstructure. It is explained how these characteristics are assessed via thermal analysis, particularly by the Aluminum Thermal Analysis System (AlTAS) which is an advanced thermal analysis system developed at the University of Windsor. Finally, an explanation of the relationship between thermal analysis parameters, the microstructural features of 319 alloy and its mechanical properties is provided. These concepts are the foundation of the knowledge-based system developed in this project.

3.2 319-Al Alloy

Aluminum-silicon alloys are classified, on the basis of their silicon content, into three categories: hypoeutectic (5 -10 wt % Si), eutectic (11 - 13 wt %Si) and hypereutectic (14 - 20 wt% Si). Based on the Al-Si system these alloys also contain varying amounts of iron, manganese, zinc and other impurity elements.

The CBR system developed in this project is based on W319-Al alloy, which is a grade of the hypoeutectic 319-Al alloy. The typical chemical composition for these alloys is presented in Table 1.

Table 1 – Chemical Composition of AA Grades of the 319 and W319 Alloys[10, 11]

Alloy Composition (wt%)

Alloy	Si	Cu	Fe	Mn	Mg	Ni	Zn	Ti
319	5.5 – 6.5	3.0 – 4.0	1.0	0.5	0.1	-	1.0	0.25
W319	6.5 – 8.0	3.0 – 4.0	0.4	0.2 – 0.3	0.10	0.02	0.15	0.25

The solidification process of 319-Al alloy starts with the formation of a dendritic aluminum network followed by the precipitation of the Al-Si eutectic phase, and later the precipitation of up to three distinct Al-Cu phases (Al_2Cu, $Al_5Mg_8Cu_2Si_6$, and a eutectic of Al_2Cu with interspersed α–Al phase[12]). If sufficient Fe is present (> 0.7 wt% depending on cooling rate and Si content[13]) intermetallic phases in the form of Al_5FeSi can also form.

The means used to analyze and predict the formation of these phases via thermal analysis will be discussed in this chapter.

3.3 Solidification of 319 Al-Si Alloy Described Via Thermal Analysis

The solidification of an alloy can be analyzed using a cooling curve obtained from a test sample. The cooling curves reflect the latent heat which is given off as a result of the formation of the phases of the alloy.

The liberation of latent heat affects the cooling rate of the sample, and as a result, the formation of each phase appears as a change in the slope of the cooling curve. The formation of a large volume phase may be described by the following three stages: the nucleation of the phase, an undercooling period which provides the driving force necessary for the formation of the phase, and a recalescence effect which indicates the growth of the given phase. Small volume phases are difficult to detect on the original curve and for this purpose the first derivative of the cooling curve is calculated[14].

The solidification process of 319-Al alloy can be described as follows. The 319-Al alloy is usually held at a pouring temperature of approximately 760°C. Once the alloy is cast and begins to solidify, at about 604°C [15] equiaxed α-Al crystals start to nucleate by different mechanisms[16] (point *a* in Figure 2). In the absence of grain refiners the molten aluminum is undercooled to the minimum temperature (point *b*), which is below the equilibrium solidification temperature. At this point, solid nuclei start to grow beyond a critical size and act as nucleation particles for new crystals slowing down the cooling rate of the metal. In the meantime the previously formed crystals start to grow. At this point, the heat generated by the nucleation of these crystals raises the temperature to a growth temperature (point *c*). After this plateau the sample starts to cool again, the dendrite structure starts to coarsen until neighboring dendrites start to impinge upon one another (point *d*) and further growth occurs only by dendrite coarsening. At this point mass feeding changes to interdendritic feeding. As a result, this point is considered as an indicator of feeding efficiency mainly because it marks the beginning of possible feeding problems which result in shrinkage and pore formation[14, 15,16].

As the dendrites continue to coarsen, the liquid in the solidification front is depleted of Al and reaches the eutectic composition. At this point (~572°C) the Al-Si eutectic starts to solidify in the interdendritic regions and in the cooling curve another undercooling effect starts followed by a long plateau (points *e,f,g*). As eutectic solidification proceeds and the fractions solid increases, feeding becomes more tortuous in the reduced interdendritic channels[16].

The first appearance of the Al_5FeSi phase occurs during the eutectic reaction but for the Fe content under consideration it is obscured by the eutectic plateau and is not detectable on the cooling curve [13].

Finally, up to three copper reactions can occur depending on the presence of modifiers and chemical composition of the alloy[15, 17]. At 549°C a simple reaction occurs leading to the formation of blocky $CuAl_2$. This reaction is only visible in cooling curves of unmodified alloy[18]. At 520°C a finely dispersed $CuAl_2$ and β-AlFeSi needles are formed along with some deposits of Si. The third reaction with noticeable heat effect is observed at 500°C (point *h*). The products of this reaction are $CuAl_2$, $Al_5Mg_8Cu_2Si_6$ with deposits of *Al* and Si[19]. The solidification of these phases is also critical for the formation of microporosity since the deposits of ternary liquid solidify when the rest of the bulk of the casting is already solid and the volumetric shrinkage in these deposits is difficult to feed[12].

At approximately 480°C the end of solidification occurs (point *i* in Figure 2). The resulting phases can be observed in Figure 3.

The characteristics of these events are affected by the chemical composition of the alloy and the cooling rate during solidification.

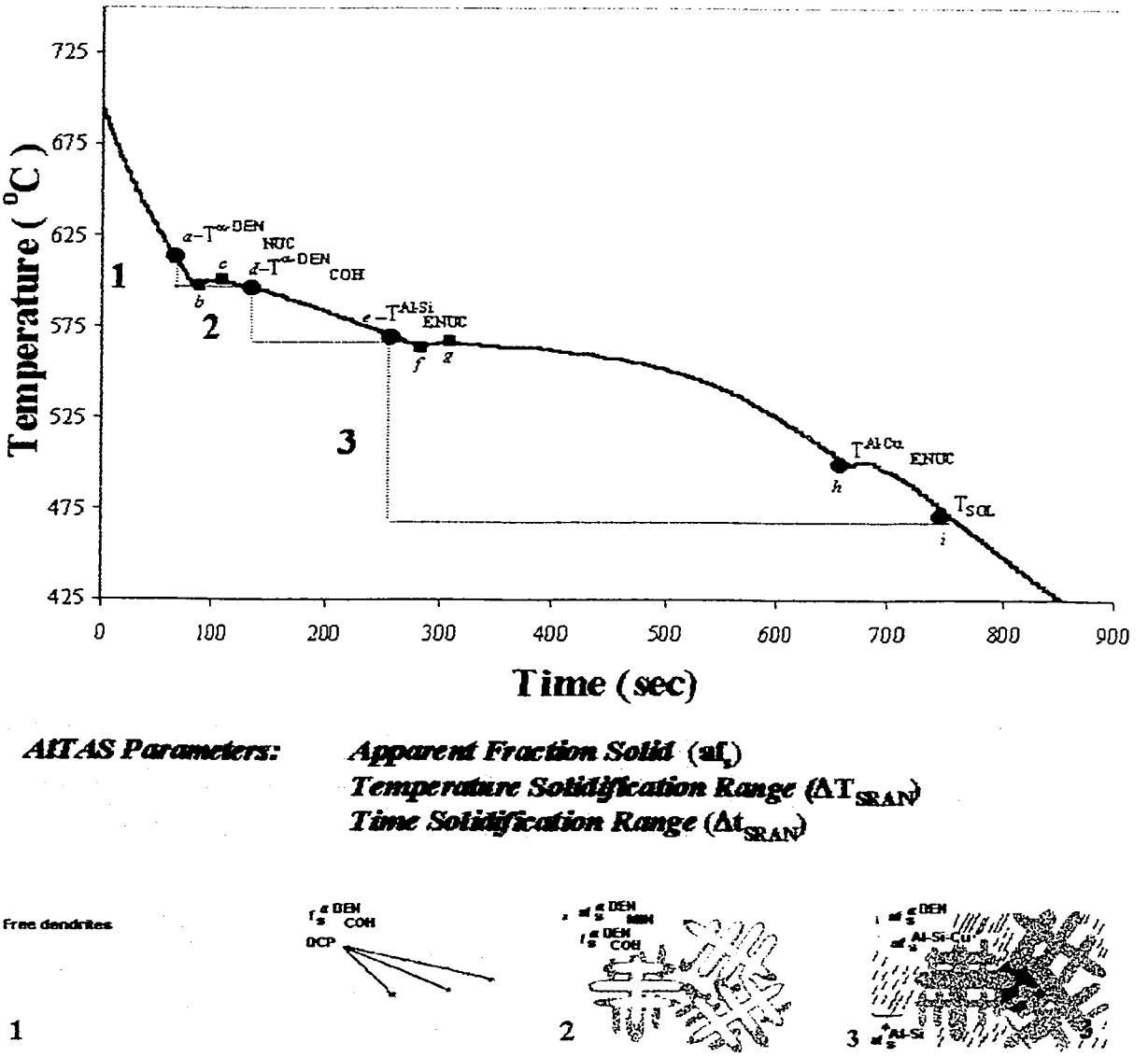

Figure 2 - Characteristic Cooling Curve of 319-Al alloy and the Different Feeding Modes that Occur During Solidification

Figure 3 – Typical Microstructure of the Unmodified 319-Al Alloy

3.4 Treatment of the 319 Al-Si Alloy

The growing use of Al-Si alloys in the automotive market places high requirements on the service performance of these materials. The required characteristics are achieved by incorporating molten metal processing techniques that optimize the metal quality prior to casting.

Common liquid metal processing techniques include:

- Fluxing, filtering and degassing, to control hydrogen level and inclusion content.
- Use of protective atmospheres to prevent re-absorption of hydrogen.
- Grain size control through the use of grain refiners.
- Addition of modifiers to refine the morphology of the Al-Si eutectic.

Different control methods are utilized on the foundry floor to evaluate the effectiveness of these treatments. Techniques such as the reduced pressure test, hydrogen measurements with AlSCAN™ units or the Porous Disc Filtration Apparatus (PODFA) are used to evaluate metal cleanliness and hydrogen content. Grain size and silicon modification are usually assessed using thermal analysis and several commercial systems have been developed for this purpose[20, 21].

3.4.1 Grain Refinement

Aluminum alloys, similar to alloys of other light metals, normally form coarse, equiaxed and columnar grains during solidification. Limiting the grain size in an aluminum alloy casting, by promoting nucleation and restricting growth during solidification is called grain refinement.
The most popular method to achieve grain refinement is the addition of grain refiners in order to increase the number of sites for the nucleation of the alpha aluminum phase. The grain size of a cast part has an inverse relationship to the number of nuclei present in the liquid. Grain refinement can take place either in-furnace or in-mould by making additions of low melting point master alloys. The latter offers advantages such as more consistent element recovery, no fading and better control of sludge formation.
There are many elements that have grain refining ability in aluminum alloys, although their effectiveness varies. The most potent of this group are Titanium and Boron, which have led to the most common grain refiners in use today, which are the Al-Ti and Al-Ti-B families of master alloys. Recent work[22] shows that, in the case of high silicon containing hypoeutectic cast AlSi alloys, AlB master alloys are most effective for the refining of primary α-Al and much better than the well known AlTiB or AlTi master alloys.

3.4.1.1 Effect of Grain Refinement on Mechanical Properties

Grain refinement has several positive effects on the properties of aluminum alloys.
The formation of finer grains prevents the growth of long dendrites, and postpones the establishment of a dendrite coherent network[16]. This causes a more even distribution of porosity and secondary phases, which improves the soundness of the metal and reduces micro and macro segregation. These benefits result in increased fatigue life, tensile strength, elongation and machinability[20, 22].

3.4.1.2 Evaluation of Grain Refinement via Thermal Analysis

Grain refinement can be related to the magnitude of the undercooling and undercooling time occurring during the α-Al reaction. When there are a great number of nuclei the shape of the curve exhibits little

undercooling (Figure 4 - dotted line). When there are few nuclei, there is more undercooling (Figure 4 -solid line).

Several time and temperature parameters have been related to the grain size of the castings[14, 20,23] as presented in Figure 4. Recent work[24] has shown that the cooling rate of the samples affects these parameters; however, for the low cooling rates (~0.2 °C/sec), which are of interest in this project the recalescence temperature ($T^{\alpha\text{-DEN}}_{G}$) provides the best correlation with the grain size of the samples.

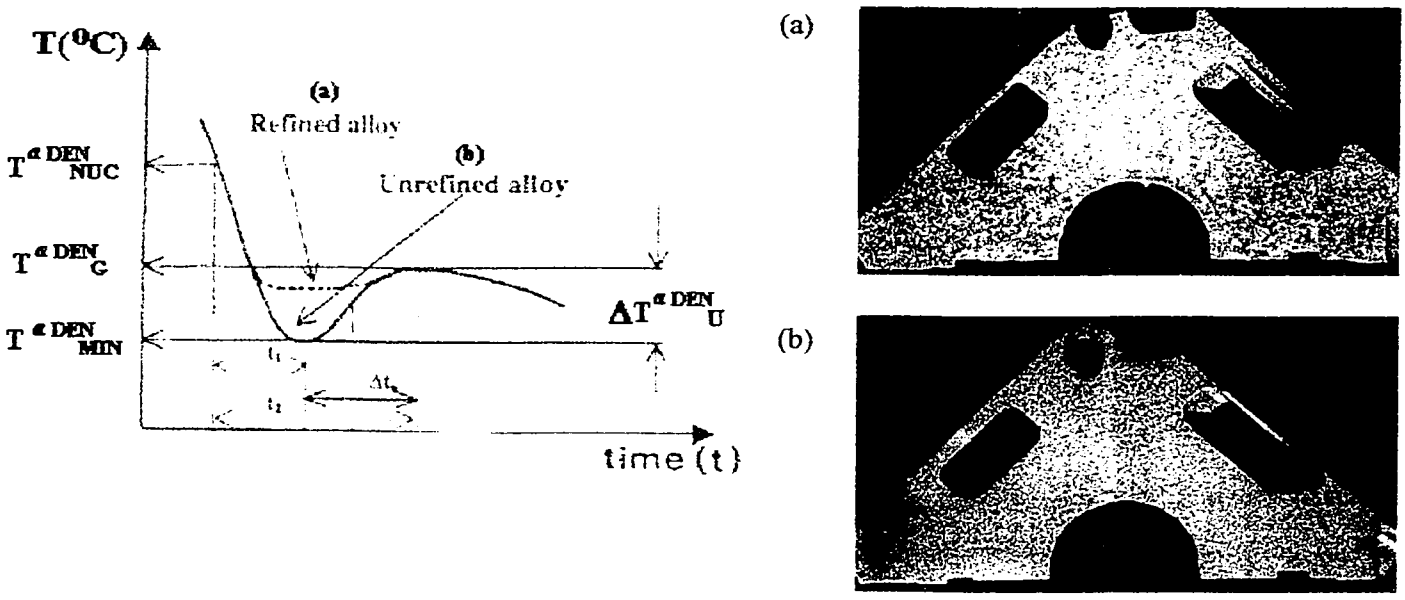

Figure 4 - Thermal Analysis Parameters Associated with Grain Size Determination and Two Different Grain Sizes in an Engine Block Cross-Section (Main Bearing Saddle)

3.4.2 Silicon Modification

At the low cooling rates typically encountered in sand castings, silicon crystals are present in the microstructure as coarse, acicular and interconnected flakes, which act as crack initiators, causing the material to fracture in a brittle mode. These needles need to be converted to a fibrous form to minimize stress.

The transition from flake to fiber is called modification and may be accomplished by the addition of modifiers, control of cooling rate, by solution treatment or by a combination of these factors[25].

Modification is usually accomplished through the use of sodium, antimony or strontium. However, strontium is the main modifier used today. It may be added to the melt in a pure metallic form, or a master alloy (either Al-10%wt Sr or Al-90%wt Sr) prior to casting. As the amount of strontium in the melt increases, the level of modification also increases.

3.4.2.1 Effect of Modification on Mechanical Properties

Silicon modification results in improved properties, especially ductility. However, the main drawback of eutectic modification is that it has been found to increase porosity and pore size, which are the most detrimental factors for both the fatigue life and tensile properties of Al-Si alloys. This effect has been explained by several mechanisms[16] such as a decrease in the critical threshold hydrogen content [26], nucleation of pores at lower fraction solid[27], or shrinkage coupled with the lack of interdendritic feeding during solidification. For this reason, modification is usually used in conjunction with grain refinement to overcome its negative effects.

3.4.2.2 Thermal Analysis Parameters for the Evaluation of Silicon Modification

Simple thermal analysis is a good tool to evaluate qualitatively and quantitatively the degree of modification[18, 28,29] prior to casting.

The net effect of the additions of strontium on a cooling curve can be quantified by the depression of the nucleation and growth temperatures of the main Al-Si eutectic reaction[28, 29] (Figure 5). The degree

of Al-Si eutectic modification has been correlated with the depression of Al-Si eutectic growth temperature ($\Delta T^{Al\text{-}Si}_{E.G}$). The $\Delta T^{Al\text{-}Si}_{E.G}$ was determined according to the following formula[28]:

Equation 2 – Calculation of the Depression of the Al-Si Eutectic Growth Temperature

$$\Delta T^{Al\text{-}Si}_{E.G} = T^{Al\text{-}Si}_{E.G\ UNMODIFIED} - T^{Al\text{-}Si}_{E.G\ MODIFIED}$$

where $T^{Al\text{-}Si}_{E.G\ UNMODIFIED}$ is the Al-Si eutectic growth temperature, that is, the maximum temperature that is achieved during the recalescence period from the nucleation temperature at a residual level of strontium, and $T^{Al\text{-}Si}_{E.G\ MODIFIED}$ is the maximum temperature after addition of strontium that is achieved during the recalescence period.

Thermal analysis can also quantify the fading of strontium in the aluminum melt[28], which results from long holding time of strontium modified melts in the furnace. The parameter $\Delta T^{Al\text{-}Si}_{E.G}$ can be used for this purpose since smaller values correspond to lower strontium levels.

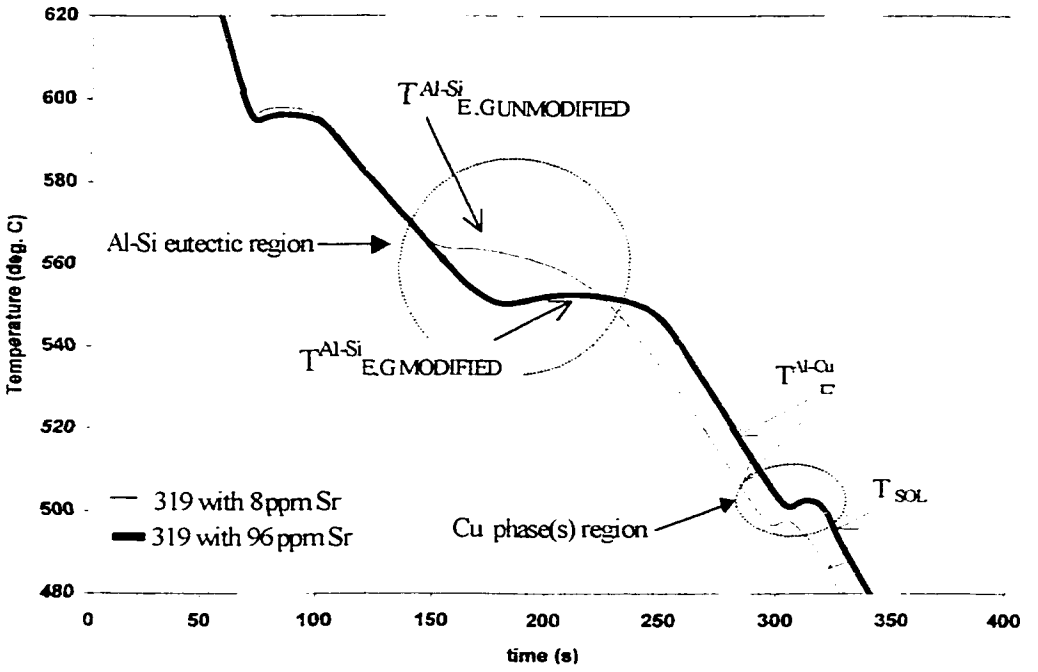

Figure 5 - Cooling Curves Showing $T^{Al\text{-}Si}{}_{E.G}$ for Modified and Unmodified Alloys[28]

3.5 Intermetallic Compounds and Their Effects on Mechanical Properties.

Iron is a common impurity in aluminum, which has a difference in solubility between the liquid and solid states[30] and as result, solidifies as an intermetallic compound. Fe intermetallics occurring in the form of needles (β–Al_5FeSi) are a particularly deleterious intermetallic compound for Al-Si-Cu based alloys.

The formation of Fe needles depends on the composition of the alloy (the threshold amount of Fe leading to formation of needles is >0.7 wt%, depending on cooling rate and Si content[13]) and its formation is controlled via Mn additions, which turns Fe needles into a form commonly named Chinese script (α-$Al_{15}(Fe,Mn)_3Si_2$). In W319 alloy iron appears in the form of Chinese Script.

It has been shown[13,31] that the existence of the β-phase acts as a stress raiser, resulting in a more brittle metal with lower tensile and fatigue properties. The β-needles also interfere with feeding and fluidity promoting shrinkage porosity and acting as pore nucleation sites, although they limit pore growth. In the absence of β-(Al_5FeSi) needles, another intermetallic, the Al_2Cu eutectic particles assist in the formation of pores, although to a lower extent.

3.5.1 Thermal Analysis that Measure the Solidification of Intermetallic Compounds

3.5.1.1 Determination of Fe Rich Phases

The possibility of quantifying iron using cooling curve analysis depends on the content of Fe in the alloy. In the case of low Fe contents such as in W319 alloy, the formation of Fe intermetallics does occur but the reaction is obscured by the Al-Si eutectic reaction and it is not possible to detect it. For higher Fe contents the reaction can be measured via the duration of the reaction, using high order time derivatives[13].

3.5.1.2 Determination of Cu Rich Phases

The last reaction in the cooling curve of 319-Al alloy corresponds to the formation of the Al-Cu eutectics. Figure 6 shows the peaks associated with the Al-Cu reactions. The possibility of detecting the peaks associated with these three reactions depends on the cooling rate of the sample, the thermocouple size and the characteristics of the test cup.

Parameters such as the nucleation temperature of the Cu phases ($T^{Al\text{-}Cu}_{NUC}$) and the solidus temperature (T_{SOL}) are indicators of the Cu content of the alloy, and also of the effect that elements such as Sr have on the proportion of the different Cu phases. Sr has been found to increase the nucleation temperature of the Al-Cu eutectic and the end of solidification as well as increasing the proportion of blocky Al_2Cu[18].

The start and end of solidification temperatures of the Al-Cu rich phases is relevant in the determination of optimum solution treatment schemes.

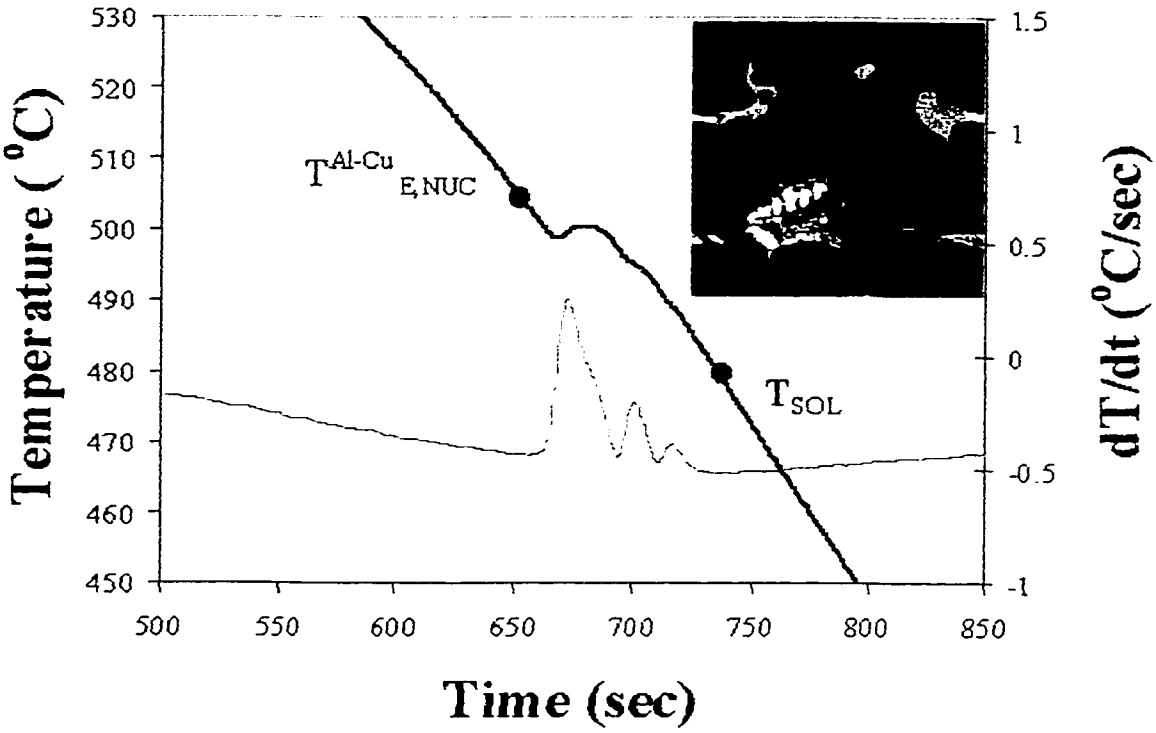

Figure 6 - Thermal Analysis Parameters Associated with the Al-Cu Rich Phases

3.6 Porosity

Three types of porosity affect aluminum castings[32] (Figure 7):

a) Hydrogen gas porosity, which is formed due to rejection of hydrogen from the solidified metal into the adjacent liquid as a consequence of the difference in solubility between the solid and liquid phases.

b) Shrinkage porosity occurring during solidification. This type of porosity is mainly determined by the feeding mechanisms (liquid, mass, interdendritic and burst feeding), and by the solidification

kinetics of the alloy in question[33]. Poor feeding of a casting during solidification will result in shrinkage pores.

c) Gas-shrinkage porosity. In most cases gas evolution and shrinkage occurs at the same time and interaction between these phenomena can be expected. Both gas and shrinkage pressure aid in the nucleation and growth of the pore.

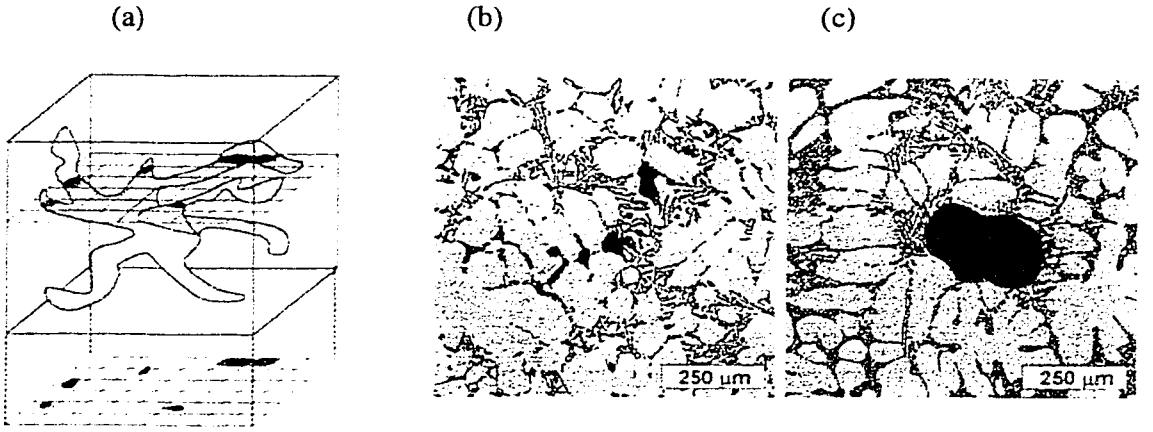

Figure 7 -(a) Schematic of a Shrinkage Pore and the Resulting Two-Dimensional Image when Sectioned[34] (b) A Typical Shrinkage Pore (c) A Typical Gas Pore[34]

3.6.1 Factors that Affect the Formation of Porosity

Basically, the higher the hydrogen content in liquid aluminum, the higher the porosity. However, other factors can also influence the hydrogen porosity formation during solidification[35]. These parameters are mainly:

a) The local pressure during solidification, the chemical composition of the alloy, since alloying elements such as Cu, Si and Mg modify hydrogen activity and affect the feeding mechanisms of the alloy.

b) Grain refinement, the amount of porosity varies inversely with titanium concentration.

c) Chemical modification, it has been determined that strontium increases the susceptibility of castings to porosity formation[32, 36].

d) The solidification range of the alloy. A wider solidification range results in higher porosity level.

e) The metal cleanliness (i.e. oxide or inclusion content in the melt). Lower melt purity leads to a higher porosity level.

3.6.2 Quantification of Porosity

The amount of porosity in good quality aluminum castings is usually less than 1% by volume and pores may vary in diameter from a few microns up to about 400 microns. Porosity is quantitatively evaluated using the Image Analysis Technique[35].
Current research efforts focus on the feasibility of determination of porosity levels using thermal analysis; however further research in this area is still required.

3.6.3 Effects of Porosity on Mechanical Properties

Hydrogen induced porosity in castings is a concern because it is always detrimental to mechanical properties, especially ductility, fracture toughness, fatigue life as well as surface finish and corrosion resistance[35].

Figure 8 displays the relationship between tensile strength and elongation and the increase in hydrogen porosity. The decrease in tensile strength and elongation is evident with the increase in porosity.

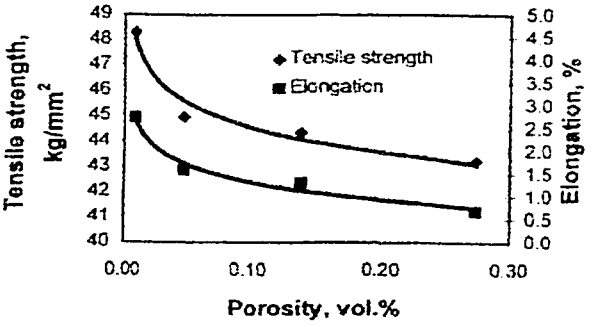

Figure 8 - Relationship of Hydrogen Porosity with Tensile Strength and Elongation for DC Casting Products (150*37.5 mm) [37]

Porosity geometry is also found to influence the mechanical properties of aluminum castings. Detrimental effects are associated with factors such as the quantity, dimension, distribution and shape of the porosity. Figure 9 shows the relationship between the number of cycles to failure and the largest pore size for the 356-foundry alloy. Large size porosity is more detrimental to the failure resistance of the castings[37].

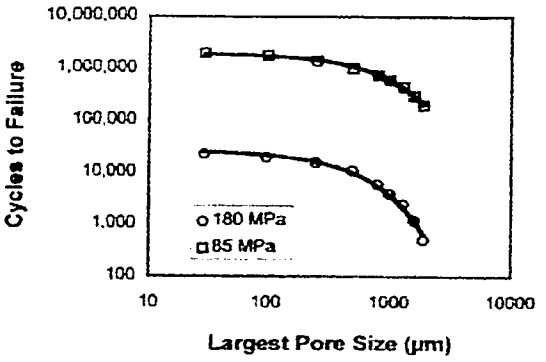

Figure 9- Relationship between the Number of Cycles to Failure and the Largest Pore Size in 356 Aluminum Castings[37]

3.7 Effects of Cooling Rate

The cooling rate of a casting section has a definite influence on the resulting type of microstructure, especially in terms of the Secondary Dendrite Arm Spacing (SDAS) as well as the size and distribution of porosity. Faster cooling rates result in finer and more homogeneous microstructure with higher Ultimate Tensile Strength (UTS), Ductility and Fatigue Properties.

Since pore growth is a diffusion-controlled process, longer solidification times increase the percent porosity, pore length and pore area[31].

Cooling rate also has an effect on the morphology of intermetallics. It has been shown[17] that at high cooling rates the Al_2Cu occurs mainly in the form of pockets of fine eutectic ($Al+Al_2Cu$) in the interdendritic regions as opposed to the coarse particles and networks that are characteristic of slower cooling rates.

CHAPTER 4

LITERATURE REVIEW - ARTIFICIAL INTELLIGENCE SYSTEMS FOR CONTROL OF ALLOY QUALITY

Several authors have addressed the use of computer systems to assist in the analysis and interpretation of cooling curves. As a result, several commercial thermal analysis systems have been developed and their capabilities range from calculation of grain refinement and modification level[21, 29,38] to statistical process control modules[20, 34] and expert systems[39, 40].

Not many knowledge-based systems have been developed for the interpretation of Thermal Analysis results and the existing are devoted to the analysis of cast iron. Li et al[41] developed two Back Propagation Neural Networks (BPNN) using properties of various cast irons with different compositions than were obtained in laboratory conditions. The BPNN are able to predict the chemical composition and mechanical properties of cast-iron components based on thermal analysis parameters. The BPNN were tested at two casting facilities and improved the results that were previously obtained by statistical methods.

Sillen[40] developed a quality control system for grey and ductile iron. This system consists of three integrated software programs. The first program measures and stores temperature/time data through an A/D converter. The second program performs the analysis of the cooling curve to obtain the characteristic temperatures; this is accomplished using analytical mathematical methods and knowledge-based functions. The knowledge base was developed by induction. This part also contains a rule-based system for a go/no go evaluation of the melt. Part three is a case-based reasoning program that correlates the results of thermal analysis to the risk of defects in the microstructure. This system was developed using data from several foundries and is intended to adapt to the characteristics of different alloys and process conditions.

Mahfoud[42] developed an intelligent heat pipe that is able to detect important treatment parameters of various aluminum alloys such as grain refinement and modification; it is also able to detect reactions related to the formation of iron, magnesium and copper bearing intermetallics for cooling rates between 0.1 to 4°C/sec. This system uses cooling-curve and derivative analysis for the calculation of metallurgical reactions. The cooling rate is controlled through a valve that is

able to adjust the airflow around the sample at any moment of solidification. The capabilities of this system allow it to calculate important characteristics of the microstructure of the alloys which determine the mechanical properties of the final castings; however, this system does not include artificial intelligence techniques to help in the analysis of the thermal analysis results nor does it provide explicitly the expected mechanical properties of the cast parts.

4.1 Motivation for the Research

To date, most of the research related to the use of artificial intelligence for cooling curve analysis and interpretation has been devoted to the cast iron industry. In the aluminum casting industry thermal analysis systems have been used mainly as indicators of the level of silicon modification and grain refinement.

In addition to these characteristics, the Aluminum Thermal Analysis System (AlTAS) developed at the University of Windsor is also able to quantify parameters related to the changes in feeding modes that occur during the solidification of 319-Al alloy. These parameters are indicators of the propensity to shrinkage porosity, which is critical to the final properties of the casting. Other parameters calculated by the AlTAS are related to the formation of Cu-rich phases, which determine the adequate heat treatment cycles. The interpretation of these important parameters requires considerable metallurgical knowledge and experience in cooling curve analysis, and therefore the implementation of this system on the foundry floor represents a suitable domain for the application of artificial intelligence techniques.

The focus of this research is on the use of knowledge-based technology and statistical methods applied towards the quality control of molten 319-Al alloy for the production of a variety of engine blocks. The resulting system will provide a state of the art thermal analysis system for the production of aluminum casting components for automobile powertrain systems.

4.2 Objectives of the Proposed Research

The main objectives of this research are as follows:

a) To carry out a repeatability and reproducibility study in order to evaluate the performance of

the AlTAS in an industrial environment and to determine potential improvements to its hardware and software. This study involves the effects of process variation and test sample variation on the recorded cooling curves and thermal analysis parameters.

b) To develop a Statistical Process Control Module for the AlTAS software using charting procedures which are adequate to the characteristics of the process.

c) Collect thermal analysis data, chemical composition, hydrogen measurements and mechanical properties from an industrial environment and incorporate them into a Case-Based Reasoning System.

d) Test the resulting Case-Based Reasoning System and Statistical Process Control Module with industrial and laboratory data to demonstrate the validity of the results.

CHAPTER 5

INDUSTRIAL IMPLEMENTATION OF THE ALUMINUM THERMAL ANALYSIS SYSTEM (AlTAS) -REPEATABILITY AND REPRODUCIBILITY STUDY

5.1 Introduction

All the experimental work for the development of this project was carried out at Ford's Windsor Aluminum Plant. This chapter provides an overview of their casting process and liquid metal treatment.

Since an understanding of measurement variability is necessary to properly monitor the variability of products and processes, a Gauge Repeatability and Reproducibility Study of the AlTAS was performed and is also presented in this chapter.

5.1.1 Overview of the Casting Process

The aluminum alloy analyzed in this project is processed using the Cosworth casting process under license by the Ford Motor Company.

In this process, zircon sand cores are produced with a cold box resin binder system. These cores are assembled to produce the mould and moved to a filling-roll-over process. The moulds are filled with aluminum from the bottom of the mould using an electromagnetic pump. The pump is submerged in liquid aluminum to a height of approximately the middle of the furnace to assure that only clean metal enters the mould. The molten aluminum is protected from hydrogen and other gases that can lead to porosity in the casting. This is achieved by means of a blanket of argon covering the metal in the furnace. The mold fill rate is closely monitored using electronic controls. This minimizes turbulence and gas pick up. The filled mould is then transferred to a Thermal Sand Removal process to separate the sand mould from the casting. Next the castings undergo a T6 treatment (solution treatment and artificial aging) to achieve the desired mechanical properties. Thermal Sand Removal is combined with solution treatment as a continuous operation (Figure 10).

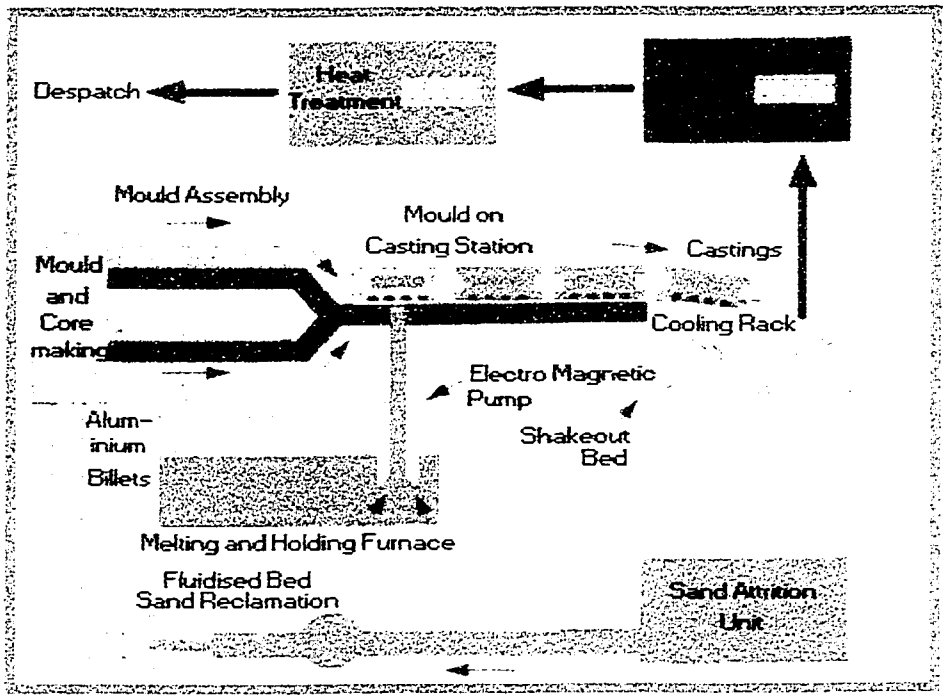

Figure 10 – Schematic of the Cosworth Casting Process [43]

5.1.2 Liquid Metal Processing

The Windsor Aluminum Plant has three holding furnaces which are fed automatically by a melting furnace to maintain a constant level. Therefore, the liquid metal treatment is a continuous process.

The thermal analysis samples of W319-Al alloy analyzed in this work were obtained from the holding furnace at the north well pump of the Windsor Aluminum Plant. Before reaching the holding furnace, the metal is degassed with argon. In the furnace, the liquid metal is maintained at 760°C, no modifier is added to the alloy and grain refiner is added in-mould.

5.1.3 The Aluminum Thermal Analysis System (AlTAS) Setup

The AlTAS is a thermal analysis system developed by the NSERC/Ford/University of Windsor Industrial Research Chair in Light Metal Casting Technology (IRC) (Figure 11). The system

consists of a stainless steel test stand protected against high frequency noise and elevated temperatures. The cabinet includes a locking mechanism to ensure the consistent location of the thermocouples within the test sample. The system offers the possibility of using two calibrated K-type thermocouples (Figure 12); one in the centre and one near the wall of the sample. The thermocouples are lowered using a pneumatic cylinder. A National Instruments Data Logger System is used for data acquisition.

The AlTAS software is installed in an industrial-type computer with an analog-to-digital (DAQ) system. It consists of a multi-channel data acquisition module and an analytical module for mathematical cooling curve analysis developed at the University of Windsor using National Instrument's LabView™ Software. This module is able to calculate a base line [11] for the estimation of fraction solid, it detects 47 cooling curve parameters (See Appendix I) using derivative analysis and calculates the modification level of the melt.

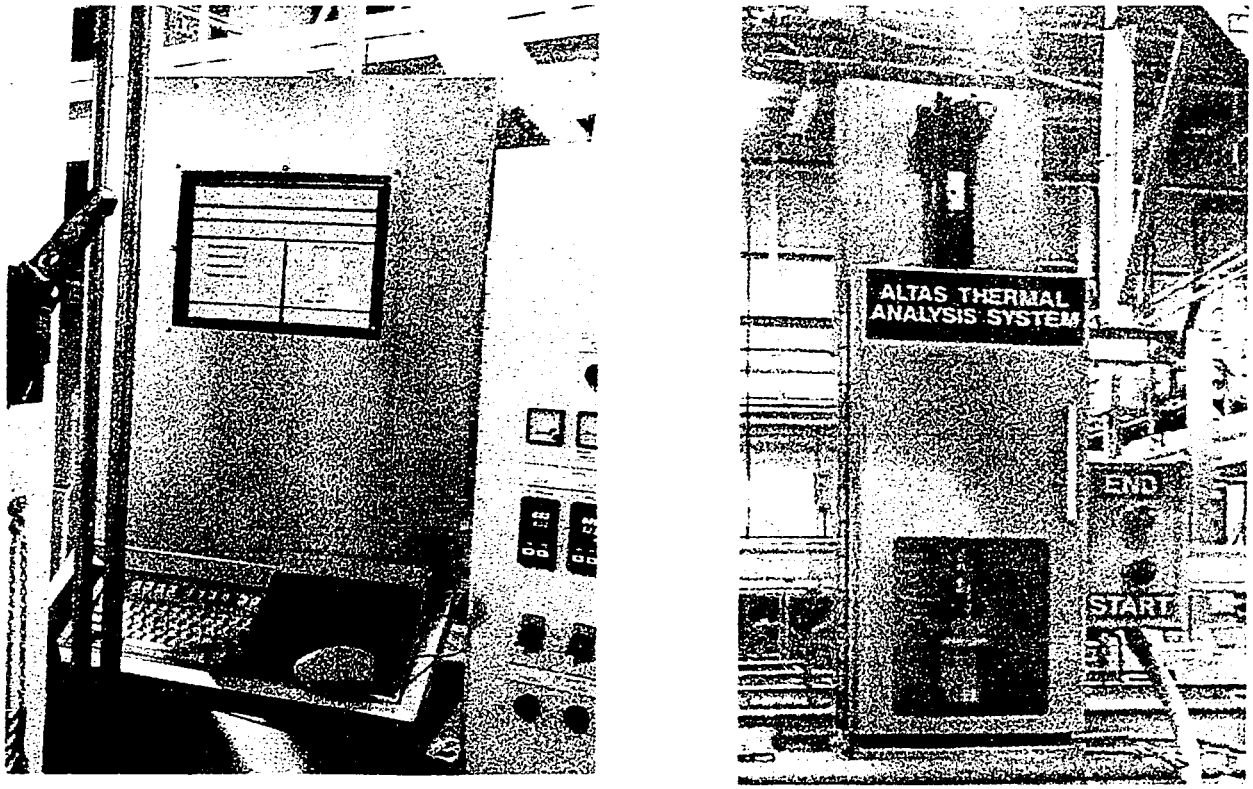

Figure 11 – The Computer Stand and Test Stand of the Aluminum Thermal Analysis System (AlTAS)

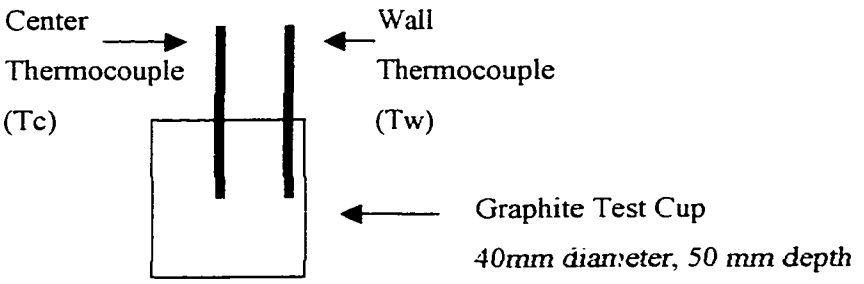

Figure 12 – Arrangement of Thermocouples in a Thermal Analysis Test Sample

5.2 Repeatability and Reproducibility (R&R) Study

The Level of Silicon Modification is a parameter that has long been studied in the aluminum casting industry. There is a generalized agreement on the temperature parameters and scales used to quantify Modification levels. Following this general agreement, the parameter $\Delta T^{AlSi}_{E.G}$ (See Appendix I) was used as the response variable during this study to measure the effect of the variation in chemical composition and operator technique on the AlTAS temperature determinations.

As described in the following sections, the study was carried out in three phases. In the third phase of the study a fraction solid ($af_s^{Al\text{-}Si}$) and a time parameter ($t_{Al\text{-}Si}$) were also evaluated. The objective of this comparison was to determine the robustness of the three different types of parameters to changes in cooling rate and identify the most suitable ones for industrial application. This was a special concern since previous studies[42] pointed at variation in cooling rate as one of the main drawbacks of traditional thermal analysis, which causes poor repeatability of results.

5.2.1 Sampling Procedure

The thermal analysis samples were obtained next to the pump well, submerging the AlTAS cylindrical graphite test cup (40mm in diameter, 50 mm deep and average cooling rate of

0.3°C/sec) into the melt. The cup was kept submerged at half the depth of the furnace for 20 seconds on average, after which it was withdrawn and rapidly placed in the stand. Two calibrated thermocouples, sheathed by stainless steel tubing, were automatically placed into the cup to record the temperature during the cooling process. The data was acquired by a National Instruments™ data logger system (SCXI-1000), analyzed by the AlTAS software and the results are stored in its database. Three plant operators from 3 different production shifts were trained on this sampling procedure (Figure 13).

All the thermocouples used in this work were calibrated using a high precision probe. For this purpose, eight temperature measurements in the working temperature range of the AlTAS (350°C – 800°C) were recorded with the high precision probe and K-type thermocouples. A logarithmic fit of the data produces a correcting equation, which is applied to all the subsequent temperature measurements.

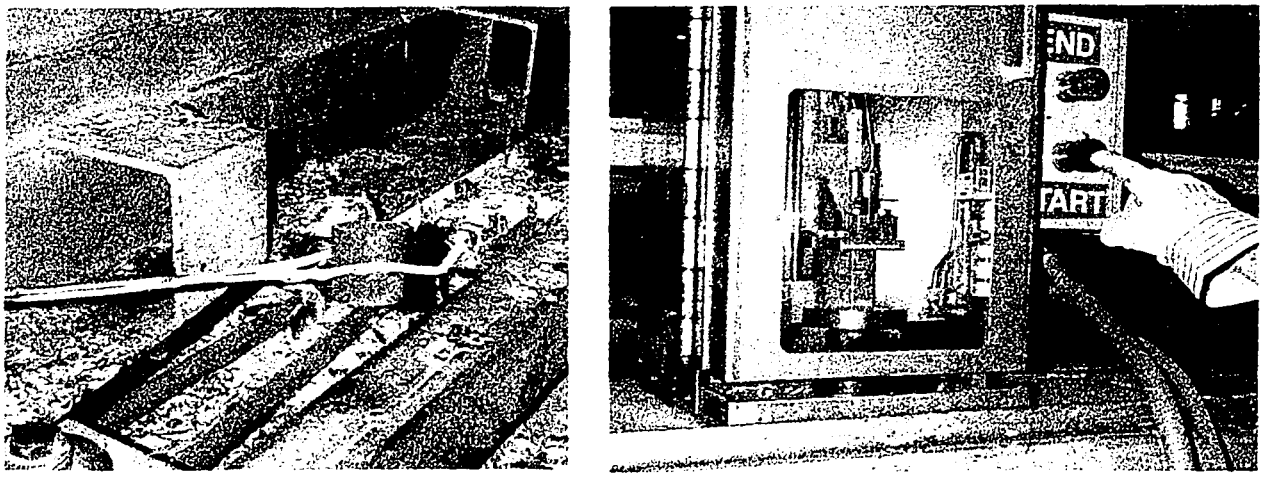

Figure 13 – The Sampling Procedure of the AlTAS

5.2.2 Chemical Analysis and Hydrogen Measurements

To verify the chemistry of the alloy and its variation during the study, the chemical composition was measured using optical emission spectrometry. The level of hydrogen in the melt was verified using an AlSCAN™ hydrogen analyzer unit.

5.2.3 Sampling Schedule for the Repeatability and Reproducibility Study

As mentioned above, the R&R study was carried out in the three phases described in Table 2:

Table 2 – Phases of the Repeatability and Reproducibility Study

Phase / Objective	Number of operators (shifts)	Number of Samples	Number of Days
I – To determine whether there is significant variation in the chemical composition of the alloy within each shift.	3	6	5
II – To carry out a preliminary estimation of Repeatability and Reproducibility.	2	8	3
III - Evaluation of Reproducibility using the Isoplot technique[45]. This analysis includes samples of 319-Al alloy with Sr additions between 7 and 100 ppm, obtained by Djurdjevic et al[18] in previous experiments using the AlTAS. The objective is to analyze R&R for the complete range of Silicon Particle Modification (1 – 6) and compare the response of three types of parameters: temperature, time and fraction solid, to test sample characteristics.	NA	NA	NA

The sampling procedure described above was followed during the three phases.

5.2.4 Statistical Analysis and Results

5.2.4.1 Phase I

The effect of variation of the chemical composition within the same shift was evaluated using a 3-factor random model. The Analysis of Variance (ANOVA) of the data was carried out with the General Linear Model of the SAS® statistical software package and the results are presented in Table 3. The range of chemical composition measured during the study is presented in Table 4.

5.2.4.1.1 Results of Phase I

A preliminary analysis of residuals of the ANOVA model indicated that the data did not meet the assumption of Equality of Variance required for the ANOVA, for this purpose, a square root variance stabilizing transformation was used prior to the computations.

The P values in Table 3, which indicate the smallest level at which the data are significant, show that the variation in alloy chemistry and process conditions within the same shift is negligible and does not have a significant effect on the thermal analysis parameter $\Delta T^{Al\text{-}Si}_{E.G}$. However, the variation between different days has a significant effect on $\Delta T^{Al\text{-}Si}_{E.G}$ and therefore, can be detected by the AlTAS (as indicated by the P value for the Different Days).

This analysis also indicated that the sampling technique of the different operators affects the AlTAS parameter.

Table 3 – Results of ANOVA for Phase I Obtained Using the Statistical Software SAS® (factors are considered significant at α=0.05)

Source of Variation	Degrees of Freedom	Mean Square	F Value	P Value (smallest significant α)
Days	2	1.10	5.25	0.0001
Operators	1	0.35	4.85	0.0409
Within Shifts	2	0.063	0.88	0.4337

Table 4 – Range of Chemical Composition Encountered During Both Phases of the Study

	Si	Cu	Fe	Mg	Mn	Zn	Ti	Sr	Ni
Mean	7.503	3.880	0.352	0.287	0.240	0.124	0.113	0.0007	0.0196
Std Dev	0.053	0.053	0.0113	0.0083	0.0044	0.0172	0.0018	0.0000	0.0022

	Sn	Pb	Cr	P	Li	B	Sb
Mean	0.0021	0.0177	0.0455	0.0004	0.0006	0.0003	0.0002
Std Dev	0.0006	0.0051	0.0040	0.0002	0.0001	0.0000	0.0002

5.2.4.2 Phase II

In the second phase of the study the variation within the same shift was discarded and the ANOVA model was simplified to a nested model. Nested models separate the variation caused by the factors of interest from the variation caused by testing physically different materials. This model is described by the equation:

Equation 3 – Nested Model for R&R study[46]

$$Y_{ijkl} = \mu + O_j + D(O)_{j(i)} + R_{k(ij)}$$

$$i = 1,..,4;\ j = 1,..,2,;k = 1,...6$$

where μ is the mean of the observations

O_j is the effect of operators

$D(O)_{j(i)}$ is the effect of changes in chemical composition and processing conditions during the days of the study

$R_{k(ij)}$ is the error among replicates

μ is a constant and O_j, $D(O)_{j(i)}$, and $R_{k(ij)}$ are independent, random variables with means equal to zero and variances σ^2_O, $\sigma^2_{D(O)}$ and σ^2 respectively.

This model was selected to take into account the fact that the samples measured by each operator are physically different[46, 47](Table 5 and Equation 4).

Repeatability was estimated using the variance component σ^2, which represents the variation among repeated samples taken by one operator.

Reproducibility describes the variation induced by having more than one operator and was quantified by the variance component σ^2_O.

The total variability of the instrument is the sum of repeatability and reproducibility.

Process variation was estimated using the variance component $\sigma^2_{D(O)}$.

Table 5 - General ANOVA Table for the Nested Model[46]

Source of Variation	Degrees of Freedom	Mean Squares	Expected Mean Squares
Operators (O)	o –1	MS_O	$\sigma^2 + dn\sigma^2 + n\sigma^2_{D(O)}$
Days (d) within Operators D(O)	o (d – 1)	$MS_{D(O)}$	$\sigma^2 + dn\sigma^2$
Replicates (n) (R)	od (n –1)	MS_E	σ^2

Equation 4 – Formulas for the Calculation of R&R Parameters

$$\hat{\sigma}^2 = MS_E$$

$$\hat{\sigma}^2_{D(O)} = \frac{MS_{D(O)} - MS_E}{n}$$

$$\hat{\sigma}^2_O = \frac{MS_O - MS_{D(O)}}{dn}$$

$$\hat{\sigma}^2_{repeatability} = \hat{\sigma}^2$$

$$\hat{\sigma}^2_{reproducibility} = \hat{\sigma}^2_{}$$

$$\hat{\sigma}^2_{process} = \hat{\sigma}^2_{D(O)}$$

The results of this phase are presented in Table 6

5.2.4.2.1 Results of Phase II

As a result of this analysis it was determined that both the variations of alloy chemistry and processing conditions and the operator's technique have a significant effect on the Al-Si Eutectic Growth Temperature.

These results prove that the AlTAS is sensitive enough to detect even small fluctuations in the chemistry of the alloy making it an excellent instrument for alloy quality control; however, the consistency of the test sample characteristics could be improved to better take advantage of its capabilities.

The mass, initial temperature and preheating conditions of the test sample are directly reflected in its cooling rate. The effect of cooling rate on temperature, time and fraction solid parameters is presented in the following section.

Table 6 – Results of ANOVA for Phase II of the R&R Study

Source of Variation	Degrees of Freedom	Mean Squares	F_0	P value
Operators (O) *(Reproducibility)*	1	113.91	42.16	0.0001
Days within operators D(O) *(Process)*	14	17.42	6.45	0.0001
Replicates (R) *(Repeatability)*	30	2.8		

For the range of chemical composition presented in Table 4, the calculation of Gauge Percent variation is presented in Table 7. According to this calculation 54% of the variation of the parameter $\Delta T^{Al\text{-}Si}_{E.G}$ was caused by elements of the AITAS (gauge), mainly the mass and temperature of the test sample. The ratio of gauge versus process variation presented in Table 7 indicates that the variation of the AITAS is greater than the variation of the process that is reflected in the AITAS parameter. However, while interpreting these results it must be kept in mind that the processing conditions established at WAP aim for a very narrow range of chemical composition without Sr or grain refiner additions. This makes process variation very small in comparison to typical processing conditions encountered in other foundries. To assess the

variation induced by the AlTAS over the complete range of chemical composition the Isoplot technique was used and the results are presented in the following section.

Table 7 – Calculation of Percent Gauge Variation for the Range of Chemical Composition Presented in Table 4

Phase II		
Variance Component	**Value**	σ
$\sigma^2_{reproducibility}$	4.02	2.005
$\sigma^2_{repeatability}$	2.702	1.643
σ^2_{gauge}	6.723	2.592
$\sigma^2_{process}$	4.09	2.214
$\sigma_{gauge}/\sigma_{process}$	117%	
$\sigma_{gauge}/\sigma_{total}$	54%	

5.2.4.2.2 Effect of Cooling Rate on Temperature, Time and Fraction Solid Parameters

Figure 14 presents the effect of cooling rate on temperature, time and fraction solid parameters. As indicated by their standard deviation, time and fraction solid parameters are affected by cooling rate while temperature parameters are more robust. For this reason, temperature parameters have better discrimination over various chemical compositions independently of the cooling rate of the test sample. The cooling rate of the test sample is determined by factors such as the test sample mass, the preheating time of the test cup inside the liquid metal, and the internal temperature of the AlTAS test stand.

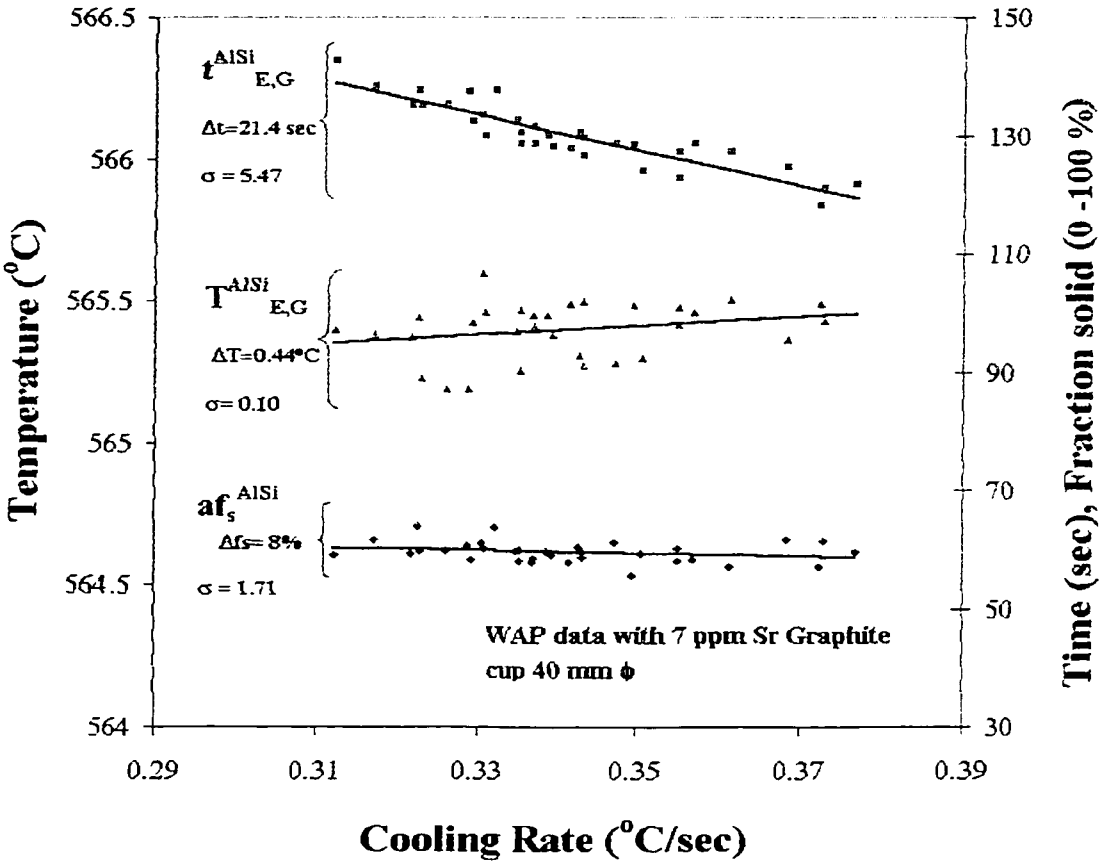

Figure 14 - Effect of Cooling Rate on Temperature, Time and Fraction Solid Parameters

5.2.4.3 Phase Three – Isoplots for Temperature, Time and Fraction Solid Parameters

In order to evaluate the repeatability of the AlTAS throughout the six levels of silicon particle modification established by the American Foundry Society, the cooling curves of samples obtained by Djurdjevic et al[18] were graphed in Isoplots along with the results of this study. This complementary data was obtained in experiments previously carried out at the University of Windsor using the AlTAS

The Isoplots are used to evaluate the capability of the AlTAS to discriminate between the different Si Modification Levels.

In the experiments of Djurdjevic et al[18] strontium additions ranging from 7 to 90 ppm were made

to the basic chemical composition presented in Table 8. The same graphite test cup, type of calibrated thermocouples, sampling procedure and analytical algorithms were used in those experiments and in the present work.

5.2.4.3.1 Construction of Isoplots

In Isoplots the X-axis represents the first measurements and the Y-axis the second measurements. If the data points fall close to a 45° line it means that the measurements are repeatable and the instrument can be considered accurate; the greater the deviation of the regression line of the measurements from a 45° line, the greater the bias of the instrument. The second step in the construction of Isoplots is to draw a boundary surrounding 95% of the measurement pairs. The length (L) of the boundary is then divided by its width (ΔM) and the larger the ratio of these two values, the better the precision and discrimination of the instrument.
The criteria presented in Equation 5 is used to determine whether a measurement instrument has adequate discrimination[45].

Equation 5 – Criteria to Evaluate the Discrimination Ratio of a Measurement Instrument[45]

Discrimination is good when:

$$\frac{\Delta P}{\Delta M} \geq 6$$

Where:

$$\Delta P = \sqrt{\frac{L^2}{2} - \frac{\Delta M^2}{2}}$$

Or:

$$\frac{L}{\Delta M} \geq 8.5$$

For each Si modification level at least two consecutive samples were used. The value of $\Delta T^{Al\text{-}Si}_{E.G}$ obtained from the thermal analysis of one sample was plotted against the value of the same parameter from the next sample. All consecutive samples were obtained from the same batch of

metal and within 15 minutes from the previous one to avoid fading of Sr. In the same manner, Isoplots for one time parameter ($t^{Al\text{-}Si}$) and one fraction solid parameter ($af_s^{Al\text{-}Si}$) were constructed. The three types of parameters have been proposed for the evaluation of Si modification. The corresponding Isoplots are presented in Figure 15, Figure 16 and Figure 17. These isoplots were also used to determine which of the parameters is the most robust for industrial conditions. The most robust is the temperature parameter.

5.2.4.3.2 Results of Isoplots

Based on the criteria presented in Equation 6, it was determined that temperature parameters are the most robust for industrial applications followed by fraction solid and lastly by time parameters. This was expected since time parameters are dependent on cooling rate, which is largely determined by the amount of metal in the test sample.

Table 8 – Chemical Composition of Samples Included in Isoplots[18]

Chemical Composition (wt %)										
Alloy	**Si**	**Cu**	**Fe**	**Mn**	**Mg**	**Ni**	**Zn**	**Ti**	**Sb**	**P**
319	7.55	0.39	3.45	0.23	0.32	0.008	0.009	0.122	0.052	0.001

To this basic chemical composition 0, 20,30, 50, 70 and 96 ppm of Sr were added (1 ppm = 0.0001 wt%). At least two samples for each level of Sr were plotted in the Isoplot.

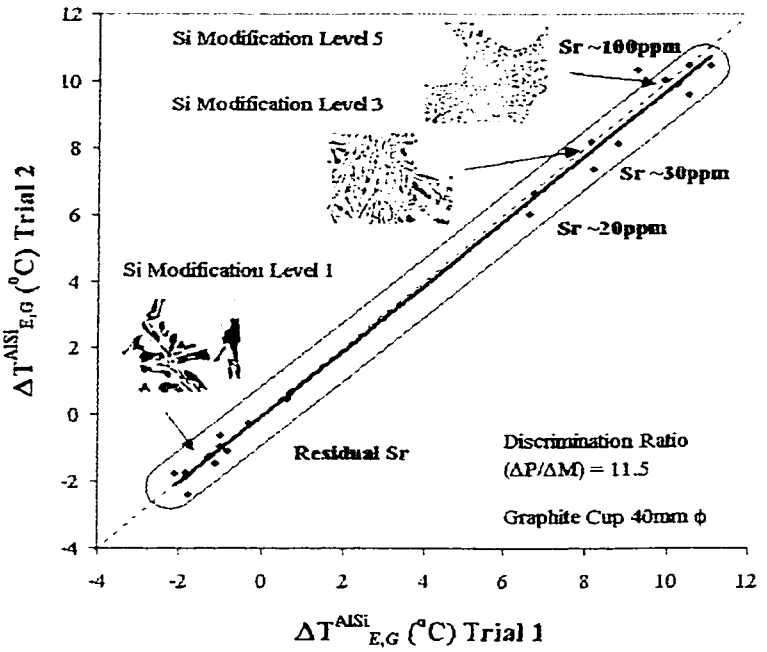

Figure 15 – Isoplot for a Thermal Analysis Temperature Parameter ($T^{Al\text{-}Si}_{E,G}$)

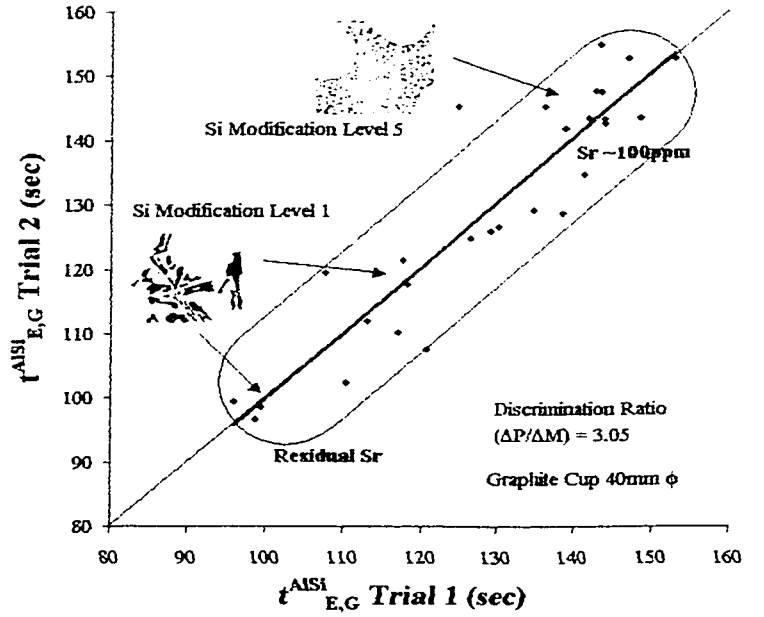

Figure 16 – Isoplot for a Thermal Analysis Time Parameter ($t^{Al\text{-}Si}$)

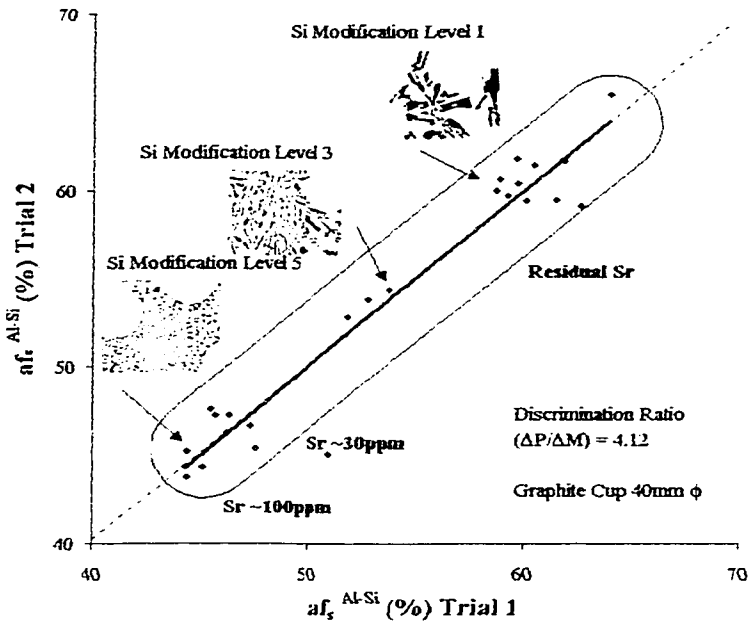

Figure 17 –Isoplot for a Thermal Analysis Fraction Solid Parameter ($af_s^{Al\text{-}Si}$)

5.3 Conclusions of R&R Study

The present R&R study clarified several aspects of the performance of the AlTAS:

a) The features of a cooling curve, its base line and its first derivative reflect minute changes in the chemical composition of the alloy, making the AlTAS a good system for alloy control. For larger variations in chemical composition (samples with different Sr levels) it was determined that temperature parameters offer adequate discrimination between the different Sr levels.

b) The traditional thermal analysis sampling method limits the applicability of fraction solid and time parameters in industrial environments due to their sensitivity to cooling rate, and therefore to the mass of the test sample. It was observed that the variability of the thermal analysis parameters and characteristic temperatures were operator dependent. Although the algorithms used by the AlTAS software were modified to improve the consistency of the results, further work is still necessary for the development of an automated sampling device that provides a better control of

the test sample mass and superheat (initial temperature). Such a device is currently being tested in the IRC laboratory.

c) All the facts learned during this study were incorporated into the AITAS knowledge base (described in the following Chapters) in order to prevent and identify faulty tests or warn of abnormal situations. These results were also considered during the acquisition of thermal analysis samples and actual engine blocks for the AITAS knowledge base.

CHAPTER 6

EXPERIMENTAL PROCEDURE

This Chapter describes the experimental procedure that was followed to obtain, analyze and interpret the samples and measurements that were later incorporated into the AlTAS Case Based Reasoning System. The results of this experimental work are also discussed.

6.1 Sampling Scenario for the Development of the CBR System

The development of the CBR system required the implementation of the AlTAS at the Ford Windsor Aluminum Plant (WAP) in order to obtain, for their established process conditions, a preliminary mapping of the values of the AlTAS parameters with the mechanical properties and microstructure of the critical sections of the engine blocks produced there. This mapping was then used by the CBR system for the prediction of mechanical properties and microstructure characteristics.

Given the high cost associated with interfering with the process by changing process parameters or alloy chemistry, the present work was limited to the chemical composition presented in Table 1 and to the standard process conditions at WAP. This method of sampling is known as observational study or passive data collection.

6.1.1 Observational Study

An observational study is a systematic approach to collect and analyze data in order to establish the current process or equipment performance[48]. This type of study is also termed passive data collection to denote that the data is gathered without making changes to the process beyond those that are part of normal production operation. The goal of this study was to establish the baseline performance of the ALTAS in an industrial operation, assessing the changes of the thermal analysis parameters that occur in response to process variation. This study would also yield initial control values for the thermal analysis parameters.

6.1.1.1 Experimental Procedure

The gauge study presented in the previous chapter set the criteria for ensuring that the measurements obtained in this study are adequate. To eliminate the operator-dependent variability, all the samples of this study were taken by the same operator who controlled the sample mass between 160 and 170 grams and ensured a preheating time of 20 seconds and an initial temperature of the sample between 700 and 720°C.
The samples were obtained during an eight-week period in order to capture the relevant sources of variability of the process.

The sampling procedure used in this study is the same described in Chapter 5. Table 9 describes the samples that were gathered simultaneously with the thermal analysis samples, it also includes the analysis performed on each type of sample.

6.1.1.2 Mechanical Testing

The tensile tests required for this work were performed at the Ford Casting Process Development Center. The standard procedures ASTM B-557 and ASTM E8-96 for mechanical testing were followed for the machining and tensile testing of the specimens. These specimens were removed from the bulkheads 2 and 3 of each casting, from the locations indicated in Figure 18. The tensile test bars had 2" gauge sections. The diameter of the gauge section was 0.505".

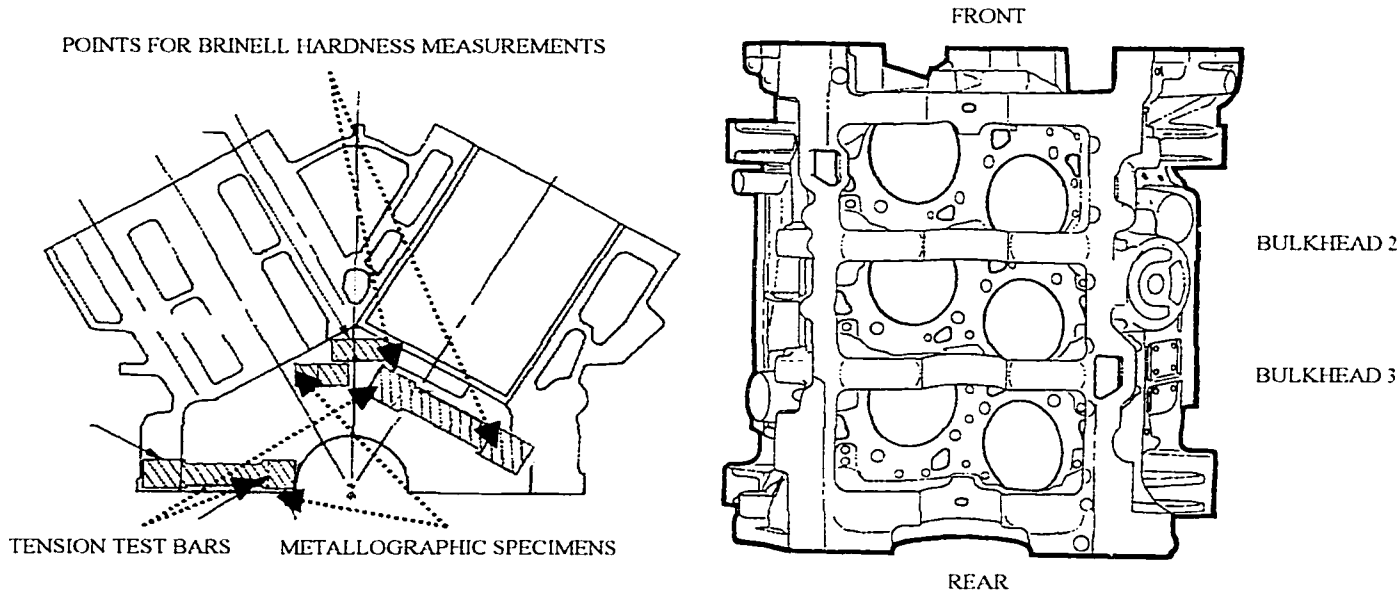

Figure 18 – 3.0L Engine Block Cross-Section Showing the Location of Test Specimens

Table 9 – Types of Samples and Analytical Procedure Used for the AlTAS Case Base

TYPE OF ANALYSIS	REQUIRED SAMPLES / DATA OBTAINED	TOTAL NUMBER OF SAMPLES
Mechanical and Metallurgical Characterization of 3.0L Engine Blocks.	Tensile test bars from Main Bearing Saddles (MBS) of bulkheads 2 and 3. (See Figure 18) *The Main Bearing Saddles are the sections with slowest cooling rate, and therefore critical areas of the casting.* a) 2% Yield strength, percent elongation and Ultimate Tensile Strength . b) Brinell hardness	80 samples
	Metallographic Specimens (See Figure 18 for locations) a) Silicon Modification Level b) Area Percent Cu phases c) Porosity	80 samples
	X-ray plates of bulkheads 2 and 3 to check for discontinuities in the microstructure.	5 plates
Thermal Analysis	Cooling curves, characteristic temperatures and parameters. Metallographic Specimens from test samples. a) Silicon Modification Level b) *Area Percent Cu phases* c) Porosity d) Vickers Hardness HV25	20 samples
Chemical Analysis	Optical Emission Spectrometry Samples (OES)	One per day of sampling (8)
Hydrogen Analysis	Melt temperature at the pump orifice and Hydrogen measurements.	24 measurements

6.1.1.3 Image Analysis Procedure and Microstructural Characterization

Metallographic samples were sectioned from both thermal analysis test samples and 3.0L engine blocks. In the thermal analysis samples, the specimens were cut from the centre of the sample, parallel to the thermocouple location. In the engine blocks, the specimens were obtained from the locations indicated in Figure 18 and mounted in cold mount resin. The specimens were prepared using standard grinding and polishing procedures on an automatic polisher to produce the surface finishing required by the Light Optical Microscope (LOM). A Leica 550IW Image Analysis System was used for this purpose. The system can be programmed to automatically scan and analyze a specified number of fields in the sample.

A description of the procedures used to characterize different features of the microstructure is presented in the following sections.

6.1.1.3.1 Measurements of Silicon Modification Level

The assessment of Silicon Modification Level is based on the American Foundry Society Chart for Microstructure Control in Hypoeutectic Aluminum Silicon Alloys, which classifies the range of modification into six levels (Figure 19). The objective of these measurements was to quantify the area fraction and modification level of the silicon particles. The perimeter of the silicon particles was measured using the LOM since it provides the best correlation with the AFS Silicon Modification Level[49].

Thirty fields were measured in each specimen using a 200X magnification. The step of the microscope was set to cover the total area of the sample. The results were statistically evaluated by the Leica Software to find the mean and standard deviation for each field and for the whole sample.

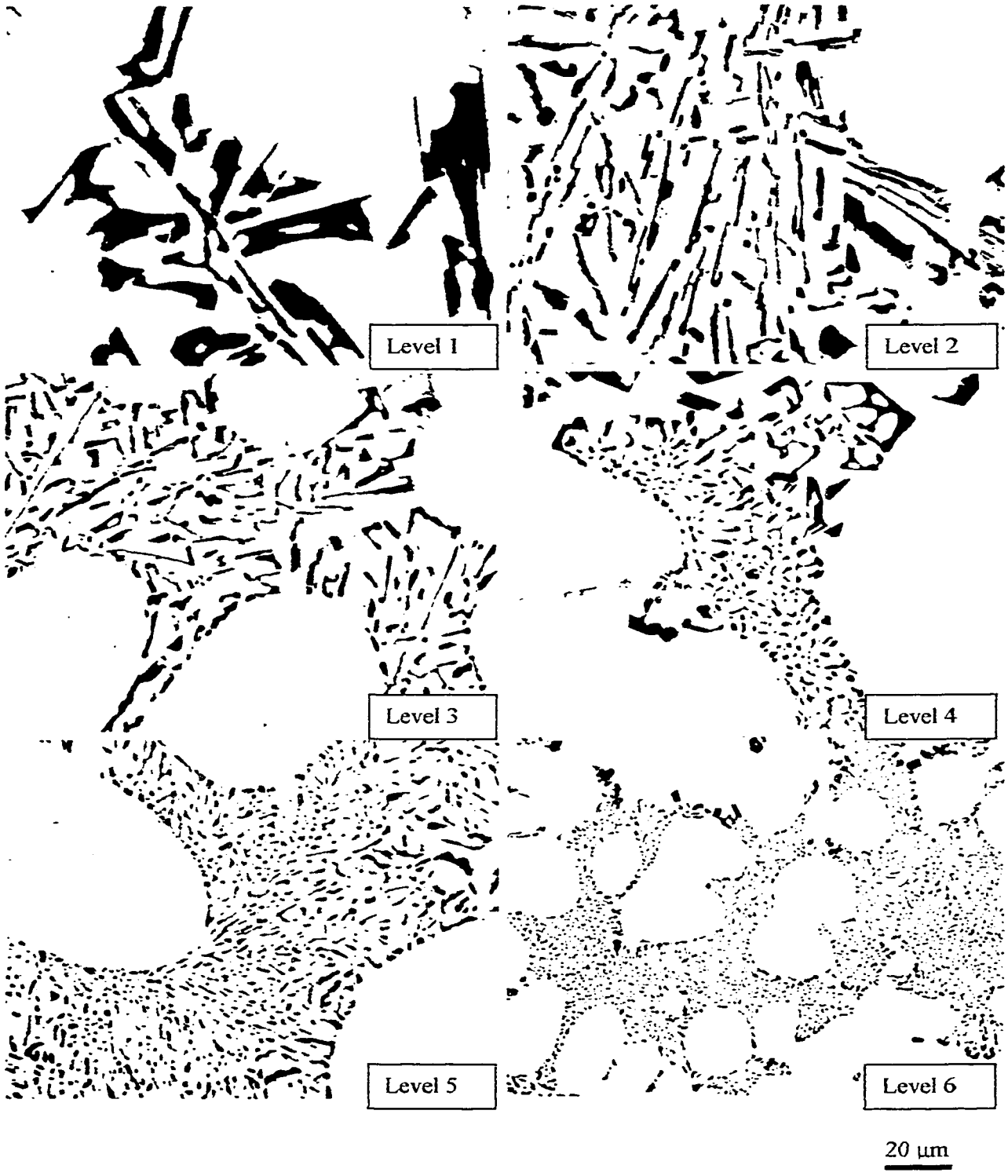

Figure 19 – Typical Morphologies of Si Structures Corresponding to the American Foundry Society Chart for Microstructure Control in Hypoeutectic Aluminum Silicon Alloys[49]

6.1.1.3.2 Measurement of the area fraction of Cu phases

To evaluate the area percent of Cu phases fifty fields from each specimen were measured at 500X magnifications. The parameter of interest was the total area fraction of the Cu phases. The mean and standard deviation were obtained for each field and for each sample; the results are summarized in Appendix II.

The $CuAl_2$ may be present in a blocky form or as a fine eutectic in which Si, $CuAl_2$ and β-AlFeSi coexist. In this work both Cu phases were considered.

6.1.1.3.3 Measurement of Porosity Area Fraction

For these measurements, fifty fields were measured at 100X magnifications. The area of the test sample that acts as a riser during solidification was not considered in the measurements. The same distance was consistently excluded in all the samples. The mean and standard deviation were obtained for each field; the results are summarized in Appendix II.

6.1.1.3.4 Microhardness Measurements

Vickers microhardness measurements were performed to characterize the α-Al matrix using a Buehler Micromet II system. The load of the indenter was set to 25 g and the load was applied during 15 seconds. A 40X objective was used to select the area of the indentation and perform the measurements.

Four measurements along each of five measuring lines were made in the central region of the image analysis samples. A Digimet system connected to the microhardness tester performed the calculations of microhardness, which are a function of the length of the two diagonals of each indentation. The mean and standard deviation of these observations were calculated. For the heat treated samples the homogeneity coefficient of the structure was calculated according to Equation 6[50] to evaluate the heat treatment cycle.

Equation 6 – Homogeneity of the Microstructure in Heat-Treated Samples Based on Microhardness Measurements[50]

$$HC = \left(\frac{(\sigma_{SAMPLE})^2 - (\sigma_{REFERENCE})^2}{(\sigma_{REFERENCE})^2} \right) \times 100$$

Where:

$\sigma_{REFERENCE}$- standard deviation of microhardness of reference sample

σ_{SAMPLE}- standard deviation of microhardness of samples after different heat treatment

6.1.1.3.5 Hydrogen Measurements

In order to measure the hydrogen level and the temperature of the melt the ceramic probe and thermocouple of an AISCAN Hydrogen Analyzer Unit were immersed in the holding furnace. One set of hydrogen and temperature measurements was completed for every thermal analysis sample collected.

6.2 Discussion of Results of the Observational Study

6.2.1 Effect of Low Melting Point Elements on Temperature Parameters

One of the objectives of the passive data collection was to detect the sources of variability of the process measured by the AlTAS.

Given the good control that is kept at WAP over metal processing and the weight percent of the main alloying elements of the melt, it was possible to observe a relationship between the level of two low melting point elements of the alloy, namely Pb and Sn, and the temperatures of the Dendrite Coherency Point ($T^{\alpha\text{-}DEN}{}_{COH}$) and Al-Si Eutectic Growth ($T^{AlSi}{}_{E.G}$).

The data was separated chronologically into two periods:

- June to July 1999, which corresponds to the R&R study
- February to May 2000, which corresponds to an intermediate monitoring period and the sampling time for the CBR system.

During these periods, it was observed that the content of Pb varied from 80 ppm (0.008 wt%) to 250 ppm (0.0250 wt%) while all the major alloying elements were kept at constant levels. From June – July 1999 the level of Sn remained constant at 20 ppm (0.002 wt%) whereas it varied from 20 to 60 ppm during February to May 2000.

The interactions of these two elements reflected on $T^{\alpha\text{-}DEN}{}_{COH}$ and $T^{AlSi}{}_{E.G}$ are presented in Figure 20 and Figure 21. According to Figure 20 Pb has the effect of postponing dendrite coherency and increasing the level of Sn in the melt further enhances this effect. Figure 21 shows a similar behaviour for the Al-Si eutectic temperature, however, when the level of Sn is increased the relationship is no longer observed. After analysing the level of Fe in both periods it was determined that Fe had a stronger influence on the behaviour of $T^{AlSi}{}_{E.G}$ than Pb and Sn during this period (Figure 22).

Although a definite trend can be observed in these two temperature parameters, this variation did not have an effect on the tensile properties or hardness of the castings. This was expected since this minor effect can be obscured by other factors such as metal cleanliness, cooling rate, level of major alloying elements or riser efficiency which determine the feeding conditions of the alloy.

Nevertheless, this result verifies that the AlTAS can be used not only to verify the level of the main alloying elements in the melt, but also the presence of impurity elements.

Such relationships have not been reported in the literature and further investigation is recommended to understand possible interactions during the evaluation of grain refiners, modifiers and feeding efficiency via thermal analysis.

These relationships account for the significant process variation reflected on $T^{AlSi}_{E.G}$ that was detected during the R&R study.

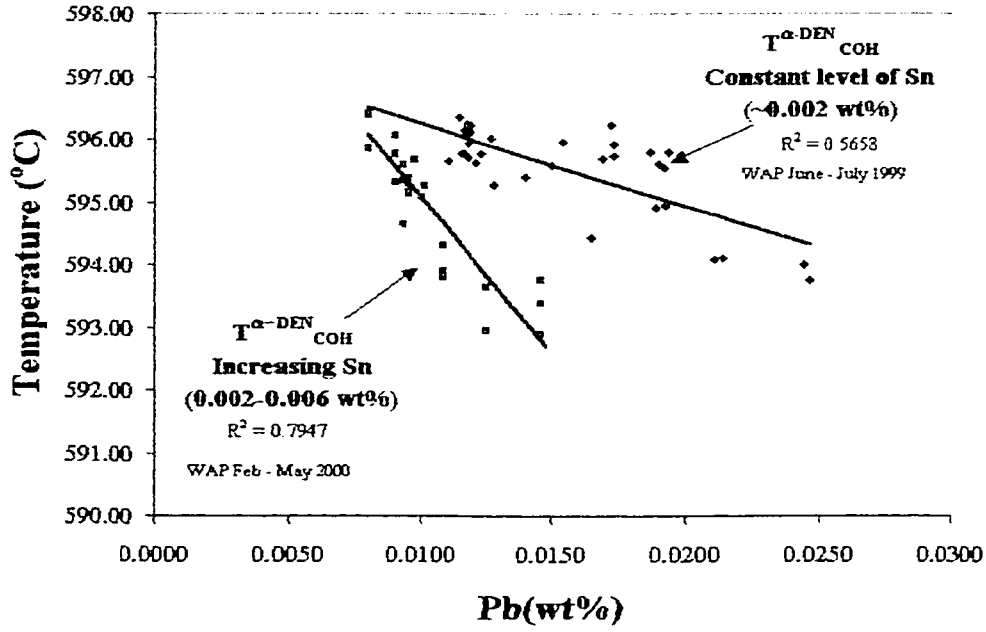

Figure 20 – Effect of Pb Content on Coherency Temperature for Various Sn Levels

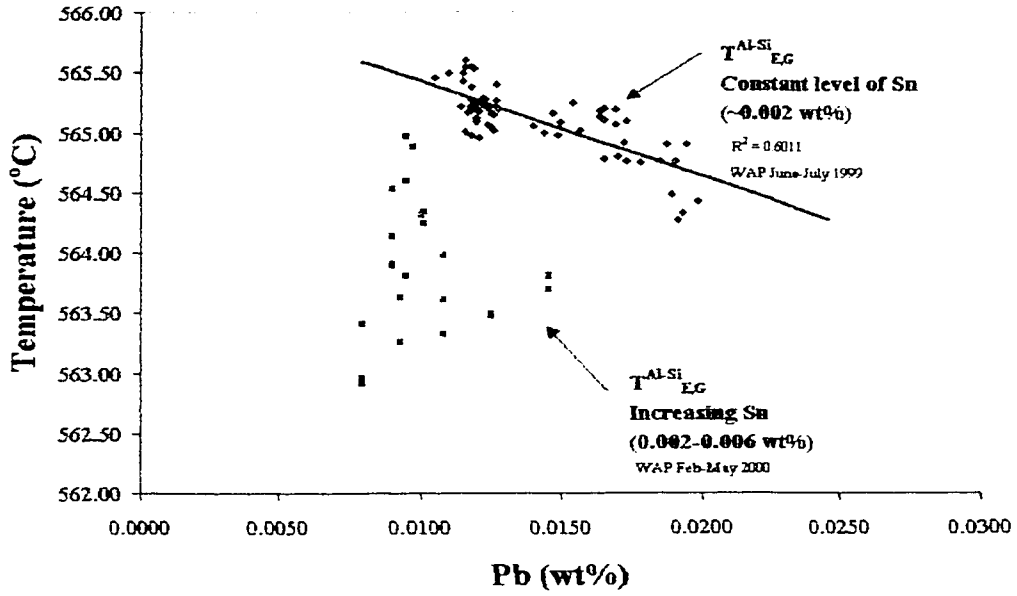

Figure 21 - Effect of Pb Content on Al-Si Eutectic Growth Temperature for Different Sn Levels

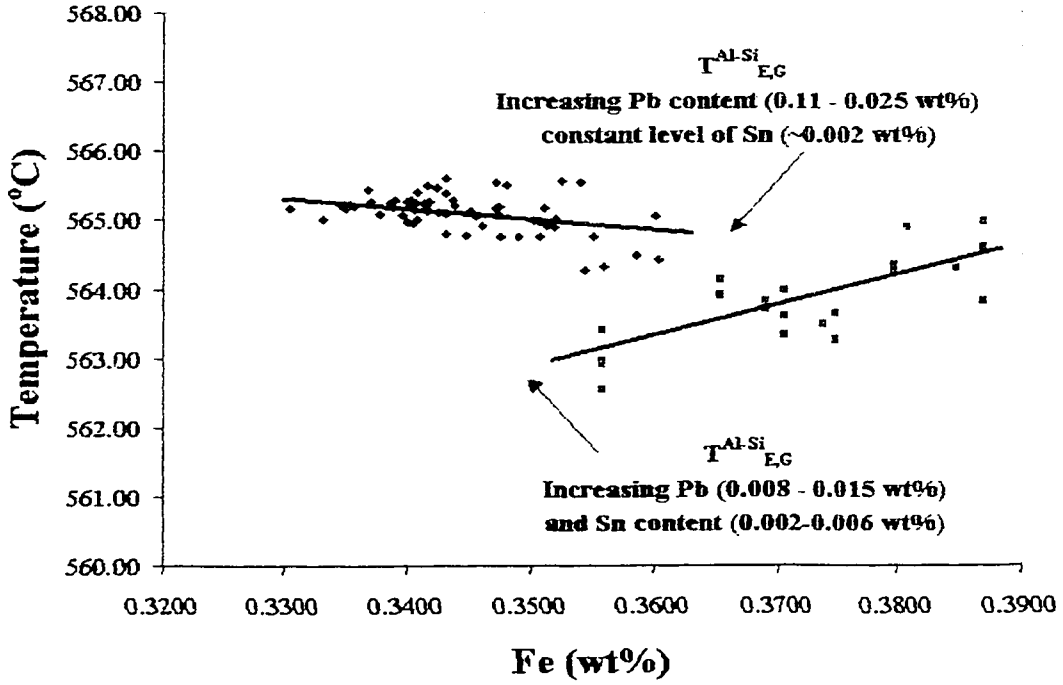

Figure 22 – Effect of Fe on the Al-Si Eutectic Growth Temperature

6.2.2 Cu Reactions

During this study two characteristic shapes of the copper reaction of the cooling curves and their first derivatives were found. Image analysis of the corresponding samples showed different proportions of Cu phases in both groups of samples (Figure 23). In the samples corresponding to cooling curve type A the copper solidified mainly as large deposits of $AlCu_2$ with interspersed α-Al, small number of blocky $AlCu_2$ and fine $Al_5Mg_8Cu_2Si_6$ eutectic deposits was observed. In the samples corresponding to cooling curve type B (prolonged solidification of Al-Cu eutectic) the situation was reversed, the fine $Al_5Mg_8Cu_2Si_6$ eutectic being the most abundant phase.

The difference in chemical composition between both groups of cooling curves is the level of low melting point elements described in the previous section. Samples with higher levels of low melting point elements present a prolonged solidification range of the Cu reaction.

This effect could be further investigated to help monitor and establish optimum solution treatment cycles.

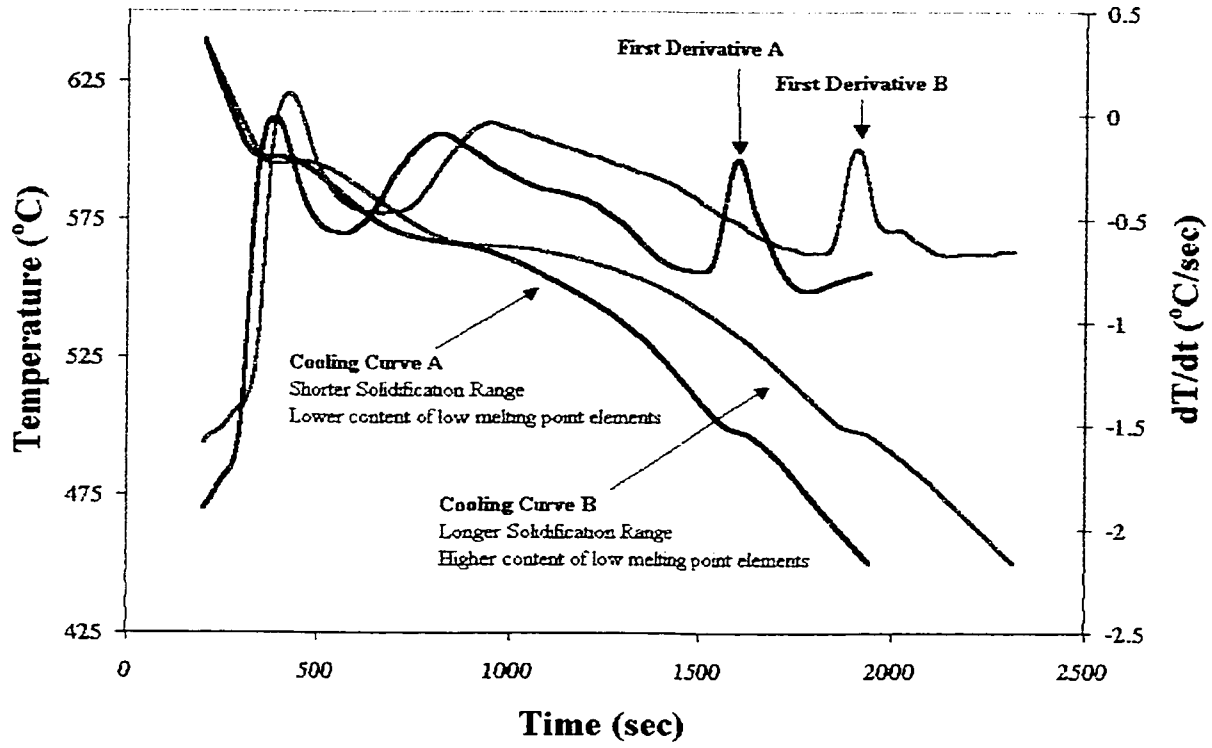

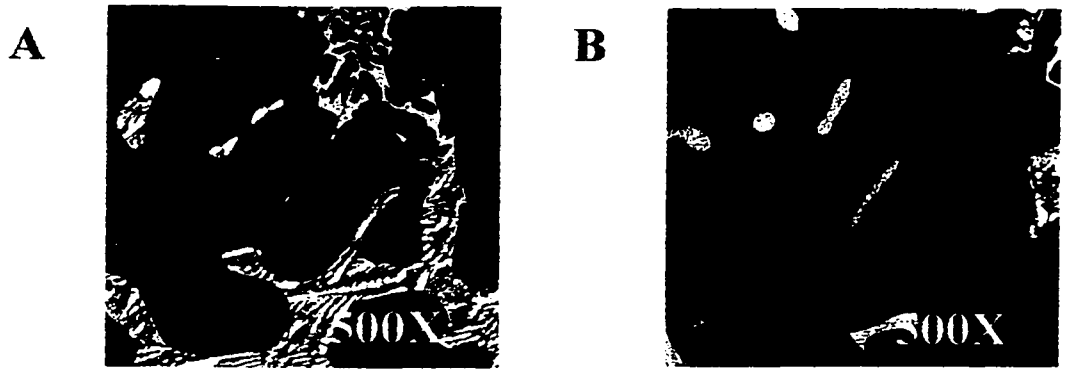

Figure 23 – Two Distinct Shapes of Cu Based Reactions Corresponding to Different Proportions of $AlCu_2$ and $Al_5Mg_8Cu_2Si_6$

6.2.3 Confidence Intervals of the Thermal Analysis Parameters.

Table 10 contains the 95% Confidence Intervals (CI) for the main TA parameters and characteristic points calculated using the statistical software SPSS®. These intervals were obtained using 50 samples with mass in the range 160-180 g and maximum temperature 660 – 696°C, the cooling rate was between 0.27 and 0.41 °C/sec. The data was collected between July 1999 and February 2000. The parameters were obtained using the two-thermocouple method.

Table 10 – 95% Confidence Intervals for the Main Thermal Analysis Parameters and Characteristic Temperatures.

Parameter	Mean	Std. Deviation	CI for mean	
			Lower Bound	Upper Bound
T^{LIQ}	605.05	3.85	604.13	605.97
T^{LIQ}_{MIN}	595.79	0.50	595.65	595.93
T^{LIQ}_{PLAT}	596.44	0.46	596.31	596.57
T^{COH}	596.16	0.52	596.01	596.31
t^{COH}	32.67	2.12	32.07	33.27
$T^{Al\text{-}Si}_{NUC}$	571.56	2.06	570.97	572.14
$T^{AlSi}_{E,G}$	565.39	0.33	565.30	565.48
T^{AlCu}_{NUC}	505.86	1.01	505.57	506.14
T^{SOL}	473.33	7.97	471.07	475.59
$af_s^{\alpha\text{-}DEN}{}_{IDF}$	20.55	2.00	19.98	21.12
$t^{Al\text{-}Si}{}_{UNDERCOOLING}$	33.89	6.13	32.16	35.63
$\Delta T^{Al\text{-}Si}{}_{E.G}$	-2.89	0.33	-2.98	-2.80
$\Delta T^{Al\text{-}Si}{}_{SRAN}$	65.70	1.97	65.14	66.26

6.3 Sequential Test of Significance

A sequential test of significance[51] was used to determine that sufficient samples had been collected. This is a test applied to determine whether a definite conclusion has been reached from an experiment, or whether more observations are needed. In the context of this project the test was used to determine whether enough variation was captured in the samples from WAP to avoid redundancy of cases in the case base.

The test decides as every new observation becomes available whether a Null Hypothesis that no change of importance has occurred can be accepted, an Alternative Hypothesis that a real change has occurred can be accepted or to continue taking observations.

For every new observation recorded a function of all the observations is plotted against the number of observations. The resulting plot is formed by boundary lines, the position of which is determined by the risks α and β of errors type I and II, and by the observations in terms of a test statistic U. Originally the procedure is designed for single-sided tests but it can be modified for double-sided tests by superimposing two single-sided tests in each of which the error type I is set to $\frac{1}{2}\alpha$ and the deviation that is desired to detect (D) is taken to be positive in one test and negative in the other.

In the upper zone of the chart the hypothesis that a real change has occurred is accepted, in the center zone the hypothesis that no important change has occurred is accepted and in the lower zone the hypothesis that a real decrease has occurred will be accepted.

The test statistic is calculated as follows. Equation 7 was developed for the case when the standard deviation of the process is unknown. The boundary lines are calculated based on predetermined tables[51] which are accessed using the deviation D and the values of α and β.

Equation 7 – Test Statistic for a Sequential Test of Significance[51]

$$U = \frac{T}{\sqrt{S}}$$

$$T = \sum (x - \mu_0)$$

$$S = \sum (x - \mu_0)^2$$

Where:

T is the sum of deviations from the standard value

S is the sum of squares

For the calculation of the chart presented in Figure 24 the following values were used: D=2 (two standard deviations from the mean value), α=0.01 and β=0.05. A value of μ_0=563.8°C resulted from the samples and σ= 0.59.

Based on this plot it was determined that the variation in the liquid metal was not sufficient and sampling was stopped to avoid redundancy in the case base. The samples were colleted over 6 different days in 8 weeks. A similar behavior was detected in other thermal analysis parameters.

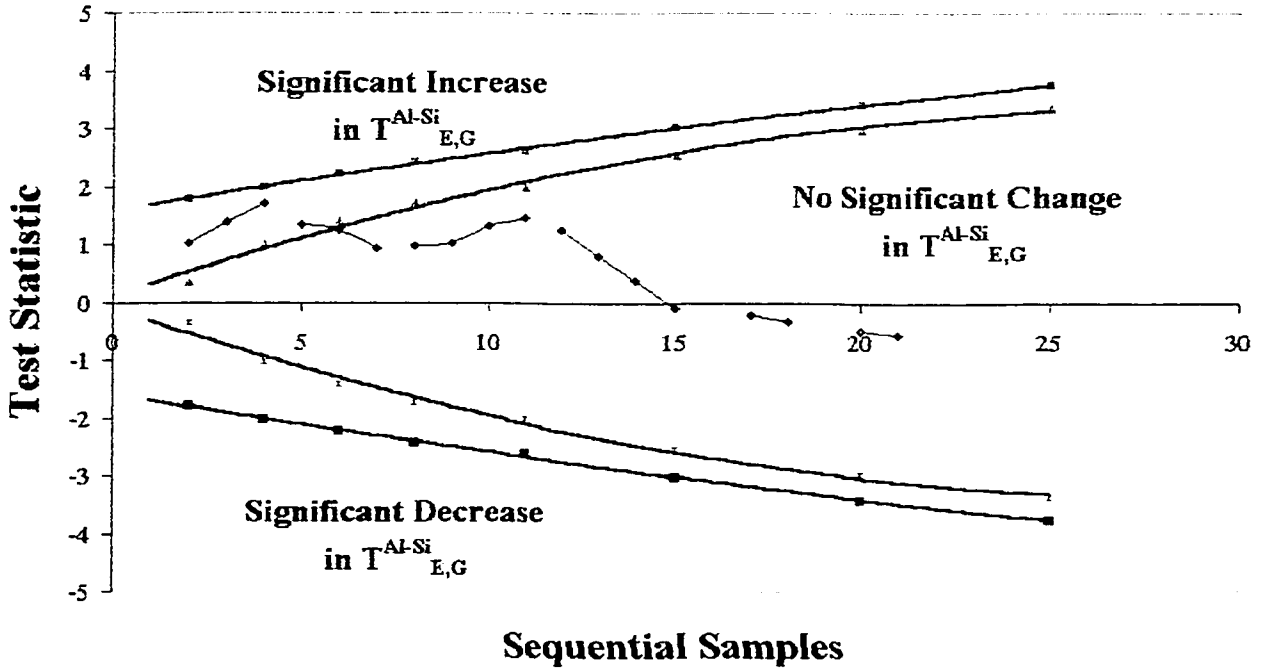

Figure 24 – Sequential Test of Significance for the Parameter $T^{Al\text{-}Si}_{E,G}$

CHAPTER 7

DEVELOPMENT OF THE STATISTICAL PROCESS CONTROL MODULE

During the development of this project the author envisioned the AlTAS as an integral system for quality control which would be able not only to test the metal and predict the outcomes of the process for given characteristics of the alloy, but also to prevent deviations in the chemical composition which would be detrimental to the quality of the casting if they were left unattended. For this purpose, a Statistical Process Control (SPC) Module was developed. The control charts plotted by the system can advise the user about trends in the process and emit an alarm if an out of control situation occurs. After this statistical analysis the results are transferred to the Case-Based System for the prediction of casting properties. The development of the SPC module will be explained in this chapter.

7.1 Introduction

Statistical Process Control is a collection of problem-solving tools for monitoring and improving process capability (scatter in the process in relation to the desired specification limits) through the control and reduction of variability.

These tools help to differentiate between natural variability of the process caused by "chance causes" and non-random variability caused by "assignable causes", such as defective materials, machine failures, etc.

The main objective of SPC is to quickly detect the occurrence of assignable causes of process shifts so that investigation and corrective actions can be taken before nonconforming units are manufactured [52]. Control charts are used for this purpose.

A control chart is formed by:

a) Lower and Upper Specification Limits – Usually set at $\pm 3\sigma$

b) A Centre Line – Set to the estimate of the mean of the process.

c) Observations – Connected by a line to visualize their evolution over time.

For a process to be "in control" most of the production must fall between the Upper and Lower Control Limits and the points must follow a random manner. Several rules such as the Western Electric Rules, or Nelson Rules[53] have been developed to assist in the search for non-random patterns in control charts and determine "out of control" conditions.

A point plotted on a control chart represents a test of the hypothesis that the mean value of the sample is equal to the established mean of the process (H_o: $x = \mu_o$). A point plotted within the control limits represents the failure to reject the hypothesis of statistical control.

The use of control charts for variables involves plotting two charts at the same time: one control chart to monitor the behaviour of the process mean and one chart to measure the variability of the process.

Important factors to determine during the design of a control chart are:

a) Selection of control limits – depending on the desired magnitude of type I and type II errors. As control limits get wider, type I error decreases (a point falling outside control limits when no assignable causes are present) but error type II increases.

b) Sample Size – in our case due to the nature of the process it is set to one sample.

c) Frequency of Sampling – Once per shift if no modifiers are added to the melt.

d) Performance of the control chart – evaluated by the average run length (average number of points to be plotted before an out of control condition occurs).

7.2 Assumptions of Control Charts

Two elemental assumptions in control charts for variables are the normality and independence of the data.

7.3 Normality

Regarding normality, several authors[52,53] have concluded that the normal control limits, with an adequate sample size ($n \geq 4$) are quite robust unless the population is extremely nonnormal. In the case of range control charts, they are more sensitive to normality than the average (x-bar) charts. Exponentially Weighted Moving Average and CUSUM charts are not sensitive to the normality of the data.

7.3.1 Normality of AlTAS Data

During the repeatability and reproducibility study presented in Chapter 5, it was not possible to make conclusive remarks about the distribution followed by the AlTAS parameters. However, its distribution appears to be close to normality as shown in Figure 25.

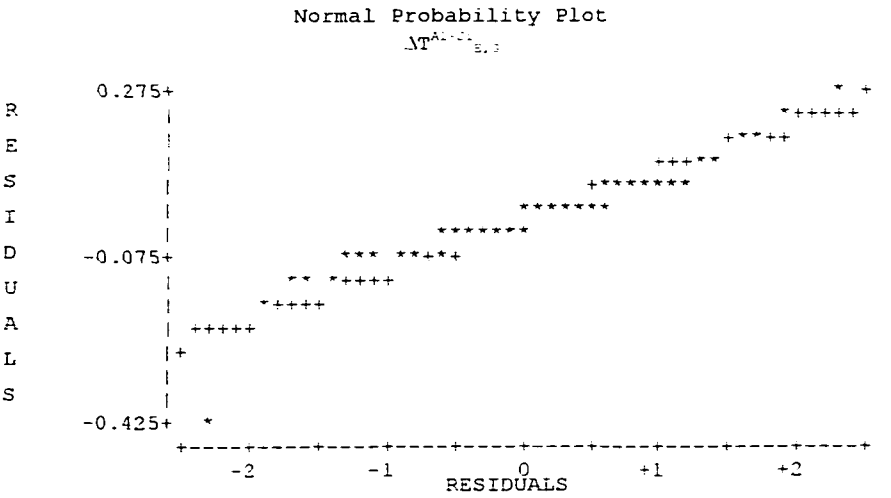

Figure 25 – Normal Probability Plot for $\Delta T^{Al\text{-}Si}_{E,G}$ Values Obtained During this Study.

7.4 Independence of Observations

More important than normality is the independence of the data points plotted in the control charts. If the data is autocorrelated, too many out of control alarms will be given (shorter in-control Average Run Length), jeopardizing the credibility of the control charts[52].

This assumption is usually violated in manufacturing processes, especially in chemical and batch processes where the measurements are made in the order of production. In such processes, the autocorrelation of the variable has an inverse relationship with the time between consecutive measurements and it can be quantified by the autocorrelation function (ρ_k) and the sample autocorrelation function (r_k).

Equation 8 – Autocorrelation Function (ρ_k) and Sample Autocorrelation Function (r_k)

$$\rho_k = \frac{Cov(x_t, x_{t-k})}{V(x_t)} \qquad r_k = \frac{\sum_{t=1}^{n-k}(x_t - \bar{x})(x_{t-k} - \bar{x})}{\sum_{t=1}^{n}(x_t - \bar{x})^2}$$

To evaluate the autocorrelation between measurements, the coefficient r_k is plotted for several consecutive lags (observations that are k periods apart from each other). If the value of this coefficient exceeds its 2σ limits, the observations are considered autocorrelated.

7.4.1 Independence of AlTAS Data

Previous process measurements done with the Alu-Delta™ system were tested for autocorrelation and a relatively high autocorrelation coefficient (r_k = 0.45) was obtained using the statistical software SPSS®.

This coefficient was also calculated for several AlTAS parameters and it was in the range $0.4 < r_k > 0.8$ –Table 11 for k = 1.

The mean values of the AlTAS parameters are another indication of autocorrelation. These values drift slowly over time instead of remaining at a constant value (Figure 26– Control chart for individuals). This is an inherent characteristic of the continuous liquid metal treatment process.

7.4.1.1 Dealing with Autocorrelated Data

To avoid the negative effect of autocorrelation on the performance of the control charts it is recommended to obtain one sample every eight hours. Sampling an unmodified melt in this time interval will control the autocorrelation of the measurements.

If during future implementations of the system the proposed schedule does not eliminate the

effects of autocorrelation the calculation of the charts can be modified to a special EWMA procedure for autocorrelated data based on the residuals of the observations[54,55]. This procedure is also recommended for modified melts, which require more frequent sampling.

Table 11 – Autocorrelation Coefficients for Several AlTAS Parameters (Sampling Frequency: 2 hours)

Parameter	r_1	Number of Autocorrelated Lags
$T^{\alpha\text{-}DEN}_{NUC}$	0.9	13
$T^{\alpha\text{-}DEN}_{MIN}$	0.8	13
$T^{\alpha\text{-}DEN}_{G}$	0.8	12
$T^{\alpha\text{-}DEN}_{COH}$	0.7	12
T^{AlSi}_{NUC}	0.9	13
T^{AlSi}_{G}	0.65	10
T^{AlCu}_{NUC}	0.7	9
T_{SOL}	0.55	9

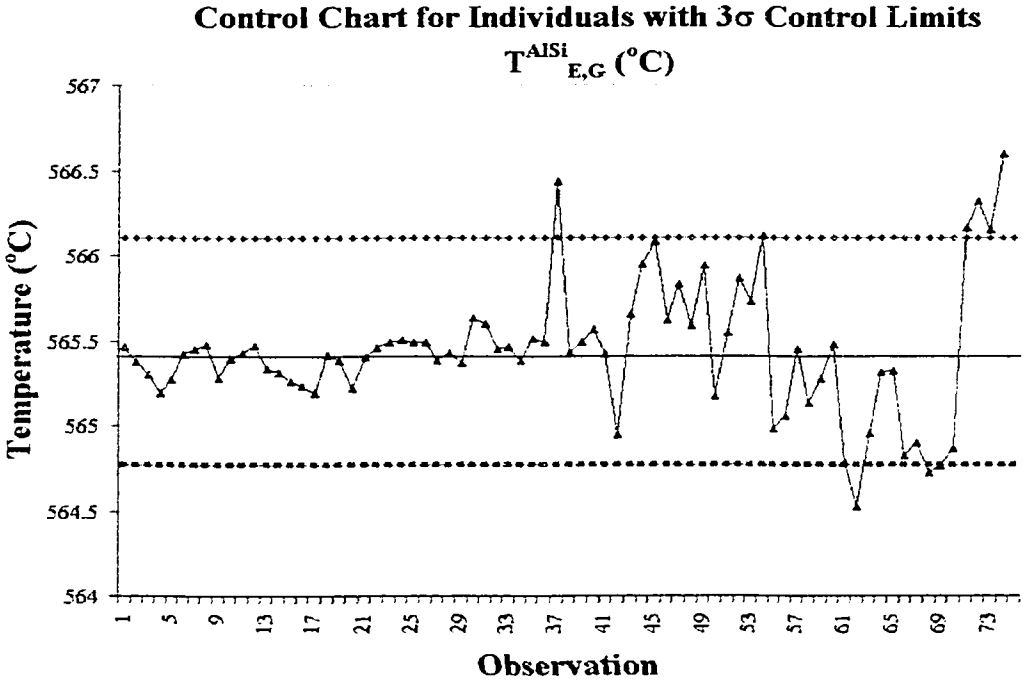

Figure 26 – Control Chart for Individuals for the Parameters $T^{Al\text{-}Si}_{E,G}$

7.5 Statistical Process Control for the AlTAS

The AlTAS SPC Module was developed using the National Instruments Labview™ Software, the module was added as a component of the original AlTAS software.

In the AlTAS SPC Module it is possible to select up to three of the thermal analysis parameters for plotting. The default parameters are:

a) $T^{AlSi}_{E,G}$ – Indicator of silicon modification

b) $a_{fs}{}^{\alpha\text{-}DEN}_{IDF}$ – Indicator of feeding efficiency

c) T_{SOL} – Indicator of the solidification range of the alloy

Since a relatively long time is necessary to complete an AlTAS test (as a result of the slow cooling rate of the test sample) and the results of consecutive samples would differ only due to sampling error, a sample size = 1 is adequate for the AlTAS Control Charts.

CUSUM charts, Exponential Weighted Moving Average (EWMA), Moving Average and Individuals are common procedures for plotting such charts. The difference between them lies in

the magnitude of the variation that can be detected effectively and their sensitivity to the underlying assumptions (normality and independence).

In the AITAS two control chart schemes were implemented:

1. ***EWMA Charts*** are useful in detecting small shifts in a process and are not based on the assumption of a normal distribution of the data. The effects of autocorrelation can be avoided if sufficient time is allowed between the samples plotted in the SPC Module.
2. ***Moving Average and Moving Range Control Charts*** were also implemented. This allows calculating an average of all the samples obtained in one production shift or any desired time interval. This type of chart can also be useful in detecting large changes in the process, depending on the number of samples used in the average. For these charts the following rules were implemented:

A: Sets of points falling outside three standard errors.

B: Eight consecutive points on one side of the centre line.

C: Six points steadily increasing or decreasing.

7.5.1 Design of EWMA Control Charts

The design parameters for EWMA charts are [52,56]:

L – is a multiple of the standard deviation

λ – is a constant $0<\lambda\leq 1$

The parameters L and λ are selected so that the desired Average Run Length performance can be obtained. Predetermined tables that include different values of these parameters and the expected performance of the charts are available in the literature[56].

The Exponentially Weighted Moving Average statistic and the control limits are defined by the following equations:

Equation 9 – Formulas for the Calculation of Center Line and Control Limits of the Exponential Weighted Moving Average (EWMA) charts[52]

$$z_i = \lambda x_i + (1-\lambda) z_{i-1}$$

$$z_0 = \mu_0$$

$$UCL = \mu_0 + L\sigma\sqrt{\frac{\lambda}{(2-\lambda)}\left[1-(1-\lambda)^{2i}\right]}$$

$$CL = \mu_0$$

$$UCL = \mu_0 - L\sigma\sqrt{\frac{\lambda}{(2-\lambda)}\left[1-(1-\lambda)^{2i}\right]}$$

7.5.1.1 Selection of Parameters λ and L

The Average Run Length of a control chart represents the number of points that must be plotted before the chart indicates an out of control condition. In processes that change quickly over time it is desirable to have a low ARL so that the change will be detected promptly. When the process is in control a large ARL is desirable so that few false alarms are emitted[54]. The ARL is determined by the values of two parameters: the smoothing parameter λ, ($0 \leq \lambda \leq 1$) and the standard deviation multiplier L.

For different ARL performance Lucas and Saccucci[56] provide tables of "optimal" λ and L parameters for specified in-control ARL and shift in the process. Using these tables, the default values of these parameters in the AITAS were set to $\lambda = 0.10$ and $L = 2.814$. These values yield a steady state ARL = 492. These values allow detecting shifts in the process lower than 0.25σ.

7.5.2 Design of Moving Average and Moving Range Control Charts

Predefined functions in the Labview™ Software were used for the development of this module. The following functions are used for calculation of the statistics and limits of the control charts.

Equation 10 – Formulas for the Calculation of Center Line and Control Limits of the Moving Range and Moving Average Control Charts[52]

$$M_t = \frac{\bar{X}_t + \bar{X}_{t-1} + \ldots + \bar{X}_{-w+1t}}{w}$$

$$CL = \bar{\bar{X}}$$

$$UCL = \bar{\bar{X}} + 3\frac{\sigma}{\sqrt{nw}}$$

$$LCL = \bar{\bar{X}} + 3\frac{\sigma}{\sqrt{nw}}$$

$$\hat{\sigma} = \frac{\bar{R}}{d_2}$$

Where

t is the size of the time step

w is the width of the moving average

X is the average of a sample size n

7.5.2.1 Interpretation of Tests

Table 12 includes the interpretation of the tests used to evaluate the Moving Average Charts. In moving average charts, the plotted points are not independent of each other. The points are interrelated through a "distance" that depends on the number of samples used for the averages. This must be kept in mind while interpreting the alarms. As a result of the averaging procedure a sudden shift in the mean shows up first in the MR chart. Changes of short duration may be shown only on the MR chart and not in the MA chart.

Table 12 – Interpretation of Run Rules and Tests Included in the AITAS Software.

Description of Test	Interpretation
One point beyond 3 standard deviations.	This signals a shift in mean, standard deviation or single outlier in the process. The R chart can be used to verify an increase in variation.
Six points in a row steadily increasing or decreasing	Detects a trend or drift in the process mean. Small trends are signaled by this test before the previous test.
Eight points in a row alternating up and down	Detects systematic effects or cyclic pattern such as alternating machines, operators, etc.

7.5.3 EWMA Control Charts

The diagram in Figure 27 shows the procedure followed in the calculation of these charts:

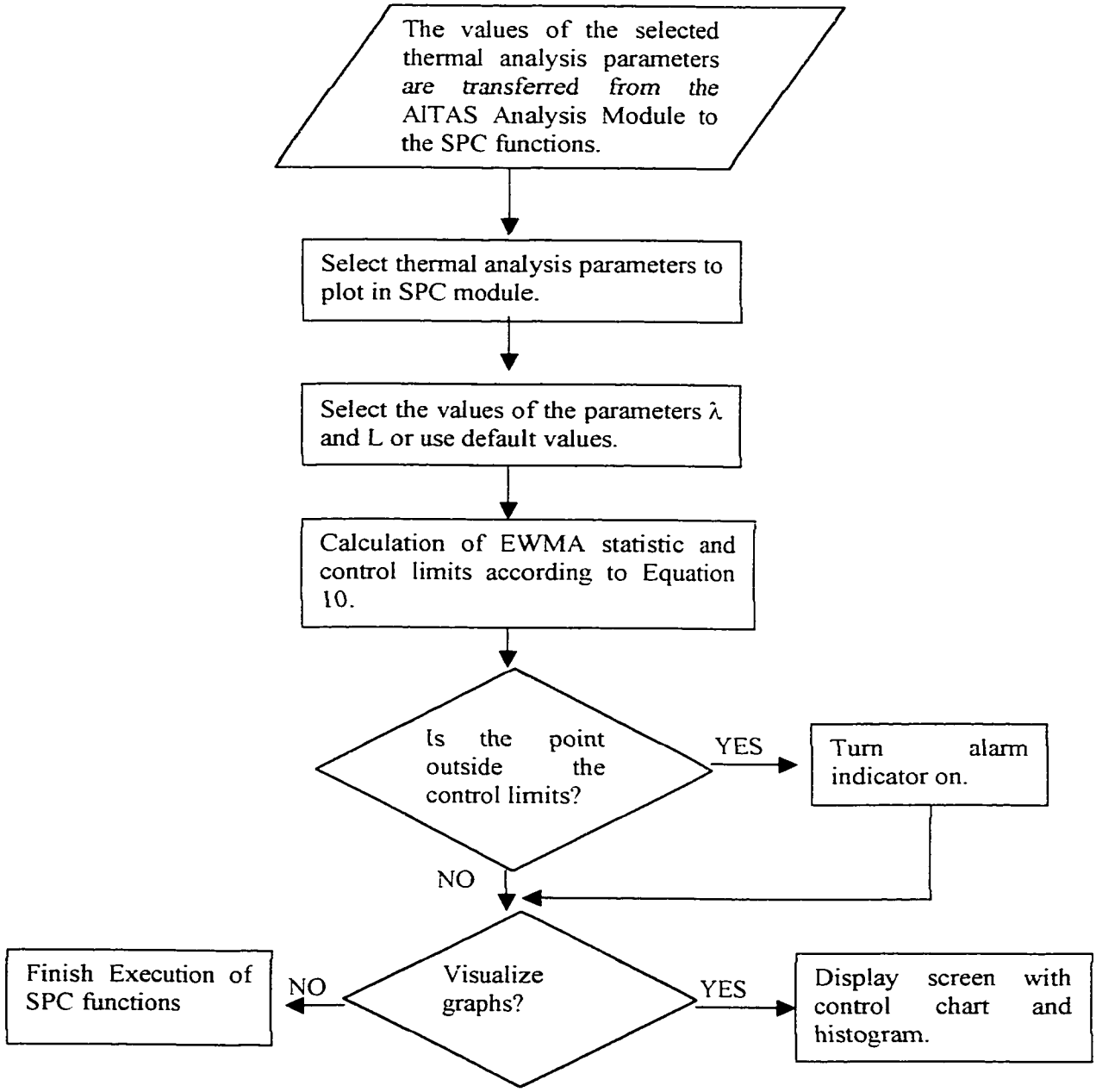

Figure 27 – Procedure for Calculation of EWMA Control Charts

7.5.4 Moving Average and Moving Range Control Charts

The diagram in Figure 28 shows the procedure followed in the calculation of these charts:

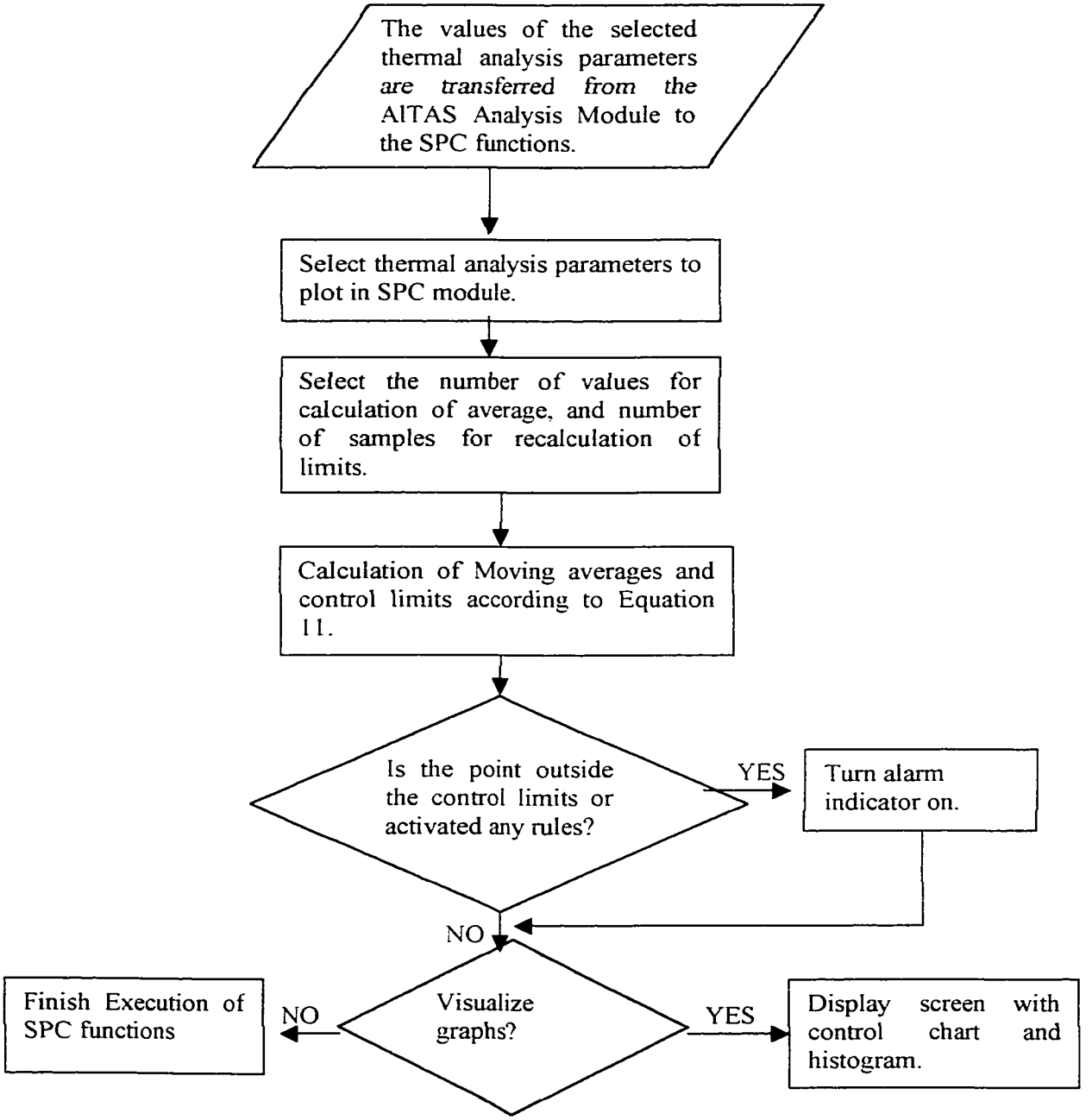

Figure 28– Procedure for Calculation of Moving Average and Moving Range Control Charts

7.5.5 User Interface

Figure 29 and Figure 30 present the screens of the AlTAS SPC Module.

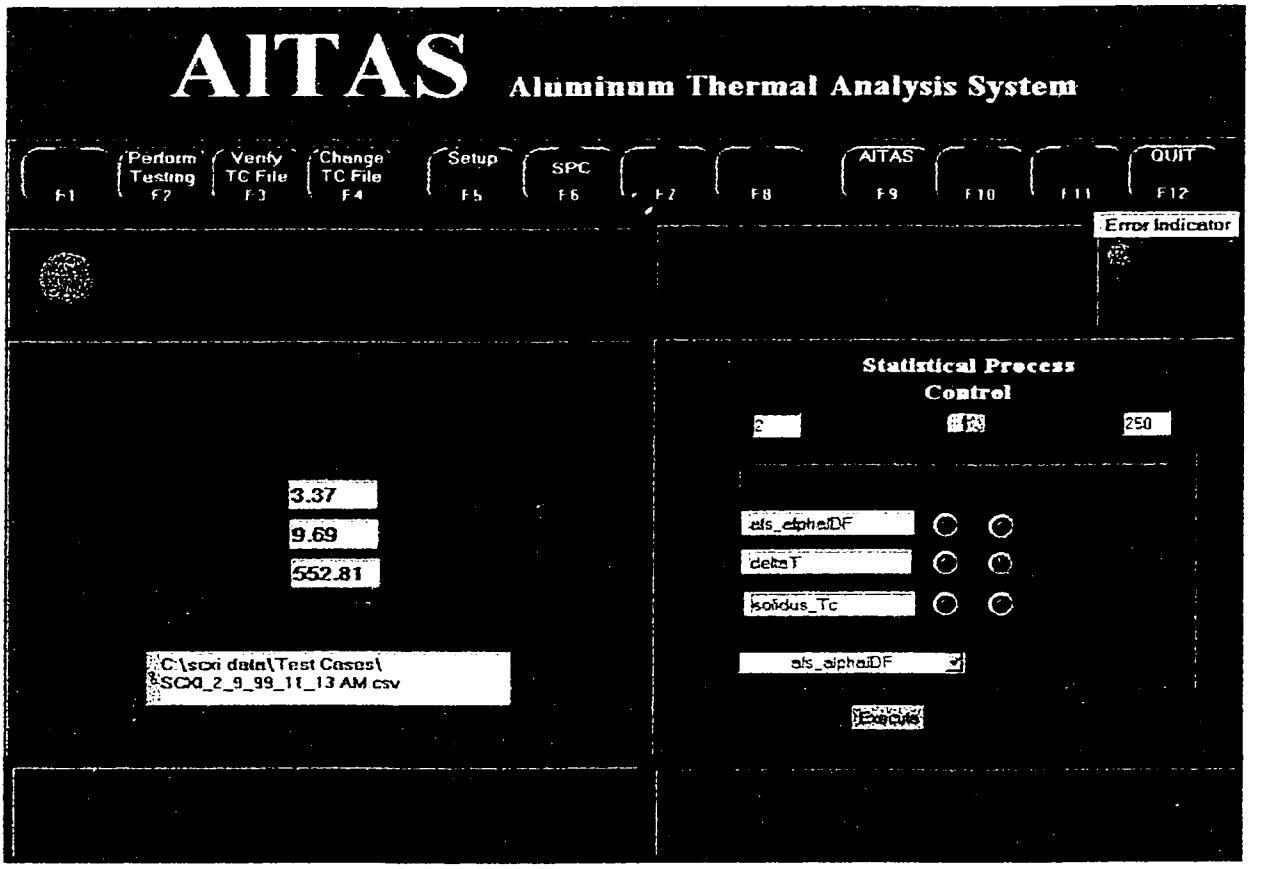

Figure 29 – Main Screen of the AlTAS with SPC Module.

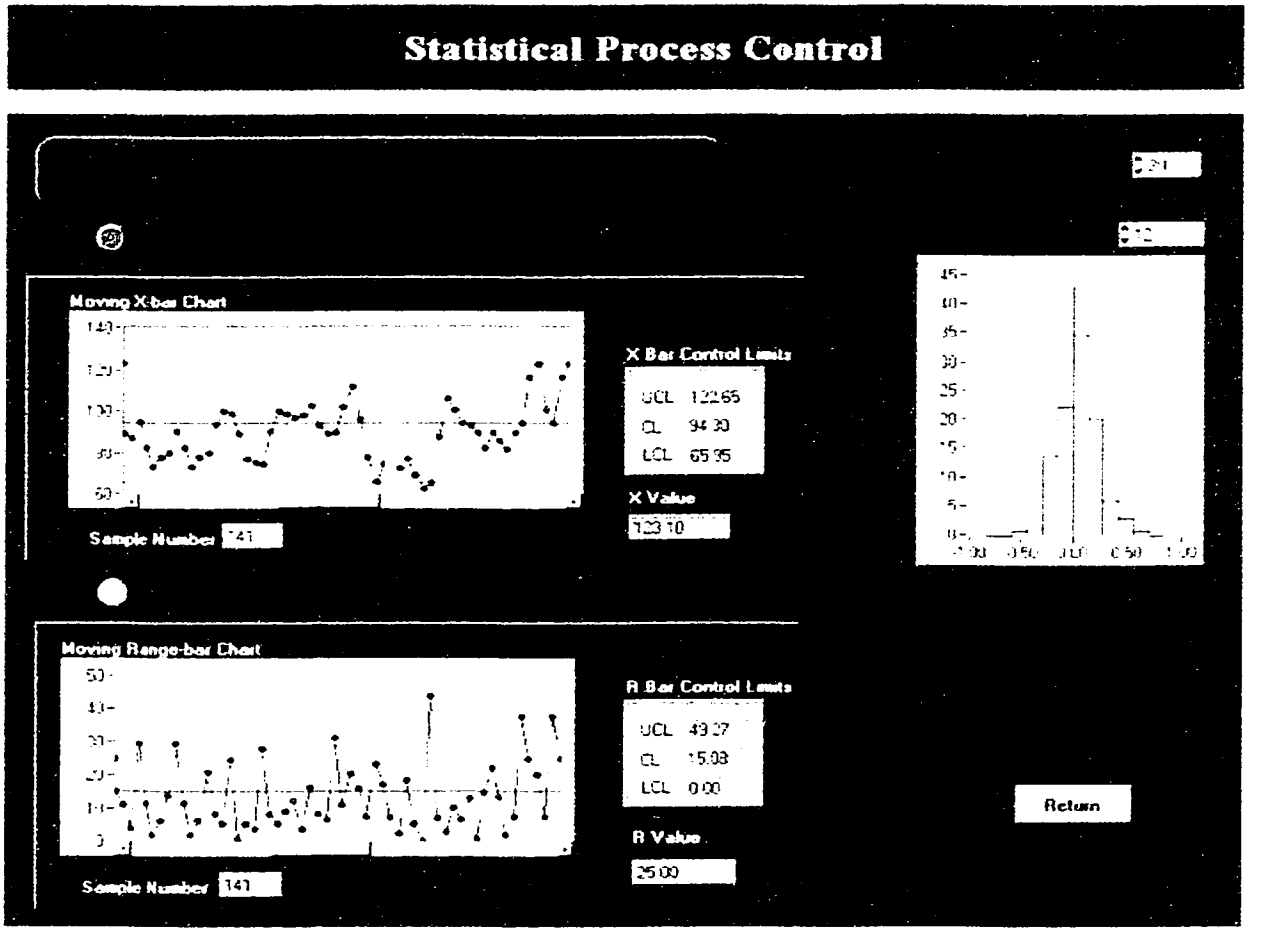

Figure 30 – Individual Screens of Control Charts in the AITAS Showing Moving Average and Moving Range Charts

CHAPTER 8

DEVELOPMENT OF THE CASE BASED REASONING SYSTEM

8.1 Introduction

The Case-Based Reasoning Module for the AITAS was built using a publicly available CBR shell built at the University of Aberystwyth (UK), called Caspian. This shell was selected after evaluating different shells[8] because it was determined to be robust enough and technically flexible to be integrated with the AITAS software.

Caspian creates a case base from a case file written in the language CASL which is a language used for case-based reasoning. Caspian uses this case file to create a case base in the computer's memory, which can be accessed to solve problems and to append new cases to the library.

8.2 System Constraints

The structure of the program, the indexing method, the procedure for calculation of similarity and the organization of the output file are determined by the characteristics of the shell and were not modified during this work.

8.3 Structure of the Case File

The following blocks compose a case file:

a) Introduction: Description of the program

b) Case definition: Definition of the fields that form the problem part of a case. The definition of a field includes the name of the field, the type of value and the weight assigned to it. It is not necessary to define the fields that form the solution part of the case.

c) Index definition: Definition of fields that will serve as indexes.

d) Modification Definition: Definition of values of the fields that will be considered similar during the matching process. Two types of definitions are possible: a symbol can be considered an abstraction of other symbols, or it is possible to define ranges over which numbers will be considered similar.

e) Pre-Processing Rule Definition: Definition of rules that will be used to modify the problem part of a case before the search is carried out.

f) Repair Rule Definition: Contains rules that are triggered as a result of differences between the new and the stored cases and are able to change fields in the solution part of a new case.

g) Cases: Group of cases that form the case base. Each case has a name, a set of input (or problem) fields and a set of solution fields.

More detailed information about the syntax of the case file is included in the CASL Manual[57].

The program code is included in Appendix III.

8.3.1 The Case Definition

Table 13 summarizes the AlTAS parameters that are used as inputs for the case-based system and are included in the *case definition* section of the program. The parameters were selected to characterize the main metallurgical reactions that take place throughout the length of the cooling curve. Higher weights were assigned to those parameters that are more representative of different melt compositions. The weights are defined on an arbitrary scale from 0 to 20.

Detailed description of all AlTAS characteristic temperatures and parameters is included in Appendix I. This Appendix includes a typical W319-Al alloy cooling curve where the parameters used as inputs for the system can be identified.

8.3.1.1 Determination of Weights

Table 13 and Table 14 include the weights that were assigned to the input parameters. To comply with the requirements of the shell Caspian the indexes (defined in Section 8.2.2) are assigned a weight of zero. The weights assigned to other parameters are based on an arbitrary scale form 0 to 20 depending on how critical the parameters are in defining the shape of the cooling curve. The relevance of each parameter is explained in Table 13 and Table 14.

Table 13 – Weights Assigned to Input Parameters

Parameter	Weight	Relevance
Cooling rate factor	0	Factor defined because of software syntax. It is obtained by adding the literals CR to the cooling rate of the sample multiplied by 100. This value is relevant because the magnitude and duration of the metallurgical reactions are determined by the cooling rate of the sample.
Modification	0	Defines the silicon modification level of the melt.
Maximum Temperature of the sample (max value)	20	This parameter largely affects the cooling rate of the sample and determines the morphology of the cooling curve.

Table 14 – Weights Assigned to Input Parameters (continued)

Parameter	Weight	Relevance
Temperature, time and fraction solid Parameters:		
$T^{\alpha\text{-DEN}}$, $T^{\alpha\text{-DEN}}_{MIN}$, $T^{\alpha\text{-DEN}}_{REC}$	5,10,0	Indicators of the grain refinement of the alloy.
$T^{\alpha\text{-DEN}}_{COH}$, $t^{\alpha\text{-DEN}}_{COH}$, $a_{fs}{}^{\alpha\text{-DEN}}_{IDF}$	5,8,5	Indicators of transition from mass to interdendritic feeding and of the feeding efficiency of the alloy.
$T^{Al\text{-}Si}_{NUC}$, $t^{Al\text{-}Si}_{NUC}$, $\Delta T^{Al\text{-}Si}_{E.G}$	0,0,10	These parameters define the beginning of the Al-Si eutectic reaction and determine the modification level.
$T^{Al\text{-}Cu}$	5	Marks the beginning of the Al-Cu eutectic reaction
T^{SOL}, t^{SOL}	10,15	Parameters that represent the end of the solidification and together with the liquidus temperature can be used to estimate the solidification range of the alloy.

8.3.1.2 Input and Output Fields of a Case

A typical case is formed by the following input (problem) and output (solution) fields. The solution fields do not need to be defined in advance and can change from case to case.

8.3.1.2.1 Input Fields

Table 15 – Input Fields of a Case

FIELD	DESCRIPTION
The following parameters are used only in internal computations and are not displayed to the user:	
Coolrate_factor	*Factor that represents the cooling rate of the sample.*
Modification	Classification of the sample according to its modification level into modified, partially modified and unmodified. This parameter is an index which is calculated internally using $\Delta T^{AlSi}_{E.G.}$
Casting_section	Section of the engine block for which the properties will be predicted. Each casting section represents a different cooling rate.
The following input parameters are presented to the user as a summary of the test:	
Target_modification_level	Expected modification level of the melt.
Initial_Sample_Temperature	*Maximum Temperature of the sample that was* recorded during the test.
Liquidus_Temperature	Thermal Analysis Parameter.
Liquidus_Undercooling_Temperature	Thermal Analysis Parameter.
Liquidus_Undercooling_Time	Thermal Analysis Parameter.
Liquidus_Recalescence_Temperature	Thermal Analysis Parameter.
Coherency_Temperature	Thermal Analysis Parameter.
Coherency_Time	Thermal Analysis Parameter.
afs_alphaDENIDF	Thermal Analysis Parameter.
AlSiNucleation_Temperature	Thermal Analysis Parameter.
AlSiNucleation_Time	Thermal Analysis Parameter.
deltaT	Thermal Analysis Parameter.
AlCuEutectic_Temperature	Thermal Analysis Parameter.
AlCuEutectic_Time	Thermal Analysis Parameter.
Solidus_Temperature	Thermal Analysis Parameter.
Solidus_Time	Thermal Analysis Parameter.

8.3.1.2.2 Solution Fields

Table 16 – Solution Fields of a Case

FIELD	DESCRIPTION
The following fields evaluate the quality of the test sample:	
Test_sample_mass	Estimated mass of the test sample.
Test_sample_temperature	Determines whether the maximum temperature of the test sample was acceptable. Low initial sample temperature.
Sample_quality	Final evaluation of the sample taking both the mass and maximum temperature into consideration.
The following fields predict modification level of the Silicon particles:	
Silicon_morphology	Classification of the sample according to its modification level into modified, partially modified and unmodified. This filed takes the same value as the index "Modification" .
AFS_silicon_modification_level	Silicon modification level according to the classification of the American Foundry Society (Figure 32).
Strontium_content	Estimated Sr content based on the relationship between the Sr level and $\Delta T^{AlSi}_{E.G}$ [49] (Figure 31)
The following fields define parameters related to the feeding conditions of the alloy and the probability of gas or shrinkage porosity:	
Hydrogen_level	As measured using an AlSCAN unit when the case data was obtained.
Solidification_range	This field evaluates qualitatively the solidification range of the alloy based on the criteria that longer solidification range promotes the formation of shrinkage porosity[12].
Grain_size	Grain size observed during microstructural evaluation by Image Analysis.
Grain_refinement	Qualitative description of the level of grain refinement of the melt.

Table 17 – Solution Fields of a Case (continued)

FIELD	DESCRIPTION
Cooling_rate_of_casting_section	Cooling rate of the casting section selected by the user. The cooling rate has paramount importance in the soundness of the casting sections, in general fast cooling rates result in low porosity level.
Propensity_to_shrinkage_porosity	Evaluation based on the parameter $af_s^{\alpha\text{-}DEN}{}_{IDF}{}^{6}$.
Area_Percent_Porosity	Porosity Area Fraction of the casting section *quantified via Image Analysis.*
The following fields evaluate the characteristics of the Cu rich phases:	
Area_Percent_Copper_Based_Phases	Area Fraction of Cu phases in the casting section (after heat treatment) quantified via Image Analysis.
Maximum_Recommended_TSR_Temp	Maximum Recommended Thermal Sand Removal / Solution treatment temperature. The calculation is described in a following section.
The following fields predict the mechanical properties of the specified casting section:	
Matrix_MicroHardness_HV	Microhardness (HV_{25}) of the α-Al matrix measured in the engine block sample.
Percent_Elongation	As measured in tensile test. The test bars were obtained from the casting section.
UTS	Ultimate Tensile Strength. As measured in tensile test. Test bars obtained from the casting section.
TwoPercent_YieldStrength	As measured in tensile test. The test bars were obtained from the casting section.
Brinell_Hardness	As measured in tensile test. The test bars were obtained from the casting section.
Sample_Microstructure	Picture illustrating the typical microstructure of the engine block sample.
The following fields present comments regarding any special conditions observed during data collection and recommendations to maintain the process in control:	
Comments	
Recommendations	

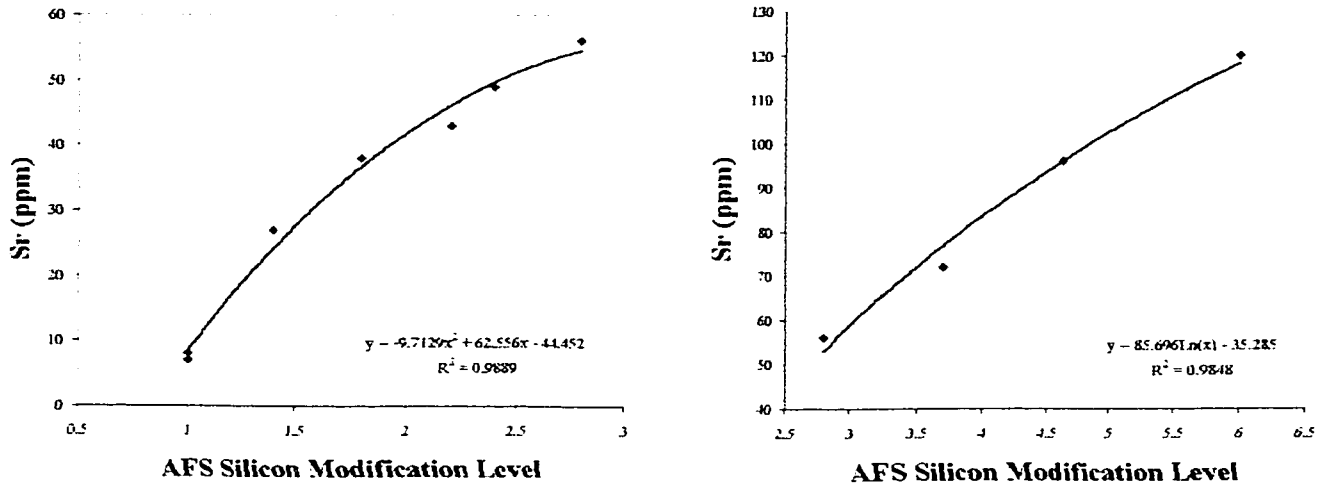

Figure 31 – Relationships for the Calculation of Sr Content in the Repair Rules of the System[49].

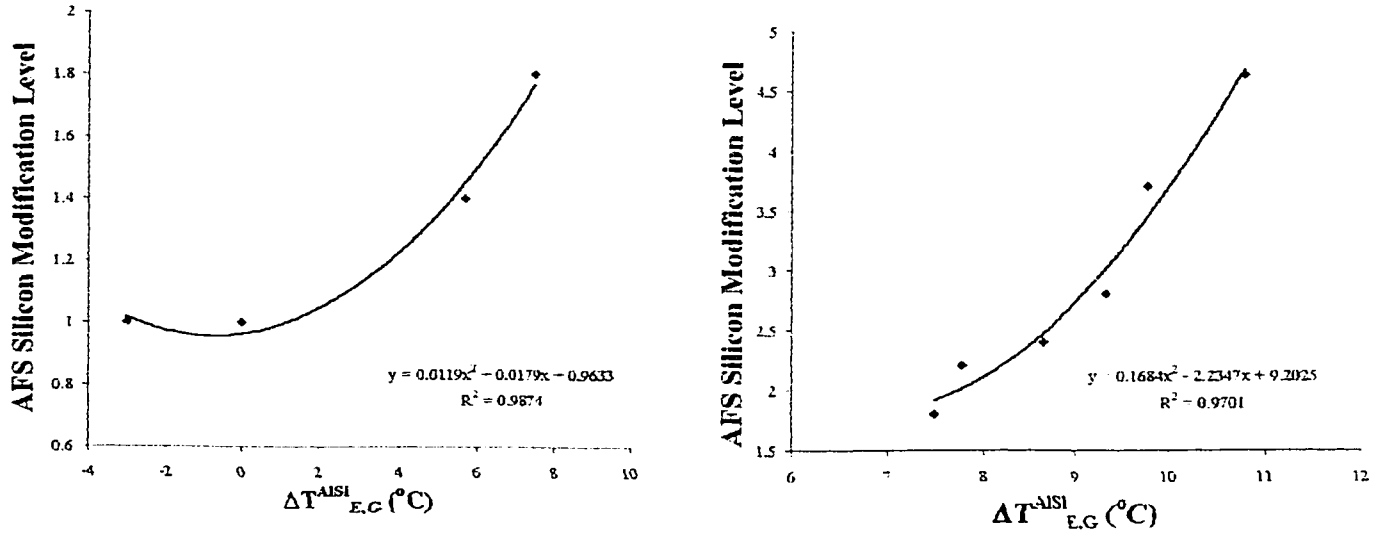

Figure 32 – Relationships for the Calculation of the AFS Level of Silicon Modification[49]

8.3.2 Index Definition

The case base is indexed using the modification level of the melt and the cooling rate of the casting section for which mechanical properties will be predicted. Figure 33 presents the organization of cases within the case-base.

8.3.2.1 Index for Modification Level

The Modification Level index can take one of three pre-established values: modified, unmodified or partially modified. The alloy sample is considered modified if the parameter $\Delta T^{Al\text{-}Si}_{E.G}$ takes values from 8.6°C to 12 °C. The index is assigned the value partially modified when $\Delta T^{Al\text{-}Si}_{E.G}$ lies between 6.6°C to 8.5°C and the value unmodified if it is within –3.5°C and 6.5°C [49].

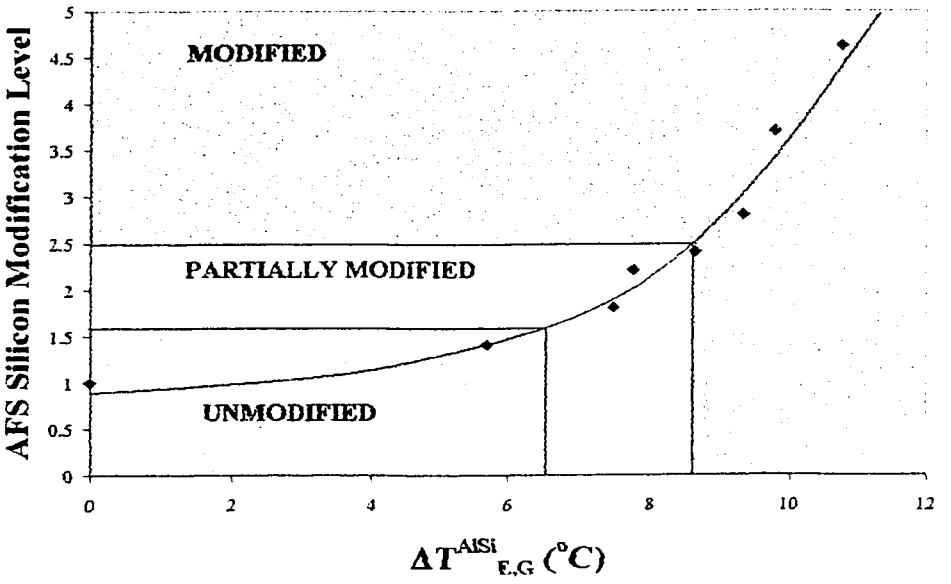

Figure 33 – Relationship between $\Delta T^{Al\text{-}Si}_{E.G}$ and the AFS Level of Silicon Particle Modification [49]

8.3.2.2 Index for the Cooling Rate of the Casting Section

The values for the index "cooling rate of casting section" can refer to 2 sections of 2 different engine blocks, which correspond to the following cooling rates:

- 2.5 L / 3.0 L Main Bearing Saddle – 0.3 °C/sec
- 2.5 L / 3.0 L Bolt Boss – 0.6 °C/sec
- 4.6 L Main Bearing Saddle – 0.2 °C/sec
- 4.6 L Bolt Boss – 0.45 °C/sec

Figure 34 presents the different cases included in the case base.

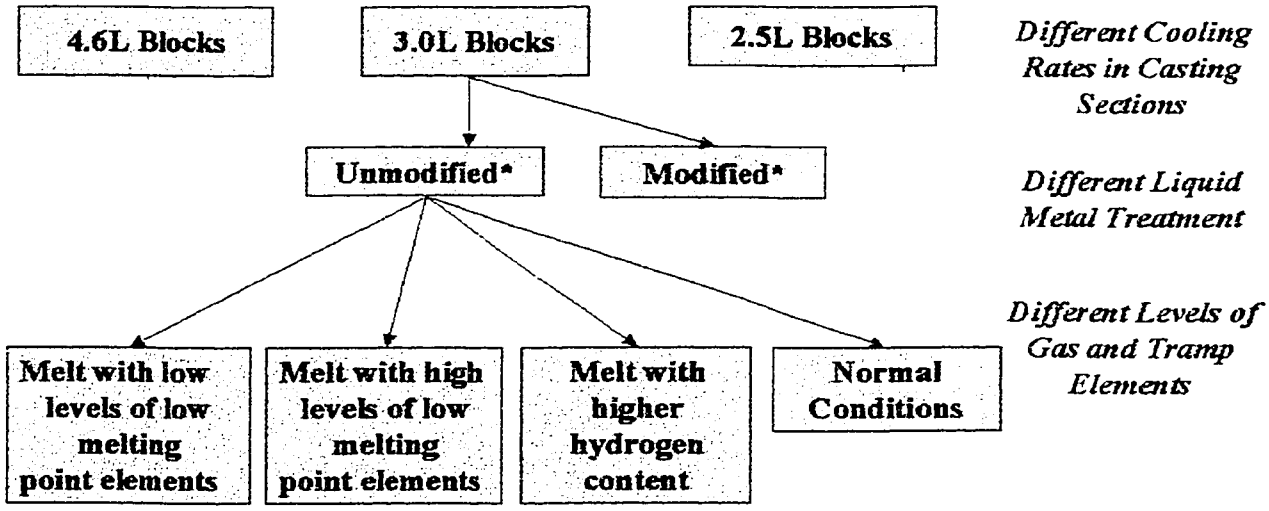

Figure 34 – Organization of Case Base

8.3.3 Modification Definition

In this section the preliminary control limits obtained for the thermal analysis parameters in Appendix V are used to define ranges over which the values of the parameters can be considered similar.

This includes ranges for the modification indicator $\Delta T^{Al\text{-}Si}{}_{E.G}$ used to distinguish between five of the possible modification levels (excluding over modification) and three intervals for the characteristic temperature $T^{\alpha\text{-}DEN}{}_{REC}$ that classify the samples qualitatively into three grain sizes.

8.3.4 Preprocessing Rule Definition

There are two rules contained in this section.

a) Rule to increase the weight of the characteristic temperature $T^{\alpha\text{-}DEN}{}_{REC}$ when its value corresponds to a grain refined melt.

For grain refined melts $T^{\alpha\text{-}DEN}{}_{REC}$ will have a more relevant role in the retrieval of similar cooling curves. This rule is included in the source code of the program presented in Appendix II, under the name "repair rule use_alternative_weights".

b) Rule to modify the value of the liquidus temperature ($T^{\alpha\text{-}DEN}{}_{NUC}$).

This rule deals with situations in which errors in the test may occur yielding incorrect values of $T^{\alpha\text{-}DEN}{}_{NUC}$. If an incorrect value for this parameter is detected, a new liquidus temperature is calculated using the mathematical equation[58] for multicomponent aluminum alloys. This equation is based on the chemical composition of the alloy (Si, Cu, Zn, Mg). In the AlTAS screen the default values of these elements correspond to the average chemical composition of W319 alloy observed during this work (Figure 35).

The rule is referred to as "repair rule adjust_liquidus" in the source code of the program. The threshold value corresponds to the Upper Control Limit obtained for this parameter (Appendix V)

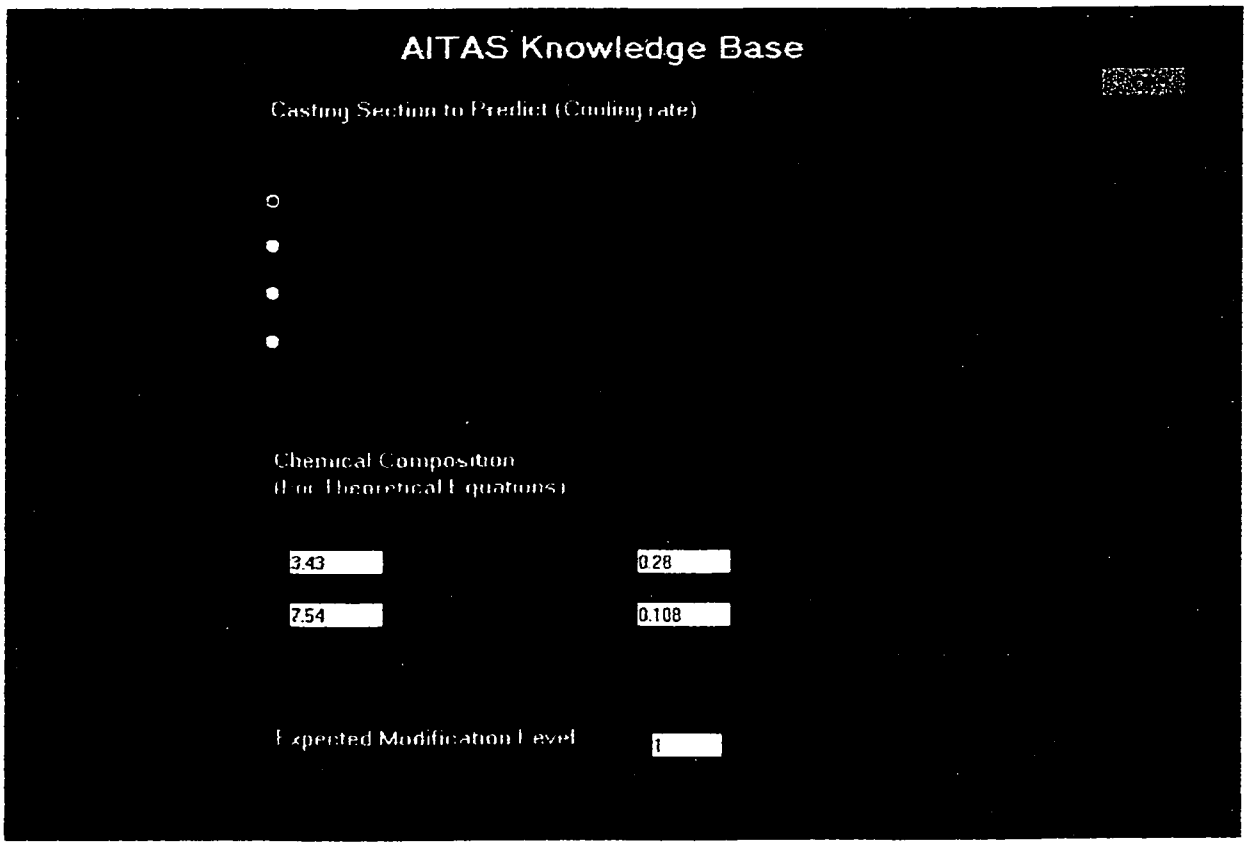

Figure 35 – Input Screen of the Case Based Reasoning System

8.3.5 Repair Rule Definition

The following rules were defined in order to modify the solution of the cases to account for differences between the new case and the existent cases:

a) Rules to determine the exact Sr content of the sample and the exact Thermal Sand Removal (TSR) temperature.

As a first step the values for the Sr content and TSR temperature are removed from the existing case. The mass of the test sample is also removed from the existing case.
After removing the original values from the stored case the new values are estimated as follows:

- The mass of the test sample is estimated as a function of the time of the Al-Cu Eutectic reaction (Figure 36). This time parameter was preferred over the total solidification time to avoid the repeatability issues that are inherent to the solidus algorithm. The equation was developed using the samples obtained during the present study.

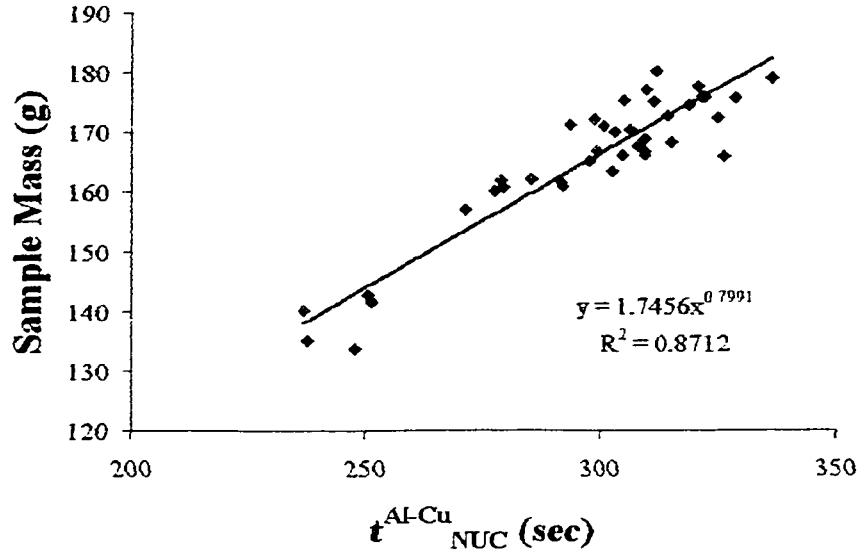

Figure 36 – Relationship Between Al-Cu Eutectic Time and the Mass of the Test Sample

- The Sr content of the melt is calculated using the relationships between the AFS Silicon Modification Level, the Sr content of the melt and the parameter $\Delta T^{Al\text{-}Si}_{E.G}$ developed at the NSERC/Ford/University of Windsor Industrial Research Chair (IRC) in Light Metal Casting Technology[51]. The relationships are included in Figure 31 and Figure 32. The data was subdivided in order to obtain a better fit for all the Modification Levels. Prior to the calculation of Sr content, the relations presented in Figure 32 obtained by the same author must be applied to calculate the AFS level of Silicon Modification based on $\Delta T^{AlSi}_{E.G}$. The verification of the estimates provided by these equations is presented in Appendix IV.

- The recommended TSR (and solution treatment) temperature is calculated using the results of studies of heating and cooling cycles carried out by the IRC to determine the

effect of isothermal holding temperature during solution treatment[59]. Solution treatment is responsible for Si particle sphereoidization and dissolution of Cu and Mg enriched phases. In conventional solution treatment the temperature must be kept below the melting point of the Cu rich phases in order to avoid incipient melting, but it should be high enough to create the required conditions for Cu and Mg dissolution and Si modification[59,60]. Previous IRC research indicates that the optimum solution treatment temperature after isothermal holding is 520°C[50] (results obtained at a cooling rate of 0.76°C/sec and presented in Figure 37), other studies[59] carried out by the IRC indicate that the recommended temperature is approximately 15°C higher than the solidus temperature recorded during the cooling cycle due to the hysteresis effect (results obtained at a cooling rate of 0.35°C/sec). Since the latter study was performed under conditions that are similar to the present work, the latter results were included in the body of a rule.

b) Rule to determine whether Sr additions to the W319-Al melt are needed.

- This rule verifies that the level of Sr in the melt is the same as the target level defined by the user. If there is a discrepancy between these two levels, the system recommends the amount of Sr that should be added to the melt to reach the target level. The equations used in this rule are those included in Figure 31. In the source code of the program, see rules "repair rule add_Sr_high" and "repair rule add_Sr_low".

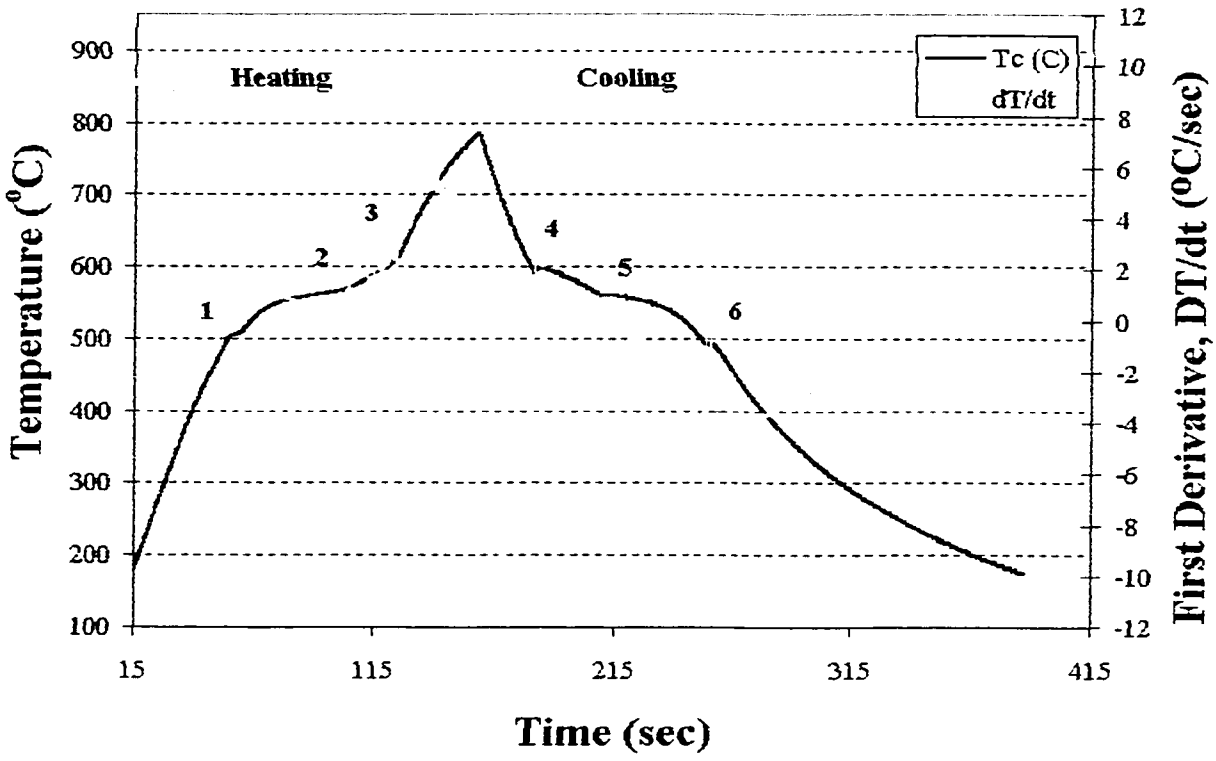

Figure 37 – Heating and Cooling Curves and First Derivative Curve of the 319-Al Alloy [50].

The Main Metallurgical Reactions During Heating and Solidification:

1. Dissolution of Cu Rich Phases

2. Dissolution of Al-Si Eutectic

3. Dissolution of α-Al Dendritic Network

4. Nucleation of α-Al Dendritic Network

5. Nucleation of the Al-Si Eutectic

6. Nucleation of Cu Rich Phases

c) Rule to change the sample microstructure display.

- For modified melts the picture of the microstructure is changed to display the correct morphology of the silicon particles (See Chapter 6). See the rule "repair rule sample microstructure" in the source code.

d) Rules to evaluate the quality of the test sample.

- When the mass of the test sample is lower than the recommended values of 165 g or the initial temperature of the sample is lower than 680°C, the system advises the user to repeat the test. Three rules were written to address this problem: "repair rule low_sample_mass", "repair rule low_initial_temperature" and "repair rule low_mass_and_temperature".

8.4 Integration of AITAS Software and the Case-Based Reasoning Module

The shell Caspian was selected mainly for the following reasons:
a) Caspian applies CBR for the recovery and matching of data. Besides the manipulation of numerical and non-numerical data, it is able to handle text to provide comments and recommendations to the user.
b) The system was developed in the C programming language for the DOS Operating System. This feature gives the user the possibility of linking the CBR application to the Graphical User Interface (GUI) of the AITAS, which runs in the Windows platform.
c) It was possible to modify the Caspian source code to match the data structures and format given by the AITAS.

Three steps were followed for the integration of the CBR into the AITAS software:
a) Modification of the Caspian source code
b) Linking of the AITAS and Caspian Software
c) Visualization of the CBR outputs in the AITAS GUI

These tasks were performed with the help of Emma Mares from the IRC.

8.4.1 Modification of the Caspian Source Code

Before mentioning the main modifications made to Caspian, it is necessary to mention that Caspian relies on a case base for matching of cases. This case base, written in the language CASL, is stored as a text file.

Originally, Caspian accessed the input values from the keyboard and presented the results in a DOS environment. These features were modified in order to read inputs automatically from the parameters generated by the AITAS and present the results in the AITAS GUI.

Thee main steps are involved in this process:

- The AITAS writes to a text file all the parameter values required in the Caspian knowledge interface.
- Caspian performs the matching of cases, retrieval and application of repair rules taking as inputs the parameters in the text file.
- The main Caspian program and its functions were compiled as a Dynamic Link library (.DLL file) for Microsoft® Windows in order to standardize the application and allow it to run under a Microsoft® Windows application.

8.4.2 Linking of the AITAS and Caspian Software

The AITAS software was developed using National Instruments LabView™ Software. Caspian is called by LabView™ as a DLL and once Caspian finishes the CBR process, the control returns to the LabView™ platform.

8.4.3 Visualization of the CBR outputs in the AITAS GUI

The outputs of Caspian are stored in a second text file. These text files are the main components for linking between platforms. Figure 38 depicts the process of linking the CBR application with the AITAS software. The AITAS program calls up the two text files and presents the values to the user in the screens presented in Figure 39a and Figure 39b.

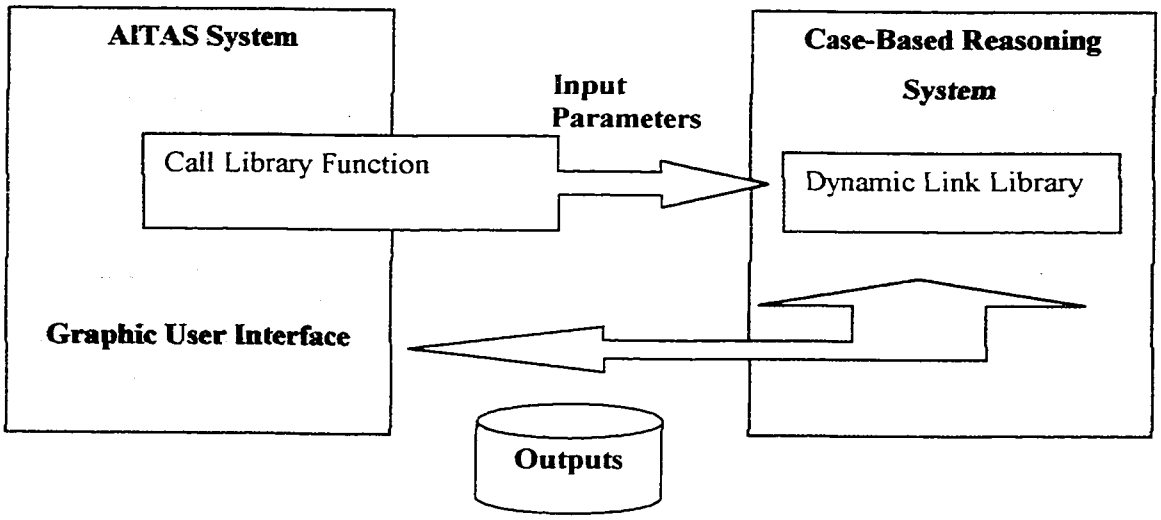

Figure 38 – Integration of Case-Based System and AlTAS System

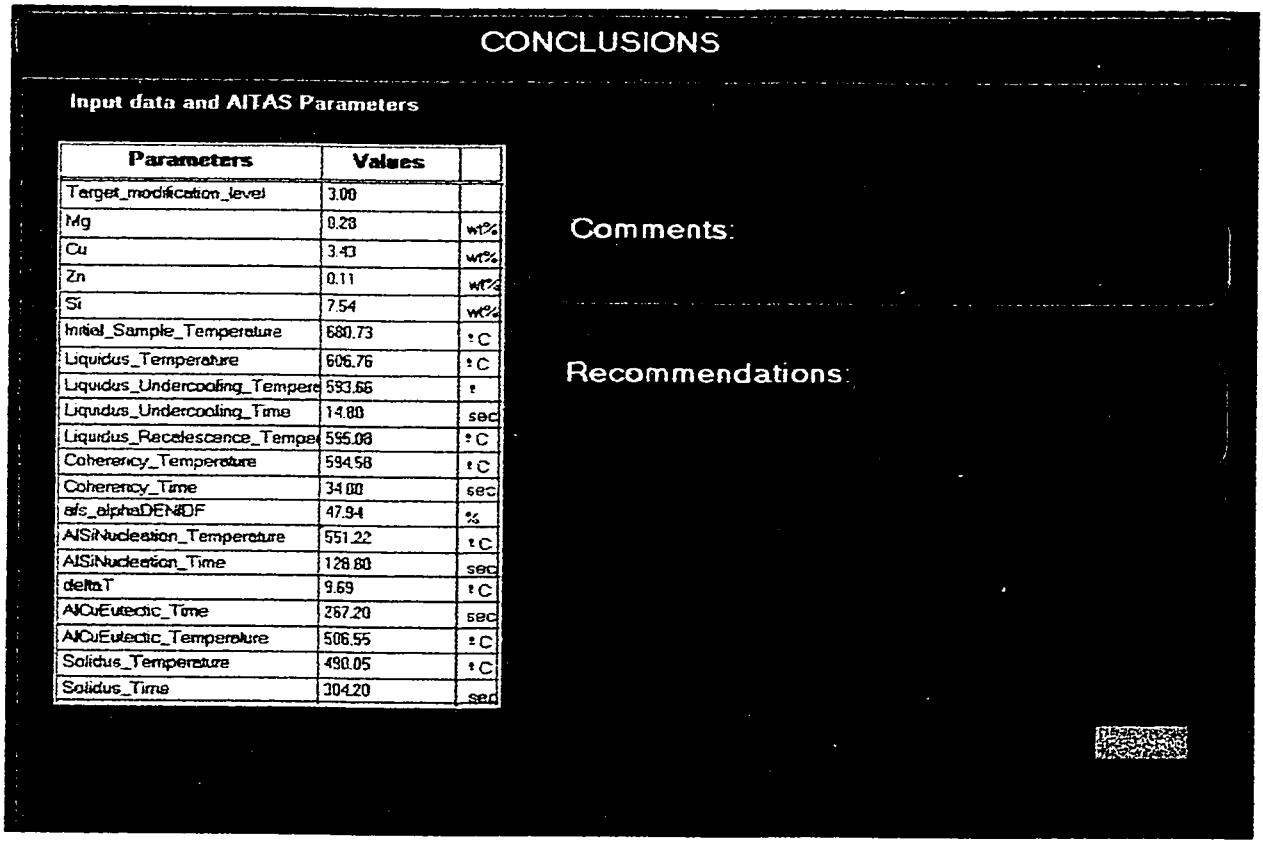

Parameters	Values	
Target_modification_level	3.00	
Mg	0.28	wt%
Cu	3.43	wt%
Zn	0.11	wt%
Si	7.54	wt%
Initial_Sample_Temperature	680.73	°C
Liquidus_Temperature	606.76	°C
Liquidus_Undercooling_Tempere	593.66	°
Liquidus_Undercooling_Time	14.80	sec
Liquidus_Recalescence_Tempe	595.08	°C
Coherency_Temperature	594.58	°C
Coherency_Time	34.00	sec
afs_alphaDENDF	47.94	%
AlSiNucleation_Temperature	551.22	°C
AlSiNucleation_Time	128.80	sec
deltaT	9.69	°C
AlCuEutectic_Time	267.20	sec
AlCuEutectic_Temperature	506.55	°C
Solidus_Temperature	490.05	°C
Solidus_Time	304.20	sec

Figure 39a – Conclusions of the CBR System and Summary of the AlTAS Results

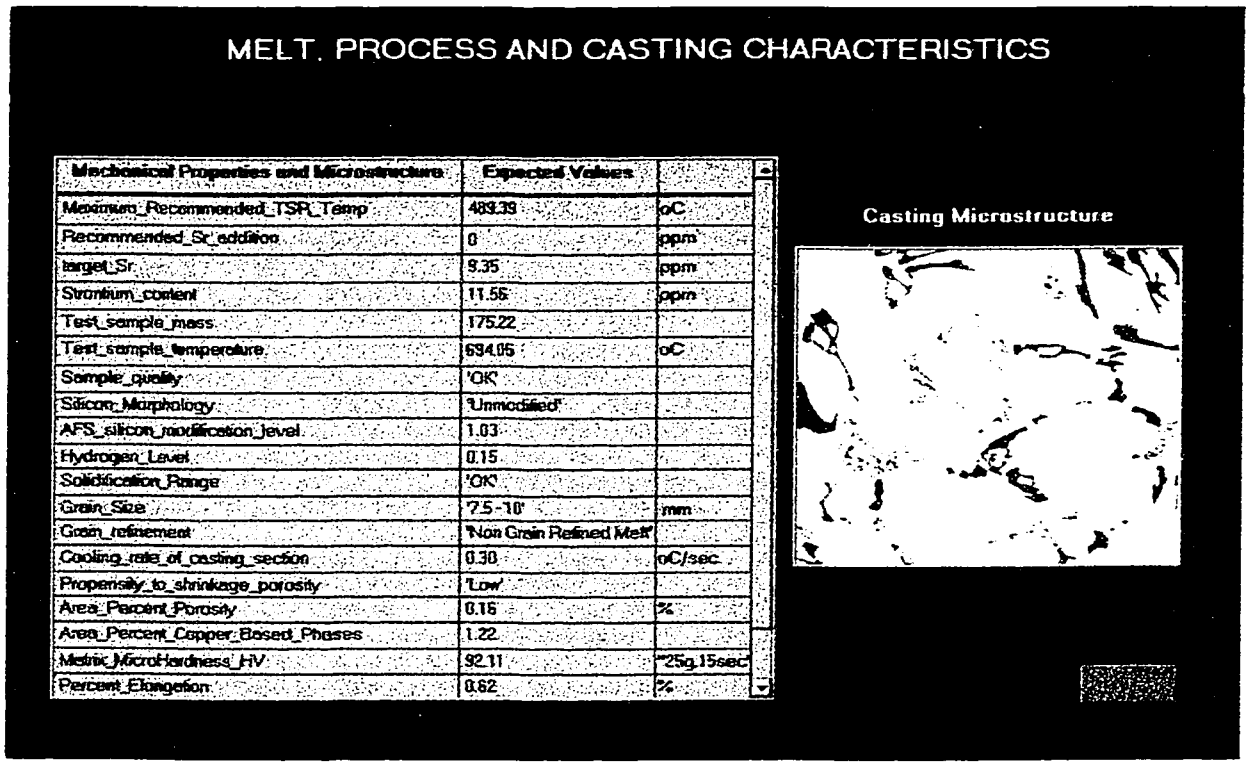

Figure 39b –Microstructure and Mechanical Properties Predicted by the CBR System

8.4.4 Execution of the CBR Module

The procedure followed by the program is described in the following diagram:

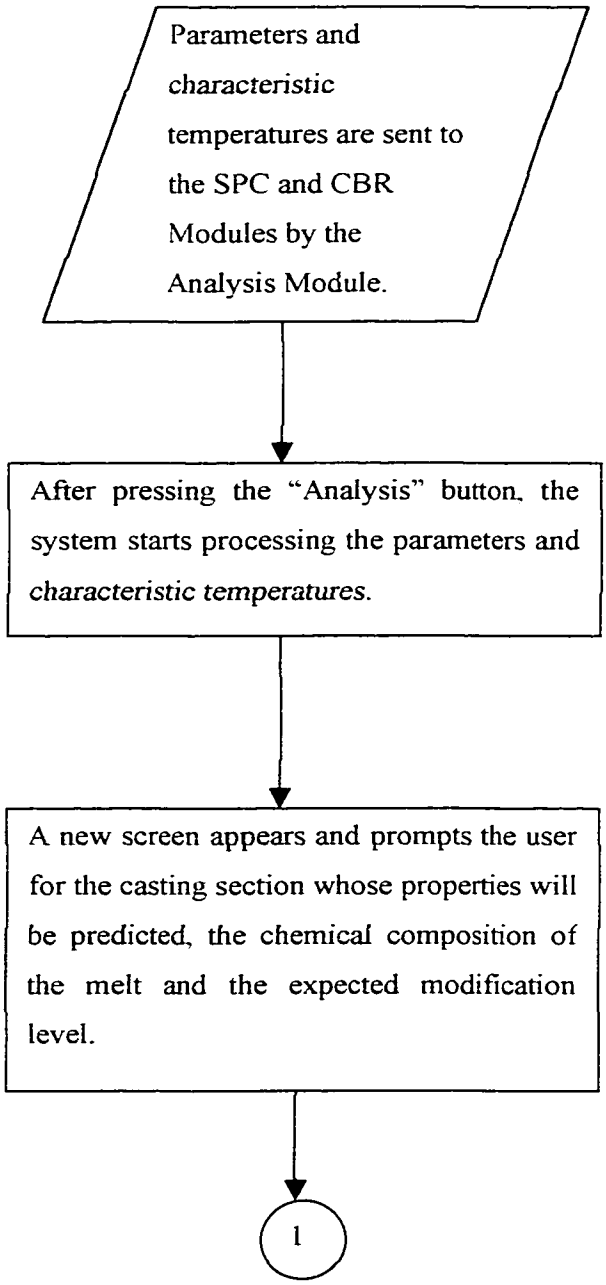

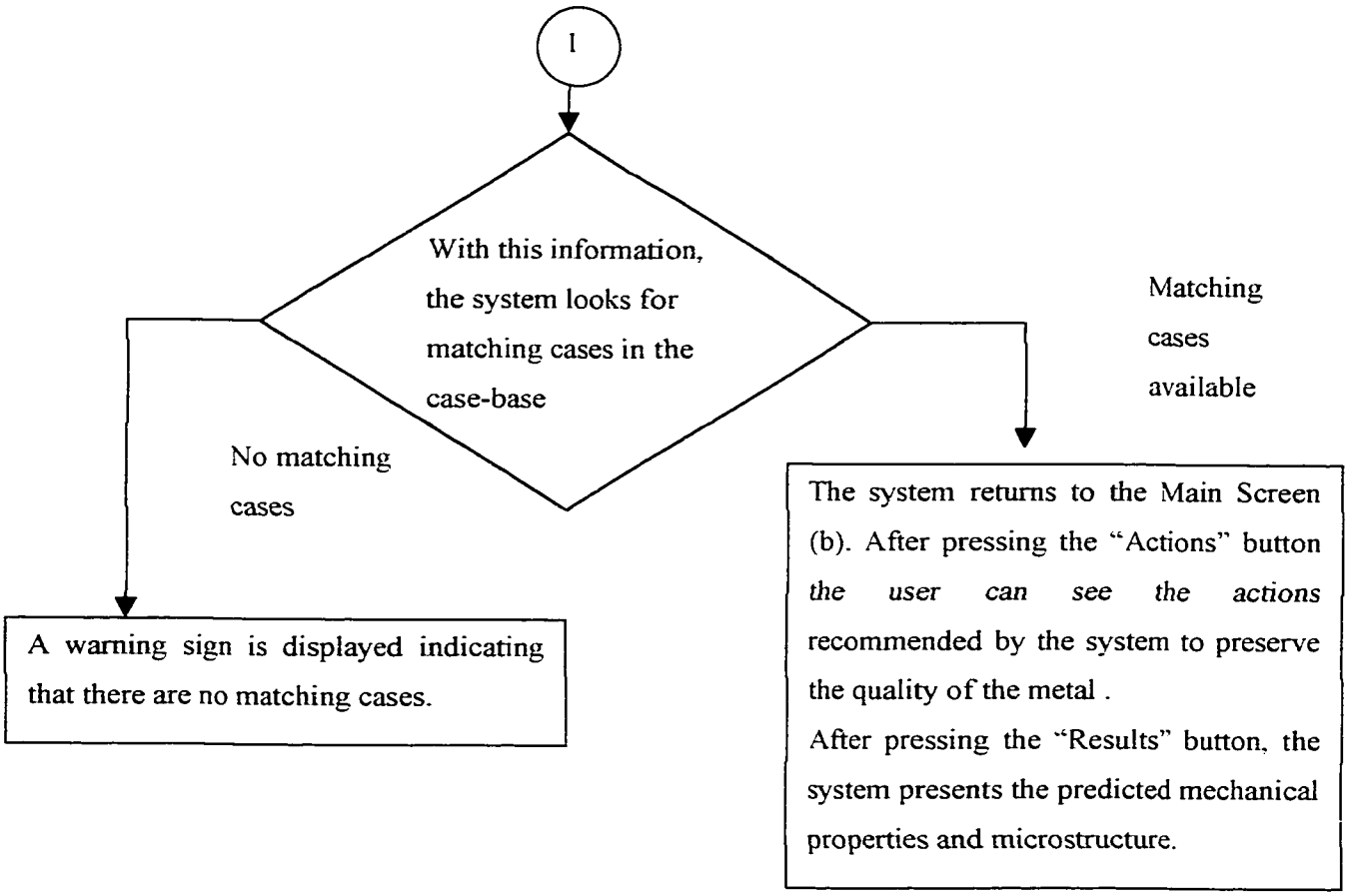

Figure 40 – Execution of the CBR Module

CHAPTER 9

VALIDATION OF THE CASE-BASED REASONING SYSTEM

9.1 Verification and Validation Methodology

A methodology proposed by Gonzales et al. [61] was followed to validate the system. This methodology uses the case library itself to evaluate the retrieval and adaptation functions of the CBR engine with respect to the domain included in the case library. This method offers advantages such as eliminating the subjectivity of the testing procedure and minimizing the involvement of domain experts.

This methodology is known as the Case Library Subset Test and includes the following three stages:
a) Retrieval test
b) Adaptation test
c) Domain coverage test

During the present validation the first two tests were carried out and domain coverage was evaluated presenting to the CBR system cases not included in the case base.

9.1.1 Validation Criteria

The validation criterion in this test is based on the evaluation of two parameters:

a) Result Acceptability Criteria (RAC) – This parameter serves as an acceptability threshold for the solutions of the system to each of the test cases executed during the validation procedure. For numerical outputs, the RAC can be defined as the Relative Error (Equation 11) of the solution when compared to a standard. For symbolic outputs a direct comparison can be made and the results classified as optimal, acceptable or unacceptable.

Equation 11 - Relative Error

$$RE = \frac{(|a-b|)}{b} * 100$$

Where:

a is the calculated value of the parameter

b is the real value of the parameter

b) System Validity Criteria (SVC) – Is the percentage of the test cases that must be acceptable (above the RAC threshold) in order to consider that the CBR system is valid. During validation this parameter is compared to a "Correctness Ratio" as defined in Equation 12:

Equation 12 – Correctness Ratio

$$CR = \frac{(c)}{t} * c$$

Where:

c is the number of correctly appraised cases

t is the total number of cases used during validation

9.1.2 Retrieval Test

This test is carried out to evaluate the correctness of the retrieval function of the CBR program. This test evaluates the indexing and case classification functions, since deficiencies in the indexing criteria would appear as poor retrieval performance.

The procedure for this test is presented in Figure 41.

As indicated in this procedure, the test is carried out using the same set of cases included in the system's case-base. The cases are included in Appendix VI.

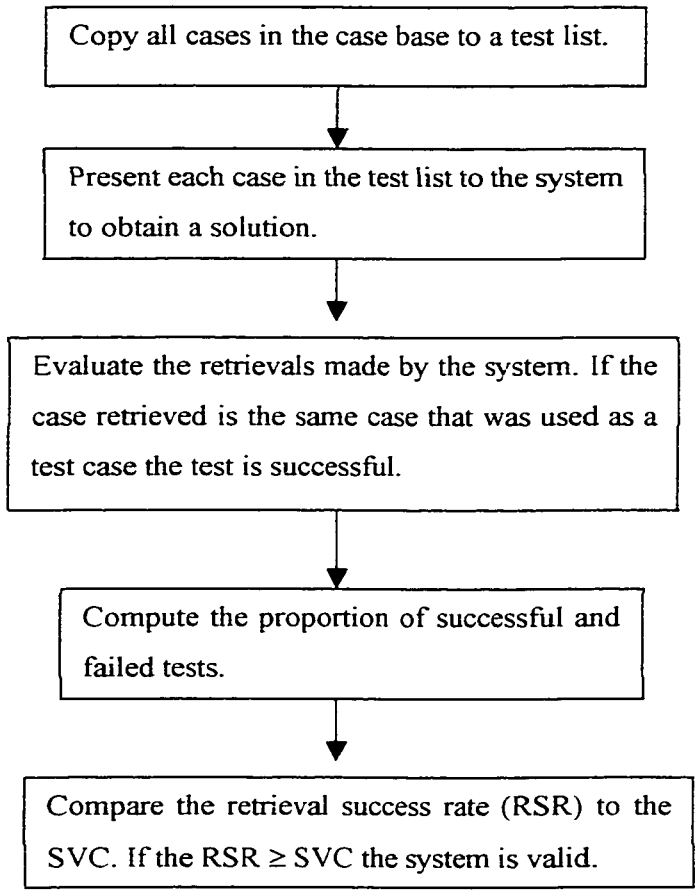

Figure 41 – Procedure for the Retrieval Test

9.1.2.1 Results of Retrieval Test

For all tests the validation criteria was defined as follows:

RAC = 20%

SVC = 95%

This means that 95% of the test cases must be retrieved with parameter values less than 20% different from their original values. Twenty percent overall RE was allowed for each case because of the narrow range of chemical composition covered by the system's cases. Table 18 presents the results of this test which was completed successfully.

The RE for each parameter in the solution part of the case was calculated and added. The overall RE is the proportion of this cumulative RE and the total possible error, which was calculated allowing a maximum RE of 100% for each parameter.

Table 18 – Results of Retrieval Test

Case	Description	Successfully Retrieved	Retrieved with Error
1	UM_GQMBS3	X	
2	UM_GQ1MBS4_6	X	
3	UM_GQBB3	X	
4	UM_GQ1BB4_6	X	
5	UM_GQ2MBS3	X	
6	UM_GQ10MBS3	X	
7	UM_GQ10BB3	X	
8	UM_GQ10MBS4_6	X	
9	UM_GQ10BB4_6	X	
10	UM_GQ13MBS3	X	
11	UM_GQ15MBS3	X	
12	UM_LS2MBS3	X	
13	UM_LS5MBS3	X	
14	UM_LS7MBS3	X	
15	M_1MBS3		X
16	M_1BB3	X	
17	M_1MBS4_6	X	
18	M_1BB4_6	X	
19	M_2MBS3	X	

Retrieval Success Rate (Correctness Ratio CR) 0.95

The system is valid because CR ≥ SVC

9.1.3 Adaptation Test

After retrieval has been determined successful, it is necessary to ensure that adaptations are correctly carried out.

This test is based on the same set of test problems described above; however, during this test the historical test that will be presented to the CBR system must be deleted from the case library of size N, so that the modified case library has only N-1 cases in it. The solution generated by the CBR system must be compared to the original solution of the case, and the Relative Error is calculated. If the Relative Error is within the RAC the test is considered successful.

The proportion of successful versus failed cases, called the "adaptation success rate", is computed and must be compared to the selected SVC.

9.1.3.1 Results of Adaptation Test

The criteria used in the retrieval test was also used in the adaptation test.

During the adaptation test it was noticed that the equation used to calculate sample mass performs better for the case of unmodified melts. Since the equation was obtained from unmodified samples, it can be concluded that one equation for each modification level is needed. However, because of the different scope of this work the task is suggested as future work.

The results of this test are included in Table 19. Appendix VII includes and example of a successfully retrieved case and a case retrieved with error.

Table 19 – Results of Adaptation Test

Case	Description	Relative Error (RE)	Successfully Retrieved	Retrieved with Error
1	UM_GQMBS3	0.08	X	
2	UM_GQ1MBS4_6	0.11	X	
3	UM_GQBB3	0.18	X	
4	UM_GQ1BB4_6	0.11	X	
5	UM_GQ2MBS3	0.12	X	
6	UM_GQ10MBS3	0.20	X	
7	UM_GQ10BB3	0.14	X	
8	UM_GQ10MBS4_6	0.29		X
9	UM_GQ10BB4_6	0.18	X	
10	UM_GQ13MBS3	0.11	X	
11	UM_GQ15MBS3	0.14	X	
12	UM_LS2MBS3	0.07	X	
13	UM_LS5MBS3	0.06	X	
14	UM_LS7MBS3	0.06	X	
15	M_1MBS3	0.11	X	
16	M_1BB3	0.14	X	
17	M_1MBS4_6	0.19	X	
18	M_1BB4_6	0.16	X	
19	M_2MBS3	0.12	X	

Retrieval Success Rate

(Correctness Ratio CR) 0.95

The system is valid because CR ≥ SVC

9.1.4 Domain Coverage Test

This test is used to determine the effect of the size of the case library and how well the CBR system can handle cases recently added to the case base.

This test is carried out in two steps:

a) Classifying the cases in the case-base according to common values of an attribute.
b) Segregating the cases in the case base into a running-case list and a test-case list. The test-case list includes cases with a common attribute.

Each case from a test list is presented as a problem to the CBR system for it to obtain a solution, until the list is empty. Once the list of cases is empty, the retrievals made by the system are evaluated. Because of the size of the case-base the segregation of cases was not possible and this test was not carried out. Instead, a set of unknown cases with different modification levels was presented to the system to evaluate the retrieval and adaptation functions. The system reacted to unknown cases as described in the following section.

9.1.4.1 Response of the System to Unknown Cases

The system responds to cases not included in the library with a non-matching index alarm. Figure 42 presents the corresponding screen of the system.

If a case cannot be automatically matched Caspian offers the possibility to match cases manually. However, in the industrial version of the AITAS CBR System this option was disabled in order to keep the access to the source program restricted to a limited number of users.

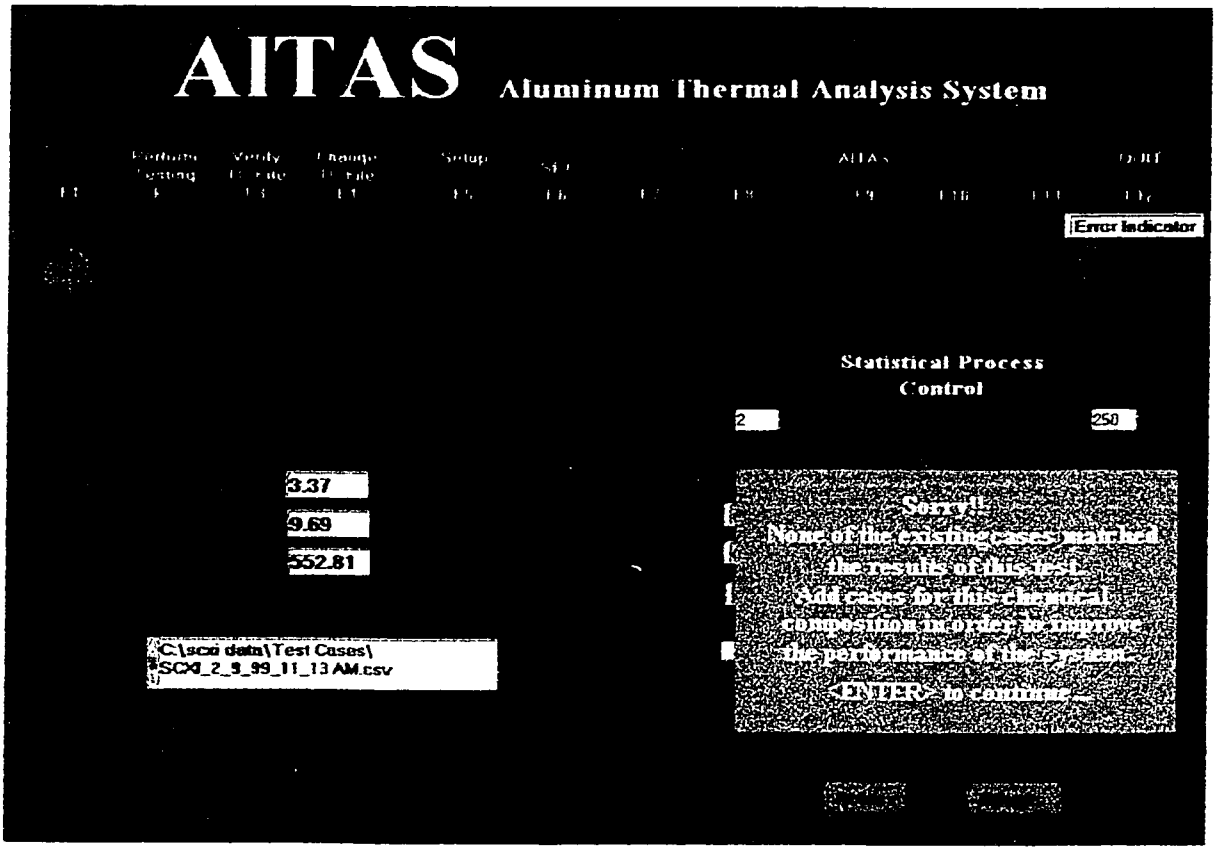

Figure 42 – Screen of the CBR System Showing the "No Matching Case" Alarm

CHAPTER 10

CONCLUSIONS

The high quality, efficiency and competitive cost requirements faced by the automotive industry, coupled with the fast growth of the aluminum casting industry have made necessary the development of proactive methods of quality control. This need motivated the development of tools such as the AlTAS. During this research the AlTAS was implemented at the Ford's Windsor Aluminum Plant proving to be a very sensitive tool capable of detecting minute variations in the chemical composition of W319-Al alloy. As a result of the implementation, the functions for determination of the Si Modification level developed by the IRC were verified in industrial conditions showing acceptable results. However, during this work it became evident that the development of an automated sampling method that guarantees constant mass and initial temperature of the test samples is an important area of opportunity for the improvement of the AlTAS.

During the collection of data, interesting relationships between the Al-Cu eutectic and solidus temperatures, the proportion of copper phases and the level of tramp elements, such as Sn or Pb in the melt were identified. However, more work is still required for a better understanding of these relationships.

This work has provided the AlTAS system with two modules to improve its capabilities as a process control tool. The SPC Module was included in the AlTAS to make it possible to prevent deviations from the required composition and the CBR system was added to provide predictions regarding the expected microstructures and mechanical properties of the engine blocks as well as interpretation of the AlTAS parameters.

Two types of control charts were included in the SPC module namely Moving Average and Exponential Moving Average. The selection of optimum values for the control chart parameters still requires a testing period under normal production conditions. A module for the calculation of process capability could be added to the SPC screen using LabView's predetermined functions if required.

The research presented in this work summarized the previous findings of the IRC in the area of thermal analysis of 319-Al alloy and included this summary in the adaptation rules and case base of the CBR system. This information was complemented with foundry data to create a system that is able to interpret thermal analysis results and predict engine block properties.

The CBR System was developed using a shell that is flexible enough to allow the use of functions and rules for modification of cases when these are available. If the functions are not available or the interrelationships between process parameters are not yet fully understood, case matching and retrieval provide a powerful resource for reaching meaningful predictions. These features make CBR a suitable artificial intelligence technique for interpretation of cooling curves and prediction of casting properties. CBR systems have advantages over other techniques such as neural networks since they require less data sets (or cases) making their development more economical.

The system is structured in such a manner that new cases or new fields for the existing cases can be easily included. During further use of the system, the maintenance of the case-base becomes an important issue to avoid the storage of redundant cases that could affect the performance of the system. For this reason and because the expert knowledge is included in the adaptation rules and the solution fields of the cases the addition of cases to the case base is a function that has been restricted to the developers of the system and engineers of the casting facilities (process experts).

The retrieval and adaptation functions of the CBR system were tested according to the established validation criteria (RAC and SVC). The results of the system are within the acceptable values of these criteria. However, the domain currently covered by the case base can be expanded to provide solutions through a wider range of chemical composition, such as different levels of modifier, grain refiner, tramp elements and impurities, hydrogen content, as well as other silicon and copper contents. High Cycle Fatigue Results could also be included in the solution part of the cases.

It is recommended that both the Statistical Process Control and the Case Based Reasoning Modules be tested for longer periods at the casting plant to determine optimum parameters for the control charts and to add more cases to the system.

REFERENCES

1. Wolfgram, D., Dear, T., Galbraith, C. **Expert Systems for the Technical Professional**. John Wiley & Sons Inc. 1987.
2. Kolodner, J. **Case-based Reasoning**. Morgan Kaufmann, 1993.
3. Pulaski, K., Casadaban, C. **Case-Based Reasoning: The Marriage of Knowledge Base and Database**. Proceedings Fourth International Conference on Data Engineering, 1998, pp. 183 -190.
4. Major, J.F. **Aluminum Automotive Castings**. An Ever Expanding Role in an Increasingly Competitive Market. Unpublished Report by Alcan International Limited.
5. Boone, G.W.; Carver, R.F.; Seese R.G. **Optimizing Grain Refiners and Modifiers in Al-Si Alloys**. Modern Casting, January 1998, pp. 52 – 54.
6. Djurdjevic, M. B., Kierkus, W. T., Mackay, R. I., Sokolowski, J. H. **Metallurgical Characterization of the 319 Alloy Solidification Process Utilizing the Aluminum Thermal Analysis System (AlTAS).** NSERC/Ford/University of Windsor Industrial Research Chair in Light Metals Casting Technology. Internal Report. April 2000.
7. Liao T.W., Zhang, Z. **Similarity Measures for Retrieval in Case-Based Reasoning Systems**. Applied Artificial Intelligence, Vol. 12, 1998, pp. 267-268.
8. Watson, I. **Applying Case-Based Reasoning: Techniques for Enterprise Systems**. Morgan Kauffman Publishers Inc. 1997.
9. Riesbeck, C.K. **Inside Case-based Reasoning**. The Institute for the Learning Sciences. Northwestern University, Evanston, Illinois. Laurence Erlbaum Associates. 1989.
10. J.R. Davis, **ASM Specialty Handbook: Aluminum and Aluminum Alloys**.
11. Bouricier, G. F., Dickinson, J., Tessandori, J. and Schiffer, D. **Aluminum Recycling Casebook**, The Aluminum Association, 1985.
12. Caceres, C. H., Djurdjevic, M. B., Stockwell, T. J., Sokolowski, J. H. **The Effect of Cu Content on the Level of Microporosity in Al-Si-Cu-Mg Casting Alloys**. NSERC/Ford/University of Windsor Industrial Research Chair in Light Metals Casting Technology. Internal Report. February 1999.
13. Mackay, R. I. **Quantification of Iron in Al-Si Foundry Alloys via Thermal Analysis.** M.Eng. Thesis. Department of Mining and Metallurgical Engineering. McGill University. December 1996.

14. **Backerud, L. Chai, G., Tamminen, J.** Solidification Characteristics of Aluminum Alloys. **Volume 2, Foundry Alloys, AFS/SKANALUMINIUM, 1990**
15. Mulazimoglu, M. H., Zaluska, A., Gruzleski, J. E. **Microstructure and Thermal Analysis of Strontium Treated Alloys.** American Foundry Society Inc., 1995.
16. StJohn, D. H., Dahle A. K., Easton M. A., Hutt J., Veldman, N. **Solidification of Hypoeutectic Aluminum-Silicon Alloys.** Materials Forum , 1999, Vol. 23, pp. 137-152.
17. Doty, H. W., Samuel, A. M., Samuel F. H. **Factors Controlling the Type and Morphology of Copper-Containing Phases in 318 Aluminum Alloy**. Transactions of the American Foundry Society. Vol 104, 1996, Paper No. 96-30, pp 893-901.
18. Djurdjevic, M., Stockwell, T., Sokolowski, M. **The Effect of Sr on the Microstructure of the Al-Si and Al-Cu Eutectics in the 319 Aluminum Alloy.** International Journal of Cast Metals Research. 1999, 12, 67-73.
19. Tenekedjiev, N., Mulazimogly, H., Closset, B., Gruzleski, J. **Microstructures and Thermal Analysis of Strontium Treated Aluminum-Silicon Alloys.** Amercian Foundry Society Inc. Des Plaines, Illinois, USA, pp 40-41, 1995.
20. Sparkman, D., Kearney, A. **Breakthrough in Aluminum Alloy Thermal Analysis Technology for Process Control.** Transactions of the American Foundry Society Vol 102 , 1994, Paper 94-13, pp. 455-460.
21. Foundry information systems. **MeltLab™ Thermal Analysis Software.** Product Information.
22. Boone, G. W.; Carver, R. F.; Seese R. G. **Optimizing Grain Refiners and Modifiers in Al-Si Alloys.** Modern casting. January 1998, pp. 52 B 54.
23. Apelian D., Sigworth G.T. et al. **Assessment of Grain Refinement and Modification of Al-Si Foundry Alloys by Thermal Analysis.** AFS Transactions. Vol. 92, 1984, pp 297-307.
24. Gloria, D., Gruzleski, J. E., **A Study of the Thermal Analysis Parameters Applied to the Grain Refinement of Al-Si Casting Alloys.** Met Soc, Light Metals 1999, pp 315-327.
25. Hetke, A., Gundlach, R.B. **Aluminum Casting Quality in Alloy 356 Engine Components.** Transactions of the American Foundry Society. Vol 102, 1994, Paper 94-137, pp. 367 –380.
26. John, D., Taylor, J., Dahle, A., K., Nogita, K. **Eutectic Solidification and Porosity Formation in Al-Si Alloys: The Role of Strontium.** Transactions of the American Foundry Society. Vol 108, 2000, Paper No. 00-115, pp 463-470.

27. Stucky, M., Gruzleski, J.E., Anson, J. **Effect of Sr Modification on the Nucleation and Growth of Microporosity During the Solidification of Aluminum -7% Silicon Foundry Alloy.** Transactions of the American Foundry Society. Vol 108, 2000, Paper No. 00-70, pp 419-426.

28. Djurdjevic, M., Gallo, P., Sokolowski, J.H., Jiang, H., **Fading of Sr in the 319 Al alloy during laboratory Thermal Analysis Test.** Transactions of the American Foundry Society, Vol 108, Paper No. 00-20, pp. 485-489, 2000.

29. Argyropoulos, S., Closset, B., Gruzleski, J.E., Oger, H. **The Quantitative Control of Modification in Al-Si Foundry Alloys Using a Thermal Analysis Technique.** Transactions of the American Foundry Society Vol 91, pp 351- 358 Paper 83-27, 1983.

30. Lanker, J. **Non-Equilibrium Solubility of Iron in Aluminum.** Key Engineering Materials. Vol 44, 1990, pp. 135-145.

31. Samuel, A.M., Roy, N. **Porosity formation in Al-Cu Alloys: Role of Intermetallics.** Light Metals Congress 1996, pp 269-284.

32. Spada A. T. **Aluminum Casters Discuss porosity, Melt Quality**. Modern Castings. February 1999 pg. 58-60.

33. Samuel A.M., Samuel F.H., Boudreault, G. Microstructural **Observations of Porosity in A319.2 alloy: Effect of Mould Type and Cooling Rate**. AFS Castexpo 99. March 1999.

34. M.K. Industrievertretungen GmbH. **Thermal Analysis System TA7604D-56459Stalhofen** a.W. Buchenweg 11. http://www.mk-gmbh.de/

35. Samuel A.M. Samuel F.H. Review, **Various Aspects Involved in the Production of Low-hydrogen Aluminum Castings.** Journal of Materials Science. Vol 27, 1992 6533-6563.

36. St. John D., et al. **Eutectic Solidification and Porosity Formation in Al-Si Alloys: The Role of Strontium.** AFS Casting Congress, Pittsburgh, 2000.

37. Liu, H., Sokolowski, J. H. **Effects of Hydrogen on Aluminum and its Alloys.** NSERC/Ford/University of Windsor Industrial Research Chair in Light Metals Casting Technology. Internal Report. June 1997.

38. Yen, C.M., Evans, W.J., Nowicki, R.M., Cole, G.S. **Measuring the Quality of Aluminum Casting Alloys with Microprocessor-Aided Thermal Analysis.** Transactions American Foundry Society Vol 93, 1985, Paper 85-26, pp 199-204.

39. Sillen, R.V. **Artificial Intelligence Technology for Adaptive Evaluation of Cooling Curves.** Ductile Iron News Number 3, 1995, pp 21-22.

40. Sillen, R.V. **Optimization and Quality Assurance of Gray and Ductile Iron by Means of Artificial Intelligence** . Indian Foundry Conference 1996.

41. Li. D., Liu, Y., Zhang, Y., Meng, F. **Study on Thermal Analysis Models Used in Gray Cast Iron Quality Prediction**. International Journal of Cast Metals Research 1999-11, pp 391-394.

42. Mahfoud, M.S. **Controlled Thermal Analysis Using Heat Pipe Technology.** Ph.D. Thesis. Department of Mining and Metallurgical Engineering, McGill University. Montreal, Canada, 1997.

43. Kanicki, D. P. **Changing Casting Demands Shape Ford's New Foundry.** Modern Casting Vol 84, 1994, N 9, pp 24-25.

44. Kierkus, W.T., Sokolowski, J.H. **Recent Advances in CCA: A New Method of Determining Base Line Equation.** Transactions of the American Foundry Society VOL107 Paper No. 99-66, 1999, pp 161-167.

45. Barth, B. A. **The Measurement Problem in Experimental Data.** Lecture Presented to the University of Windsor Class 85-222-01, November 1998.

46. Montgomery, D.C., Runger, G.C. **Gauge capability Analysis and Designed Experiments. Part II: Experimental Design Models and Variance Component Estimation.** Quality Engineering, 6(2), 1993-94, pp. 289-305.

47. Dolezal, K. K., Burdick, R.K. Birch, N.J**. Analysis of a Two-Factor R&R Study with Fixed Operators.** Journal of Quality Technology. Vol. 30, 1998, No. 2.

48. Czitrom, V., Spagon, P.D. **Statistical Case Studies for Industrial Process Improvement.** American Statistical Association. Chapter 6, pp 63 –113.

49. Jiang, H.,Sokolowski, J.H., Djurdjevic, M.B., Evans, W.S. **Recent Advances in Automated Evaluation and on-line prediction of Al-Si Eutectic Modification Level.** Transactions of the American Foundry Society. Vol 108, 2000, Paper No.00-23, pp 505-510.

50. Kasprzak, M., Kasprzak, W., Kierkus, C.A., Kierkus, W.T., Sokolowski, J. H., Evans, W. **The Structure and Matrix Microhardness of the 319 Aluminum Alloy After Isothermal Holding During the Solidification Process.** American Foundry Society Transactions, in press.

51. Box, G.E.,Connor, L. R. et al. **The Design and Analysis of Industrial Experiments**. Imperial Chemical Industries Limited, 1956.

52. Montgomery, D. C., **Introduction to Statistical Quality Control.** John Wiley & Sons, Inc. 1996. Western Electric. Statistical Quality Control Handbook. Western Electric Coorporation, Indianapolis, Ind. 1956

53. Nelson, L. S. **The Shewhart Control Chart – Test for Special Causes.** Journal of Quality

Technology. 1984, Vol. 16.

54. Lu, C., Reynolds, M.R. **Control Charts for Monitoring the Mean and Variance of Autocorrelated Processes.** Journal of Quality Technology. Vol. 31, No. 3, July 1999, pp 259-274.
55. Montgomery, D. C., Mastrangelo, C. M. **Some Statistical Process Control Methods for Autocorrelated Data.** Journal of Quality Technology, Vol. 23.
56. Lucas, J.M., Saccucci, M.S. **Exponentially Weighted Moving Average Control Schemes: Properties and Enhancements.** Technometrics. Feruary 1990, Vol. 32, No.1, pp 1-29.
57. Caspian the Case-based Reasoner. **Caspian and CASL Manuals.** http://www.scs.ryerson.ca/~dgrimsha/courses/cps820/CBRCaspian.html
58. Djurdjevic, M.B., Kierkus, W.T., Byczynski, G.E., Sokolowski, J.H. ***Calculation of Liquidus Temperature for Aluminum 3XX Series of Alloys.*** American Foundry Society Transactions. Vol 98-47 pp. 143 –147.
59. Djurdjevic, M. B., Kierkus, C. A., Northwood, D. O., Sokolowski, J. H. **Improvement of 319 aluminum Alloy Casting Durability by High Temperature Solution Treatment.** Journal of Advanced Material Processing Technology, in press.
60. Campbell, G. T., Danilak S.A. **Enhanced Ti-Al Grain Refiners.** Light Metals. The Minerals, Metals and Materials Society, 1991, pp 831-836.
61. Gonzales, A. J., Xu, L., Gupta, U. M. **Validation Techniques for Case-Based Reasoning Systems.** IEEE Transactions on Systems, Man and Cybernetics – Part A: Systems and Humans, Vol. 28, No. 4, July 1998.

APPENDIX I

DESCRIPTION OF THERMAL ANALYSIS PARAMETERS

The following figure identifies the time, temperature and fraction solid parameters used during this work:

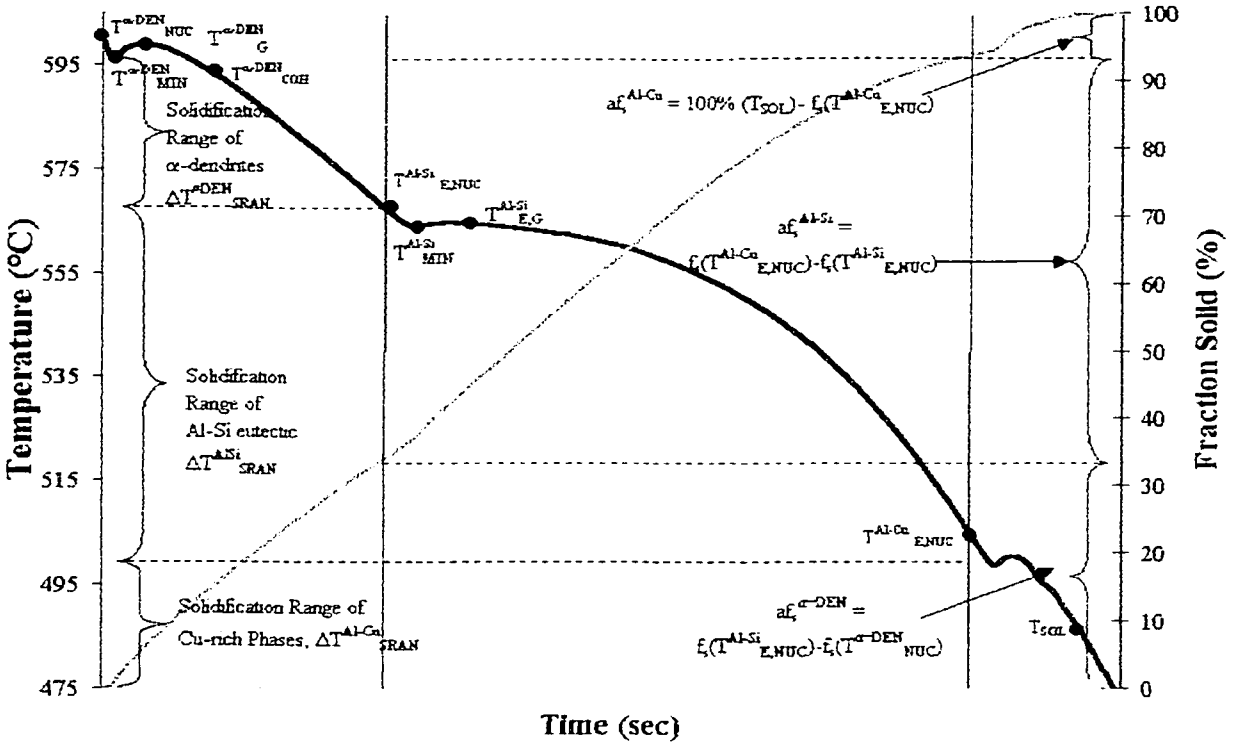

Figure I-1 – Identification of Characteristic Points and Parameters on a Cooling Curve and Fraction Solid Curve of Unmodified and Non Grain Refined W319-Al Alloy.

The metallurgical meaning of these parameters is presented in Table I-1[6].

Table I-1 – Description of Thermal Analysis Parameters[6].

AlTAS Symbol			Description	Metallurgical Significance
Temperature (°C)	**Time (sec)**	**Fraction Solid (%)**		
$T^{\alpha DEN}_{NUC}$	$t^{\alpha DEN}_{NUC}$	$fs^{\alpha DEN}_{NUC}$	α-Al dendrite nucleation	This is the point at which stable α-Al dendrites nucleate and begin to solidify in the melt. This point also marks the beginning of mass feeding.
$T^{\alpha DEN}_{MIN}$	$t^{\alpha DEN}_{MIN}$	$fs^{\alpha DEN}_{MIN}$	α-Al dendrite undercooling	Point at which the latent heat generated during dendrite nucleation equals the heat loss of the sample. After this point the temperature of the melt rises to the steady state growth temperature.
$T^{\alpha DEN}_{G}$	$t^{\alpha DEN}_{G}$	$fs^{\alpha DEN}_{G}$	α-Al dendrite growth (or recalescence)	Steady state growth temperature of the α-Al dendrites. After this point the heat loss of the sample starts again.
$T^{\alpha DEN}_{COH}$	$t^{\alpha DEN}_{COH}$	$fs^{\alpha DEN}_{COH}$	Dendrite Coherency Point (DCP)	At this point the dendrite tips of neighboring grains come in contact becoming fixed at their locations forming a skeleton throughout the sample. This point marks the transition from mass feeding to interdendritic feeding.

Table I-2 – Description of Thermal Analysis Parameters (continued)

AlTAS Symbol			Description	Metallurgical Significance
Temperature (°C)	**Time (sec)**	**Fraction Solid (%)**		
$T^{Al\text{-}Si}_{E.NUC}$	$t^{Al\text{-}Si}_{E.NUC}$	$fs^{Al\text{-}Si}_{E.NUC}$	Al-Si Eutectic Nucleation	As dendrites nucleate in the samples, the composition of the remaining liquid reaches the eutectic composition and the Al-Si eutectic begins to nucleate and grow.
$T^{Al\text{-}Si}_{E.MIN}$	$t^{Al\text{-}Si}_{E.MIN}$	$fs^{Al\text{-}Si}_{E.MIN}$	Al-Si Eutectic Minimum	Point after stable co-precipitation of Al and Si when latent heat generation equals the heat loss of the sample and appears as a minimum in the Al-Si region of the cooling curve.
$T^{Al\text{-}Si}_{E.G}$	$t^{Al\text{-}Si}_{E.G}$	$fs^{Al\text{-}Si}_{E.G}$	Al-Si Eutectic Growth	Point at which considerable eutectic growth occurs. These parameters are used to gauge the morphology of the Al-Si structure.
$T^{Al\text{-}Cu}_{E.NUC}$	$t^{Al\text{-}Cu}_{E.NUC}$	$fs^{Al\text{-}Cu}_{E.NUC}$	Al-Cu Eutectic Nucleation	Start of the formation of the Al-Cu eutectic as the remaining liquid becomes enriched with Cu and Si. The temperature and duration of this phenomenon can be used to establish adequate solution treatment parameters.

Table I-3 – Description of Thermal Analysis Parameters (continued)

AlTAS Symbol			Description	Metallurgical Significance
Temperature (°C)	**Time (sec)**	**Fraction Solid (%)**		
T_{SOL}	t_{SOL}	fs_{SOL}	Solidus	End of the solidification process.
$\Delta T^{\alpha\text{-}DEN}{}_{SRAN}$	$\Delta t^{\alpha\text{-}DEN}{}_{SRAN}$	$af_s{}^{\alpha\text{-}DEN}{}_{SRAN}$	Solidification range of α-Al dendrites prior to Al-Si nucleation	These parameters measure the temperature range, duration and fraction solid that forms during mass feeding.
$\Delta T^{\alpha\text{-}DEN}{}_{IDF}$	$\Delta t^{\alpha\text{-}DEN}{}_{IDF}$	$af_s{}^{\alpha\text{-}DEN}{}_{IDF}$	Solidification range of α-Al dendrites after DCP and before Al-Si Nucleation.	These parameters characterize the interdendritic feeding mode of the alloy. The longer the solidification time between DCP and prior to Al-Si nucleation the higher the surface area of the dendrites that will form making feeding of shrinkage voids through interdendritic channels more tortuous.
$\Delta T^{Al\text{-}Si}{}_{SRAN}$	$\Delta t^{Al\text{-}Si}{}_{SRAN}$	$af_s{}^{Al\text{-}Si}{}_{SRAN}$	Solidification range of the Al-Si eutectic	These parameters represent the solidification temperature range, duration and fraction solid that forms within the test sample during the Al-Si eutectic reaction.

Table I-4 – Description of Thermal Analysis Parameters (continued)

AlTAS Symbol			Description	Metallurgical Significance
Temperature (°C)	**Time (sec)**	**Fraction Solid (%)**		
$\Delta T^{Al\text{-}Cu}{}_{SRAN}$	$\Delta t^{Al\text{-}Cu}{}_{SRAN}$	$af_s^{Al\text{-}Cu}{}_{SRAN}$	Solidification range of Al-Cu Eutectic	These parameters represent the solidification temperature range, duration and fraction solid that forms within the test sample during the Al-Cu eutectic reaction.
$\Delta T^{Al\text{-}Si}{}_{E.G.MOD}$	-	-	Al-Si eutectic depression	This parameter is calculated by comparing the Al-Si eutectic growth temperature of an unmodified and a modified alloy. This parameter is commonly used to determine silicon particle modification.
$\Delta T^{\alpha\text{-}DEN}{}_{U}$	-	-	Grain Refiner Potential	The difference between the α-Al minimum and growth temperatures is a parameter commonly used to evaluate the potency of grain refiners and therefore the level of grain refinement of the structure.

APPENDIX II

EXPERIMENTAL RESULTS

Table II-1 – Experimental Results

Day of Sampling	Thermal Analysis Sample Number	Thermal Analysis Parameters									
		Cooling rate (°C/sec)	T^{a-DEN}_{NUC} (°C)	t^{a-DEN}_{MIN} (sec)	T^{a-DEN}_{MIN} (°C)	Σ_{CS-DEN} MIN (%)	t^{a-DEN}_{D} (sec)	T^{a-DEN}_{D} (°C)	Σ^{a-DEN}_{D} (%)	t^{a-DEN}_{CEM} (sec)	T^{a-DEN}_{CEM} (°C)	Σ^{a-DEN}_{CEM} (%)
1	1	0.36	613.59	22.20000076	595.00	5.78	28.80	595.44	9.77	31.80	595.24	11.44
	2	0.38	617.71	26.39999962	595.50	7.31	28.00	595.52	8.26	34.40	595.13	11.85
	3	0.36	610.49	20	595.39	5.72	26.40	595.65	9.48	30.40	595.39	11.68
	4	0.36	610.85	19	595.52	5.21	25.80	595.89	9.27	29.40	595.67	11.26
2	1	0.35	613.57	26.60	595.42	8.22	26.60	595.42	8.22	36.00	594.64	13.38
	2	0.34	608.20	17.20	595.03	4.65	28.00	595.79	10.99	31.40	595.58	12.81
	3	0.31	613.09	25.60	595.32	6.10	33.60	595.64	10.43	38.40	595.34	12.83
3	1	0.35	616.28	26.80	595.79	7.86	28.40	595.82	8.77	35.60	595.33	12.64
	2	0.35	618.91	27.60	595.97	7.00	33.20	596.13	10.17	38.60	595.76	13.03
	3	0.31	606.19	15.40	595.42	3.70	27.80	596.18	10.23	30.60	596.06	11.60
	4	0.33	607.61	16.40	595.13	4.09	28.00	595.93	10.49	31.20	595.77	12.12
4	1	0.36	630.44	28.60	596.76	5.42	36.80	597.28	10.31	40.40	597.06	12.30
	2	0.31	611.36	21.80	596.21	5.23	30.60	596.61	9.70	34.20	596.42	11.40
	3	0.29	605.28	13.40	595.15	2.73	27.60	596.46	9.98	29.60	596.40	10.91
	4	0.29	605.65	15.00	595.08	3.24	27.80	595.99	9.60	31.00	595.86	11.06
2	4	0.26	603.62	15.80	594.75	3.21	34.40	596.18	11.97	27.60	595.96	8.88
2	5	0.27	604.39	16.80	594.71	3.78	32.80	595.90	11.65	34.20	595.88	12.29
3	5	0.27	604.59	15.80	594.96	3.16	34.20	596.49	11.56	27.80	596.28	8.75
4	5	0.26	604.50	17.40	595.80	3.71	34.40	596.99	11.44	42.80	596.46	14.77
5	1	0.36	623.29	29.6	594.61	7.03	29.60	594.61	7.03	37.00	592.89	10.79
	2	0.37	608.63	19.6	594.31	6.03	19.60	594.31	6.03	29.00	593.38	11.11
	3	0.40	613.95	22.2	594.45	7.19	22.20	594.45	7.19	28.20	593.76	10.84
6	1	0.35	606.23	19	594.21	5.97	19.00	594.21	5.97	26.20	593.66	9.80
	2	0.36	611.80	23.4	594.04	6.75	23.40	594.04	6.75	31.40	592.95	10.97
7	1	0.35	613.00	23.2	593.47	5.49	32.60	593.96	11.05	36.00	593.79	12.92
	2	0.34	609.16	19.8	593.37	5.06	30.60	594.00	11.36	33.40	593.89	12.88
	3	0.34	606.48	16.6	593.43	4.07	30.00	594.49	11.86	33.40	594.32	13.67
8	1	0.36	608.89	17	595.43	4.75	25.40	595.72	9.78	31.40	595.26	13.09
	2	0.37	609.99	18.8	595.39	5.64	25.40	595.62	9.67	30.40	595.27	12.52
	3	0.37	609.65	18.6	595.22	5.56	25.00	595.42	9.46	30.40	595.07	12.54

Table II-2 – Experimental Results (continued)

t^{ABS}_{NUC} (sec)	T^{ABS}_{NUC} (°C)	ξ^{ABS}_{NUC} (%)	t^{ABS}_{MIN} (sec)	T^{ABS}_{MIN} (°C)	ξ^{ABS}_{MIN} (%)	t^{ABS}_{α} (sec)	T^{ABS}_{α} (°C)	ξ^{ABS}_{α} (%)	t^{ABS}_{NUC} (sec)	T^{ABS}_{NUC} (°C)	ξ^{ABS}_{NUC} (%)	t^{SOL} (sec)	T^{SOL} (°C)	$a\xi_{ABS-DEN}$ (%)	$a\xi^{ABS}$ (%)	$a\xi^{ABS}_{\alpha}$ (%)	Hydrogen level (ml H$_2$/100 gAl)	Cooling rate (°C/sec)
74.20	576.45	27.62	126.60	563.81	49.65	126.60	563.81	49.65	270.00	506.25	92.19	318.40	481.64	16.18	64.57	7.81	0.101	0.41
84.60	572.52	31.49	120.60	564.59	47.47	120.60	564.59	47.47	262.20	506.81	91.88	312.40	480.92	19.65	60.39	8.12	0.114	0.44
81.40	572.60	30.61	117.60	564.97	46.05	117.60	564.97	46.05	268.80	506.45	91.89	321.20	479.47	18.93	61.27	8.11	0.114	0.41
85.60	570.97	32.52	119.40	564.88	47.45	119.40	564.88	47.45	266.40	506.36	91.97	317.20	480.36	21.26	59.45	8.03	0.105	0.41
88.20	571.97	32.13	131.40	563.25	49.84	131.40	563.25	49.84	286.20	505.13	92.47	346.80	474.57	18.76	60.34	7.53	0.144	0.40
90.40	569.63	33.91	124.80	563.63	48.40	124.80	563.63	48.40	278.60	505.24	92.75	336.00	475.16	21.10	58.83	7.25	0.144	0.39
97.80	572.19	31.95	145.40	563.26	49.31	145.40	563.26	49.31	319.80	504.48	92.59	384.20	475.13	19.12	60.63	7.42	0.138	0.36
94.00	570.28	33.98	128.60	563.91	48.30	128.60	563.91	48.30	283.80	506.06	92.50	337.00	480.34	21.34	58.52	7.50	0.149	0.43
92.20	572.83	32.41	134.80	563.89	49.57	134.80	563.89	49.57	287.00	506.21	92.38	340.40	480.12	19.38	59.97	7.62	0.123	0.40
68.20	582.59	24.84	129.20	564.52	45.30	129.20	564.52	45.30	305.40	505.02	92.38	359.40	481.37	13.24	67.54	7.62	0.138	0.34
94.40	569.21	33.75	126.00	564.13	46.51	126.00	564.13	46.51	288.60	505.47	92.44	342.00	479.78	21.63	58.69	7.56	0.138	0.37
99.60	569.09	34.21	133.20	563.40	48.67	133.20	563.40	48.67	279.80	507.02	93.04	327.60	480.80	21.91	58.82	6.96	0.153	0.46
101.40	570.07	32.70	144.00	562.96	48.22	144.00	562.96	48.22	316.20	505.52	92.77	371.20	480.46	21.31	60.07	7.23	0.153	0.35
102.60	569.14	33.51	142.80	562.91	47.73	142.80	562.91	47.73	322.60	504.66	92.88	375.60	481.32	22.60	59.37	7.12	0.153	0.33
66.60	584.68	23.31	147.80	562.54	49.39	147.80	562.54	49.39	321.60	504.87	93.09	373.20	481.54	12.25	69.78	6.91	0.153	0.33
135.60	566.85	40.46	165.20	564.18	50.42	165.20	564.18	50.42	366.00	503.02	93.35	429.20	476.38	31.58	52.89	6.65	0.138	0.29
110.60	570.90	34.68	162.80	563.76	52.26	162.80	563.76	52.26	347.40	505.34	93.56	414.80	473.33	22.40	58.88	6.44	0.144	0.31
103.20	575.00	31.51	165.00	564.40	50.85	165.00	564.40	50.85	353.00	505.14	93.12	409.80	480.76	22.76	61.61	6.88	0.138	0.30
78.20	585.79	24.61	181.80	563.22	53.45	181.80	563.22	53.45	379.20	503.01	94.00	436.40	477.63	9.84	69.39	6.00	0.153	
57.40	582.54	18.48	117.00	563.70	42.68	117.00	563.70	42.68	278.40	504.53	92.03	362.20	455.16	7.69	73.55	7.97	0.108	0.46
78.00	570.46	29.32	110.20	563.80	43.38	110.20	563.80	43.38	266.40	503.75	91.90	348.00	453.93	18.21	62.58	8.10	0.108	0.44
80.40	568.16	32.74	102.40	563.80	43.60	102.40	563.80	43.60	245.40	504.67	91.87	321.60	455.89	21.90	59.13	8.13	0.108	0.49
77.00	571.63	28.12	113.00	563.49	42.81	113.00	563.49	42.81	279.20	503.60	92.06	358.80	458.31	18.32	63.94	7.94	0.105	0.41
73.40	573.08	26.27	112.00	563.48	42.39	112.00	563.48	42.39	271.80	504.40	91.71	356.00	453.77	15.30	65.44	8.29	0.102	0.44
89.20	572.57	33.22	130.20	563.32	50.13	130.20	563.32	50.13	276.00	505.81	92.41	338.40	471.81	20.30	59.19	7.59	0.123	0.42
86.80	572.21	32.93	126.60	563.60	49.26	126.60	563.60	49.26	274.80	506.22	92.61	335.60	472.51	20.05	59.67	7.39	0.123	0.41
85.20	572.59	32.36	124.80	563.98	48.34	124.80	563.98	48.34	277.40	505.77	92.75	337.40	472.73	18.69	60.39	7.25	0.12	0.40
78.80	573.58	30.78	121.40	564.24	48.89	121.40	564.24	48.89	267.60	506.46	92.49	329.20	471.18	17.69	61.71	7.51	0.108	0.42
76.80	574.07	30.60	117.60	564.34	48.23	117.60	564.34	48.23	261.20	506.16	92.44	321.40	471.04	18.08	61.84	7.56	0.101	0.43
83.00	571.32	32.95	118.20	564.31	48.66	118.20	564.31	48.66	261.00	506.14	92.56	320.00	471.61	20.41	59.61	7.44	0.109	0.43

Table II-3 – Experimental Results (continued)

Test Sample Microstructures							Micro Hardness		Chemical Composition								
Porosity		Silicon		Copper													
Area Fraction	Area Percent	Modification Level	Area Fraction	Area Percent	Area Fraction	Area Percent	HV25	Stdlev	Si (wt%)	Cu (wt%)	Fe (wt%)	Mg (wt%)	Mn (wt%)	Zn (wt%)	Ti (wt%)	Sr (wt%)	Ni (wt%)
0.003	0.30	1	0.08	8.00	0.03	2.91	75.01	9.27	7.6164	3.3592	0.3871	0.3007	0.2387	0.1376	0.1145	0.0008	0.019
0.002	0.20	1	0.07	7.29	0.04	3.70	72.33	6.71	7.6164	3.3592	0.3871	0.3007	0.2387	0.1376	0.1145	0.0008	0.019
0.002	0.20	1	0.08	8.17	0.04	3.54	75.62	8.56	7.6164	3.3592	0.3871	0.3007	0.2387	0.1376	0.1145	0.0008	0.019
0.002	0.2	1	0.08	7.62	0.02	2.26	72.99	8.36	7.5547	3.4303	0.3808	0.3091	0.2376	0.1375	0.1137	0.0008	0.0194
0.002	0.22	1.00	0.08	8.12	0.03	3.06	71.67	6.22	7.5424	3.3654	0.3749	0.276	0.2476	0.1198	0.1174	0.0007	0.0215
0.002	0.23	1.00	0.08	7.70	0.03	2.73	77.33	9.11	7.5424	3.3654	0.3749	0.276	0.2476	0.1198	0.1174	0.0007	0.0215
0.002	0.23	1.00	0.08	7.95	0.02	2.44	76.79	8.45	7.5424	3.3654	0.3749	0.276	0.2476	0.1198	0.1174	0.0007	0.0215
0.003	0.25	1.00	0.08	7.68	0.04	3.47	73.08	9.06	7.484	3.3943	0.3653	0.2648	0.2432	0.1183	0.1171	0.0007	0.0168
0.002	0.23	1.00	0.08	7.81	0.03	2.92	70.87	8.60	7.484	3.3943	0.3653	0.2648	0.2432	0.1183	0.1171	0.0007	0.0168
0.002	0.24	1.00	0.08	7.87	0.02	2.33	75.55	8.05	7.484	3.3943	0.3653	0.2648	0.2432	0.1183	0.1171	0.0007	0.0168
0.003	0.26	1.00	0.08	7.66	0.03	3.22	76.95	6.89	7.484	3.3943	0.3653	0.2648	0.2432	0.1183	0.1171	0.0007	0.0168
0.002	0.24	1.00	0.07	7.42	0.03	2.27	74.59	9.63	7.5355	3.4084	0.3558	0.2806	0.2399	0.09	0.1169	0.0007	0.0175
0.002	0.24	1.00	0.08	7.88	0.03	3.32	70.43	7.17	7.5355	3.4084	0.3558	0.2806	0.2399	0.09	0.1169	0.0007	0.0175
0.002	0.26	1.00	0.08	7.91	0.03	2.83	76.18	10.05	7.5355	3.4084	0.3558	0.2806	0.2399	0.09	0.1169	0.0007	0.0175
0.002	0.20	1.00	0.07	7.35	0.04	3.54	73.57	8.08	7.5355	3.4084	0.3558	0.2806	0.2399	0.09	0.1169	0.0007	0.0175
0.002	0.21	1.00	0.07	7.50	0.02	2.43	74.34	7.14	7.4947	3.3302	0.3775	0.2733	0.2449	0.1195	0.1179	0.0007	0.0214
0.002	0.23	1.00	0.08	7.88	0.03	2.89	72.45	9.38	7.4947	3.3302	0.3775	0.2733	0.2449	0.1195	0.1179	0.0007	0.0214
0.002	0.22	1.00	0.08	7.77	0.03	2.84	77.08	5.88	7.484	3.3943	0.3653	0.2648	0.2432	0.1183	0.1171	0.0007	0.0168
0.003	0.25	1.00	0.08	7.57	0.03	3.36	72.48	9.58	7.5355	3.4084	0.3558	0.2806	0.2399	0.09	0.1169	0.0007	0.0175
0.001	0.14	1	0.07	7.29	0.03	2.54	71.77	6.72	7.577	3.48	0.369	0.2804	0.2509	0.1046	0.1154	0.0007	0.0201
0.002	0.20	1	0.08	8.27	0.03	2.73	73.62	9.87	7.577	3.48	0.369	0.2804	0.2509	0.1046	0.1154	0.0007	0.0201
0.002	0.25	1	0.08	8.00	0.03	2.82	70.76	7.18	7.577	3.48	0.369	0.2804	0.2509	0.1046	0.1154	0.0007	0.0201
0.002	0.25	1	0.07	7.29	0.03	2.65	73.40	7.42	7.5562	3.3703	0.3738	0.2794	0.2481	0.0945	0.1162	0.0007	0.0213
0.001	0.08	1	0.07	7.23	0.26	2.62	76.16	6.26	7.5562	3.3703	0.3738	0.2794	0.2481	0.0945	0.1162	0.0007	0.0213
0.002	0.18	1	0.08	8.14	0.03	2.54	74.57	3.58	7.5147	3.5814	0.3705	0.2934	0.24	0.1088	0.1124	0.0007	0.0157
0.002	0.23	1	0.08	7.76	0.03	2.60	73.50	8.20	7.5147	3.5814	0.3705	0.2934	0.24	0.1088	0.1124	0.0007	0.0157
0.002	0.17	1	0.07	7.40	0.03	2.82	71.69	6.84	7.5147	3.5814	0.3705	0.2934	0.24	0.1088	0.1124	0.0007	0.0157
0.002	0.24	1	0.07	7.39	0.03	3.15	73.08	9.76	7.5883	3.5071	0.3797	0.2896	0.2421	0.13	0.1205	0.0007	0.0222
0.003	0.30	1	0.08	7.95	0.03	2.85	70.43	8.75	7.5883	3.5071	0.3797	0.2896	0.2421	0.13	0.1205	0.0007	0.0222
0.003	0.30	1	0.07	7.22	0.03	3.02	74.59	5.36	7.5857	3.4486	0.3848	0.2835	0.2443	0.1303	0.1205	0.0007	0.0219
							REF VAL		8.36								

Table II-4 – Experimental Results (continued)

Chemical Composition				3.0L Casting Mechanical Properties						3.0L Casting Microstructures				
					Tensile Properties				HB500	Porosity		Silicon		
Sn (wt%)	Pb (wt%)	Cr (wt%)	Sb (wt%)	Casting Number	2% YS(Mpa)	2% YS(KSI)	UTS (Mpa)	UTS (KSI)	Percent Elongation	Inboard	Area Fraction	Area Percent	Modification	Area Fraction
0.0037	0.0095	0.0488	0.0002	142196	33.25	229.34	33.8	232.86	0.58	104.5	0.001	0.093	1	0.07
				bh3	31.9	219.47	33.7	232.27	0.43	104.5	0.002	0.157	1	0.07
0.0037	0.0095	0.0488	0.0002	142144	36.9	254.06	37.1	255.55	0.79	96.5	0	0.07	1	0.07
				bh3	35.45	244.36	37.25	256.51	0.525	96	0.002	0.157	1	0.07
0.0037	0.0095	0.0488	0.0002	142211	30.9	212.76	32.3	222.51	0.74	98	0.002	0.231	1.1	0.07
				bh3	32.1	221.375	33.55	231.34	0.825	100	0	0.100	1	0.07
0.0041	0.0097	0.0489	0.0002	142213	32.75	225.69	34.4	236.90	0.81	100	0.001	0.062	1	0.07
				bh3	31.6	217.605	32.75	225.71	0.44	98	0.006	0.600	1	0.08
0.0026	0.0093	0.0684	0.0005	204848	29	199.86					0.001	0.128	1	0.08
				bh3	29.35	202.015					0.002	0.174	1	0.07
0.0026	0.0093	0.0684	0.0005	204782	26.7	183.84	31.15	214.82	0.47	94.5	0.000	0.026	1	0.09
				bh3	31.4	216.445	33.85	232.94	0.745	96.5	0.000	0.007	1	0.08
0.0026	0.0093	0.0684	0.0005	204859	29.95	206.21	33.45	229.84	0.68	100	0.001	0.131	1	0.07
				bh3	31.9	219.815	33.8	232.79	0.61	94.5	0.001	0.13	1	0.07
0.0031	0.0090	0.059	0.0001	734585	32.1	220.94	32.9	226.69	0.705	96.5	0.001	0.100	1	0.07
				bh3	32.2	221.84	33.2	228.84	0.815	98	0.002	0.237	1	0.08
0.0031	0.0090	0.059	0.0001	734596	28.7	197.87	33.25	229.07	0.455	93	0.001	0.126	1	0.08
				bh3	33.2	228.565	34.8	239.70	0.61	98	0.003	0.3	1	0.07
0.0031	0.0090	0.059	0.0001	734567	32	220.5	32.4	223.50	0.58	104.5	0.005	0.541	1	0.07
				bh3	29.9	206.04	33.5	230.95	0.68	104.5	0.001	0.122	1	0.09
0.0031	0.0090	0.059	0.0001	734597	32	220.365	34	234.30	0.83	96.5	0.002	0.188	1	0.08
				bh3	30.5	210.145	32.8	225.94	0.705	94.5	0.002	0.24	1	0.07
0.0026	0.0080	0.0618	0.0004	221673	30.6	210.99	27.1	187.01	0.445	96.5	0.003	0.281	1	0.08
				bh3	30.2	208.36	31.9	219.99	0.645	102.5	0.021	0.207	1	0.07
0.0026	0.0080	0.0618	0.0004	221685	24	165.145	28.05	193.01	0.6	93	0.002	0.173	1	0.08
				bh3	29	199.9	31.25	215.33	0.76	96.5	0.002	0.244	1	0.07
0.0026	0.0080	0.0618	0.0004	221862	30.5	209.995	30.8	212.27	0.585	96.5	0.002	0.223	1	0.08
				bh3	29.97	206.46	31.55	217.40	0.32	101	0.001	0.096	1	0.07
0.0026	0.0080	0.0618	0.0004	221876	30.1	207.38	31.3	215.57	0.9	96.5	0.002	0.173	1	0.07
				bh3	27.85	191.885	31.05	214.18	0.785	96.5	0.001	0.071	1	0.07
0.0026	0.0097	0.0674	0.0006	204852	30.44	209.6	31.2	215.28	0.93	94.5	0.002	0.226	1	0.07
				bh3	28.85	198.7	31.45	216.77	0.75	94.5	0.002	0.169	1	0.08
0.0026	0.0097	0.0674	0.0006	204877	31.55	217.29	32.55	224.29	0.48	93	0.002	0.174	1	0.08
				bh3	29.65	204.185	32.5	223.82	0.56	94.5	0.002	0.21	1	0.08
0.0031	0.009	0.059	0.0001	734600	29.3	201.755	31.5	216.83	0.455	100	0.002	0.239	1	0.07
				bh3	30	206.76	31.6	217.70	0.87	100	0.001	0.116	1	0.08
0.0026	0.0080	0.0618	0.0004	221674	30.25	208.52	31.85	219.45	0.72	93	0.004	0.379	1	0.08
				bh3	27.7	190.97	32	220.69	0.59	96.5	0.003	0.298	1	0.08
0.006	0.0146	0.0508	0.0005	-										
0.006	0.0146	0.0508	0.0005	-										
0.006	0.0146	0.0508	0.0005	-										
0.0064	0.0125	0.0563	0.0002	-										
0.0064	0.0125	0.0563	0.0002	-										
0.0044	0.0108	0.0556	0	-										
0.0044	0.0108	0.0556	0	-										
0.0044	0.0108	0.0556	0	-										
0.0038	0.0101	0.0594	0.0003	-										
0.0038	0.0101	0.0594	0.0003	-										
0.0038	0.01	0.0597	0.0003	-										

Table II-5 – Experimental Results (continued)

	3.0L Casting Microstructures							
	Silicon	Copper		Micro Hardness				
	Area Percent	Area Fraction	Area Percent	HV25	StdDev	Homogeneity Factor
				92.79	5.37	0.36
	7.37	0.02	2.00	96.65	11.50	-0.38
	7.14	0.02	1.73	101.00	3.18	0.62
	6.84	0.01	0.52	95.81	6.81	0.18
	7.32	0.00	0.32	98.71	6.44	0.23
	7.28	0.02	1.68	93.71	5.51	0.34
	7.28	0.01	1.23	91.47	5.23	0.37
	7.49	0.01	1.31	96.69	6.65	0.20
	7.86	0.00	0.41	95.90	6.51	0.22
	7.73	0.01	1.39	97.71	5.75	0.31
	6.89	0.01	0.55	92.15	7.19	0.14
	8.42	0.02	2.44	100.11	4.28	0.49
	7.89	0.02	1.76	99.81	4.19	0.50
	7.24	0.02	1.68	93.51	9.41	-0.13
	7.20	0.01	1.24	95.55	7.52	0.10
	7.47	0.02	2.45	89.61	4.81	0.42
	7.56	0.02	1.53	92.13	5.28	0.37
	8.20	0.01	1.33	94.07	3.48	0.58
	7.40	0.01	1.11	96.79	5.72	0.32
	7.50	0.01	1.22	91.39	8.31	0.01
	9.37	0.01	1.15	89.87	5.76	0.31
	7.54	0.02	2.39	86.84	9.13	-0.09
	7.27	0.02	1.75	91.78	8.14	0.03
	8.16	0.02	1.77	94.27	7.73	0.07
	6.50	0.01	1.49	92.38	6.37	0.24
	7.74	0.02	2.29	87.53	5.73	0.31
	7.02	0.02	1.85	93.05	6.81	0.19
	8.21	0.02	1.70	96.70	4.77	0.43
	7.01	0.01	1.45	88.78	5.75	0.31
	7.44	0.02	2.23	96.14	4.72	0.43
	6.57	0.01	1.26	94.24	6.71	0.20
	7.36	0.01	1.46	95.33	6.86	0.18
	7.72	0.02	1.96	96.56	6.25	0.25
	8.03	0.02	2.34	93.12	7.92	0.05
	8.31	0.02	1.79	87.87	6.37	0.24
	7.20	0.02	1.88	98.27	6.76	0.19
	8.18	0.01	1.07	91.44	5.26	0.37
	7.78	0.01	0.64	94.85	7.73	0.07
	8.14	0.01	1.08	99.56	8.11	0.03

APPENDIX III

SOURCE CODE OF THE CASE BASED REASONING SYSTEM

This appendix includes the source code of the system except the case library. One case is included at the end of the code as an example and the rest of the cases are summarized in the form of a Table in Appendix VI.

```
~AlTAS case base including information for 2 sections of 2 types of
blocks
~representing four possible cooling rates


introduction is

      '\t\t\t\tAlTAS Case-Base'

end;

~This section defines all the input variables

case definition is

      field coolrate_factor type is (CR50,CR49,CR48,CR47,CR46,CR45,CR44,
                                     CR43,CR42,CR41,CR40,CR39,CR38,
                                     CR37,CR36,CR35,CR34,CR33,CR32,
                                     CR31,CR30,CR0)
            weight is 5
            prompt is ['Enter the cooling rate:'];
      field Modification type is (mod,unmod,part_mod)
            weight is 0
            prompt is ['Enter modification level:'];
      field casting_section type is (BB46,MBS46,BB3_25,MBS3_25)
            weight is 0
            prompt is ['Enter the casting section to predict:'];
      field Target_modification_level type is number
            weight is 0
            prompt is ['Enter the expected modification level'];
      field Mg type is number
            weight is 0
            prompt is ['Enter the Mg level'];
      field Cu type is number
            weight is 0
            prompt is ['Enter the Cu level'];
      field Zn type is number
            weight is 0
            prompt is ['Enter the Zn level'];
      field Si type is number
            weight is 0
            prompt is ['Enter the Si level'];
      field Initial_Sample_Temperature type is number
```

```
            weight is 20
            prompt is ['Enter the Initial_Sample_Temperature:'];
      field Liquidus_Temperature type is number
            weight is 10
            prompt is ['Enter Liquidus Temp:'];
      field Liquidus_Undercooling_Temperature type is number
            weight is 10
            prompt is ['Enter the Liquidus Min Temp:'];
      field Liquidus_Undercooling_Time type is number
            weight is 10
            prompt is ['Enter the Liquidus Min time:'];
      field Liquidus_Recalescence_Temperature type is number
            weight is 0
            prompt is ['Enter the Liquidus_Recalescence_Temperature:'];
      field Coherency_Temperature type is number
            weight is 10
            prompt is ['Enter the Coherency_Temperature:'];
      field Coherency_Time type is number
            weight is 5
            prompt is ['Enter the Coherency_Time:'];
      field afs_alphaDENIDF type is number
            weight is 5
            prompt is ['Enter the afs_alphaIDF:'];
      field AlSiNucleation_Temperature type is number
            weight is 0
            prompt is ['Enter the AlSiNucleation_Temperature:'];
      field AlSiNucleation_Time type is number
            weight is 0
            prompt is ['Enter the AlSiNucleation_Time:'];
      field deltaT type is number
            weight is 10
            prompt is ['Enter deltaT :'];
      field AlCuEutectic_Time type is number
            weight is 5
            prompt is ['Enter the AlCuEutectic_Time:'];
      field AlCuEutectic_Temperature type is number
            weight is 5
            prompt is ['Enter the AlCuEutectic_Temperature:'];
      field Solidus_Temperature type is number
            weight is 10
            prompt is ['Enter the Solidus_Temperature:'];
      field Solidus_Time type is number
            weight is 15
            prompt is ['Enter the Solidus_Time:'];

end;

~The case base structure is based on the cooling rate of the casting
~for which properties will be predicted, modification condition
~and finally based on the cooling rate of the test sample

index definition is

      index on Modification;
      index on casting_section;
end;


modification definition is
```

```
~Define similar cooling rates
      abstraction CR48 is (CR50);
      abstraction CR49 is (CR50);
      abstraction CR44 is (CR45);
      abstraction CR43 is (CR45);
      abstraction CR46 is (CR45);
      abstraction CR47 is (CR45);
      abstraction CR36 is (CR35, CR37);
      abstraction CR37 is (CR35, CR36);
      abstraction CR33 is (CR35, CR34);
      abstraction CR34 is (CR35, CR33);
      abstraction CR38 is (CR39, CR40);
      abstraction CR41 is (CR40, CR42);
      abstraction CR42 is (CR40, CR41);
      abstraction CR31 is (CR30, CR32);
      abstraction CR32 is (CR30, CR31);
      abstraction any_section is (BB46,MBS46,
                        BB3_25,MBS3_25);

      abstraction CR45 is (CR44, CR43, CR46, CR47);
      abstraction CR35 is (CR36, CR37, CR33, CR34);
      abstraction CR40 is (CR38, CR41, CR42);
      abstraction CR39 is (CR40);
      abstraction CR30 is (CR31, CR32);

~Define similiar ranges for TA parameters

~For different modification levels
      field deltaT similar range -3.5 to 6.5;
      field deltaT similar range 6.6 to 8.5;
      field deltaT similar range 8.6 to 9.75;
      field deltaT similar range 9.8 to 10.5;
      field deltaT similar range 10.6 to 12;

~For correct and incorrect liquidus interval
      field Liquidus_Temperature similar range 599 to 610.5;
      field Liquidus_Temperature similar range 610.6 to 635;

~For WAP range without grain refiner, high and low
      field Liquidus_Recalescence_Temperature similar range 597.5 to
599;
      field Liquidus_Recalescence_Temperature similar range 595.2 to
597.42;
      field Liquidus_Recalescence_Temperature similar range 590 to
595.2;

~Normal WAP range
      field AlCuEutectic_Temperature similar range 503.6 to 506.98;

~Correct and low temperature range
      field Solidus_Temperature similar range 470 to 482;
      field Solidus_Temperature similar range 454.16 to 469.9;

~Samples with high mass, low cooling rate
      field Solidus_Time similar range 353 to 434;

~Adequate sample size and cooling rate
```

```
      field Solidus_Time similar range 297 to 352;

~Correct and low Initial Temperature
      field Initial_Sample_Temperature similar range 680 to 710;
      field Initial_Sample_Temperature similar range 650 to 679.9;
end;



~These rules to modify the input parameters
~to compensate for sample defects or to increase
~the weight of parameters under certain conditions


preprocess rule definition is

      ~Rule 1 Change weights for grain refined melts

      repair rule use_alternative_weights is
            when
                  Liquidus_Recalescence_Temperature > 599
            then
                  change weight of Liquidus_Recalescence_Temperature to
10;
            end;



      ~Rule 2 Repair liquidus temperature and times for
      ~defective samples

      repair rule adjust_liquidus is
            when
                  Liquidus_Temperature > 610.5
            then
                  evaluate Liquidus_Temperature to
            (660.452 - 6.11 * (Si + ((0.35 * Cu) -
            (0.027*Cu^2)) +   ((0.0258 * Mg) + (0.0088 * Mg^2)) +
            ((Zn * 0.1227) - (0.0002 * Zn^2))) -
            0.057 * (Si + ((Cu * 0.35) - (0.027 * Cu^2)) +
            ((0.0258 * Mg) + (0.0088 * Mg^2)) + ((Zn * 0.1227) -
            (0.0002 * Zn^2)))^2);
            end;

end;



~Rules to modify outputs according to difference in
~input parameters of new and stored cases.

repair rule definition is

      repair rule remove_values is
            when
                  1=1
            then
                  change Strontium_content to undefined;
                  change AFS_Silicon_Modification_Level to undefined;
```

```
                change Maximum_Recommended_TSR_Temp to undefined;
          end;

     repair rule remove_mass is
          when
                deltaT<=8.5
          then
                change Test_sample_mass to undefined;
          end;


     repair rule calculate_mass is
          when
                Test_sample_mass is undefined
          then
                evaluate Test_sample_mass to
                      1.7456 *(AlCuEutectic_Time^0.7991);
          end;

     repair rule low_sample_mass is
          when
                Test_sample_mass < 165 and Initial_Sample_Temperature
> 679
          then
                change Sample_quality  to
                      'low mass of test sample REPEAT TEST';
                change Recommendations1 to
                      'Obtain a new sample with adequate mass';
          end;

     repair rule low_initial_temperature is
          when
                Test_sample_mass >= 165 and Initial_Sample_Temperature
<= 679
          then
                change Test_sample_temperature to
                      'Low temperature of the test sample';
                change Sample_quality  to
                      'Insufficient preheating time';
                change Recommendations3 to
                      'Verify the condition of the thermocouples';
                change Recommendations4 to
                      'Preheat the test cup for 20 seconds';
                change Recommendations5 to
                      'Obtain a sample of adequate size';
          end;

     repair rule liquidus_zero is
          when
                Liquidus_Temperature = 0
          then
                change Comments to 'Error ocurred during test.
REPEAT!';
                change Recommendations1 to
                      'Verify the condition of the thermocouples';
                change Recommendations2 to
                      'Preheat the test cup for 20 seconds';
                change Recommendations3 to
                      'Obtain a sample of adequate size';
```

```
            end;


      repair rule low_mass_and_temperature is
            when
                  Test_sample_mass < 165 and Initial_Sample_Temperature
<= 679
            then
                  change Comments to
                  'BAD SAMPLE Repeat Test';
                  change Recommendations31 to
                  'Verify the condition of the thermocouples';
                  change Recommendations4 to
                  'Preheat the test cup for 20 seconds';
                  change Recommendations5 to
                  'Obtain a sample of adequate size';
            end;


      ~for modification levels 1 to 2
      repair rule calculate_Sr_low is
            when
                  Strontium_content is undefined and
                  deltaT <= 7.5
            then
                  evaluate AFS_silicon_modification_level to
                  ((0.0119*deltaT^2)+(0.0179*deltaT)+0.9633);
                  evaluate Strontium_content to
                  ((-9.7129*AFS_silicon_modification_level^2)+
                  (62.556*AFS_silicon_modification_level )-44.452);
            end;


      ~for modification levels 2 to 5
      repair rule calculate_Sr_high is
            when
                  Strontium_content is undefined and
                  deltaT > 7.5
            then
                  evaluate AFS_silicon_modification_level to
                  ((0.1684*deltaT^2)-(2.2347*deltaT)+9.2025);
                  evaluate Strontium_content to
                  ((85.696* log(AFS_silicon_modification_level))-
35.285);

            end;


      ~when target modification level is different from calculated
      repair rule add_Sr_low is
            when
                  Target_modification_level !=
AFS_silicon_modification_level and
                  deltaT <= 7.5
            then

                  evaluate target_Sr to
                  ((-9.7129*Target_modification_level ^2)+
```

```
                  (62.556*Target_modification_level)-44.452);

                  evaluate Recommended_Sr_addition to
                        (target_Sr - Strontium_content);
            end;

      repair rule add_Sr_high is
            when
                  Target_modification_level !=
AFS_silicon_modification_level and
                  deltaT > 7.5
            then

                  evaluate target_Sr to
                  ((85.696* log(Target_modification_level))-35.285);
                  evaluate Recommended_Sr_addition to
                        (target_Sr - Strontium_content);
            end;



      repair rule calculate_TSR is
            when
            Maximum_Recommended_TSR_Temp is undefined
            then
            evaluate Maximum_Recommended_TSR_Temp to Solidus_Temperature
+ 15;
            end;


      repair rule sample_microstructure is
            when
                  deltaT > 8.5
            then
                  change Microstructure to 'modified.jpg';
            end;

end;


case instance UM_GQ1MBS3 is
~4_19_2000_4_42 Cooling rate 0.32

coolrate_factor = CR34;
Modification = unmod;
casting_section = MBS3_25;
Target_modification_level = 1;
Initial_Sample_Temperature = 705.13;
Liquidus_Temperature = 606.19;
Liquidus_Undercooling_Temperature = 595.42;
Liquidus_Undercooling_Time = 15.4;
Liquidus_Recalescence_Temperature = 596.18;
Coherency_Temperature = 596.06;
Coherency_Time = 30.6;
afs_alphaDENIDF = 13.24;
AlSiNucleation_Temperature = 582.59;
AlSiNucleation_Time = 98.2;
deltaT = -2.02;
AlCuEutectic_Temperature = 505.02;
```

```
AlCuEutectic_Time = 322.6;
Solidus_Temperature = 481.37;
Solidus_Time = 359.4;

solution is

Test_sample_mass = 164.9;
Test_sample_temperature = 'OK';
Sample_quality  = 'OK';

Silicon_morphology = 'Unmodified';
AFS_silicon_modification_level = 1;
Strontium_content = 7;

Hydrogen_level = 0.138; ~mlH2/100grAl
Solidification_range = 'OK';
Grain_size = '7.5 - 10';
Grain_refinement = 'Non Grain Refined Melt';
Cooling_rate_of_casting_section = 0.3;

Propensity_to_shrinkage_porosity = 'Low';
Area_Percent_Porosity =0.10;

Area_Percent_Copper_Based_Phases = 1.22;
Maximum_Recommended_TSR_Temp = 496.37;

Matrix_MicroHardness_HV = 94.41;
Percent_Elongation = 0.7;
UTS= 218.64;
TwoPercent_YieldStrength = 199.88;
Brinell_Hardness = 96.3;
Sample_Microstructure = 'unmodified.jpg';

Comments = 'High level of hydrogen in the melt';
Recommendations1 = 'Verify with Reduced Pressure Test';
Recommendations2 = 'Verify melt temperature and degassing efficiency';

end;

case instance UM_GQ1MBS4_6 is
~4_19_2000_4_42 Cooling rate 0.2

coolrate_factor = CR34;
Modification = unmod;
casting_section = MBS46;
Target_modification_level = 1;
Initial_Sample_Temperature = 705.13; ~400
Liquidus_Temperature = 606.19;
Liquidus_Undercooling_Temperature = 595.42;
Liquidus_Undercooling_Time = 15.4;
Liquidus_Recalescence_Temperature = 596.18;
Coherency_Temperature = 596.06;
Coherency_Time = 30.6;
afs_alphaDENIDF = 13.24;
AlSiNucleation_Temperature = 582.59;
AlSiNucleation_Time = 98.2;
deltaT = -2.02;
AlCuEutectic_Temperature = 505.02;
AlCuEutectic_Time = 322.6;
```

```
Solidus_Temperature = 481.37;
Solidus_Time = 359.4;

solution is

Test_sample_mass = 164.9;
Test_sample_temperature = 'OK';
Sample_quality  = 'OK';

Silicon_morphology = 'Unmodified';
AFS_silicon_modification_level = 1;
Strontium_content = 7;

Hydrogen_level = 0.138; ~mlH2/100grAl
Solidification_range = 'OK';
Grain_size = '7.5 - 10';
Grain_refinement = 'Non Grain Refined Melt';
Cooling_rate_of_casting_section = 0.2;

Propensity_to_shrinkage_porosity = 'Low';
Area_Percent_Porosity  = 0.19;

Area_Percent_Copper_Based_Phases = 1.22;
Maximum_Recommended_TSR_Temp = 496.36;

Matrix_MicroHardness_HV = 87;
Percent_Elongation = 0.5;
UTS= 214;
TwoPercent_YieldStrength = 195;
Brinell_Hardness = 92.6;
Sample_Microstructure = 'unmodified.jpg';

Comments = 'High level of hydrogen in the melt';
Recommendations1 = 'Verify with Reduced Pressure Test';
Recommendations2 = 'Verify melt temperature and degassing efficiency';

end;
```

APPENDIX IV

VERIFICATION OF EQUATIONS USED IN THE CALCULATION OF Sr CONTENT AND AFS LEVEL OF SILICON PARTICLE MODIFICATION.

The results presented in Table IV-1 correspond to thermal analysis of the samples used during the validation of the case base and were obtained in past experiments by the IRC.

Table IV-1 – Verification of the Equations Used in the Calculation of Sr Content and AFS Silicon Particle Modification Level.

Target Sr content during experiments (ppm)	$\Delta T^{AlSi}_{E,G}$ (°C)	Sr content calculated as a function of AFS Si Modification Level (ppm) (1)	Sr content calculated as a function of AFS Si Modification Level and $\Delta T^{AlSi}_{E,G}$ (ppm) (2)
7	-2	8.4	7.3
7	-3.5	8.4	10.4
20	6.61	24.1	27.7
20	6.73	24.1	29.3
50	8.5	51.2	50.9
50	9.89	55.0	51.2
70	9.8	72.1	71.5
70	13.09	72.1	65.3
100	11	102.6	102.6
100	10.4	102.6	87.2

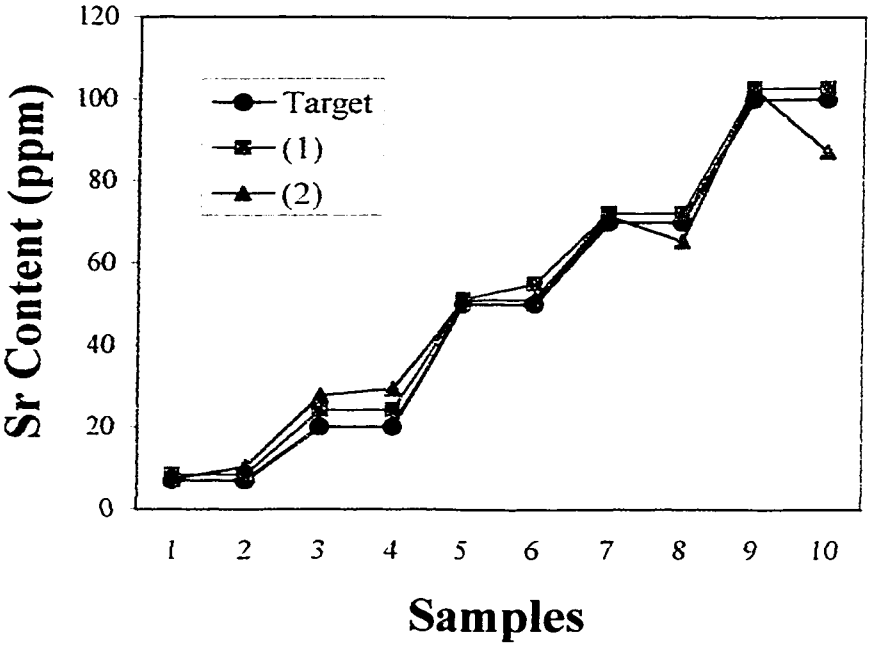

Figure IV-1 – Comparison of Sr Results with Different Equations

APPENDIX V

PRELIMINARY CONTROL LIMITS

The following control limits were calculated according following the Exponentially Weighted Moving Average method with parameters $\lambda = 0.1$ and $L = 2.814$:

Table V-1 – Preliminary Control Limits for the AlTAS Parameters and Characteristic Points

Parameter	Mean	Std. Deviation	EWMA Control Limits	
			UCL	LCL
T^{LIQ}	605.05	3.85	607.53	602.56
T^{LIQ}_{MIN}	595.79	0.50	595.46	596.11
T^{LIQ}_{PLAT}	596.44	0.46	596.74	596.14
T^{COH}	596.16	0.52	596.50	595.82
t^{COH}	32.67	2.12	34.04	31.31
$T^{Al\text{-}Si}_{NUC}$	571.56	2.06	572.89	570.23
$T^{AlSi}_{E,G}$	565.39	0.33	565.60	565.18
T^{AlCu}_{NUC}	505.86	1.01	506.51	505.21
T^{SOL}	473.33	7.97	478.47	468.18
$af_s^{\alpha\text{-}DEN}{}_{IDF}$	20.55	2.00	21.84	19.26
$t^{Al\text{-}Si}{}_{UNDERCOOLING}$	33.89	6.13	-2.68	-3.10
$\Delta T^{Al\text{-}Si}{}_{E,G}$	-2.89	0.33	66.97	64.43
$\Delta T^{Al\text{-}Si}{}_{SRAN}$	65.70	1.97	37.85	29.94

These limits were used to define similar ranges for the AlTAS parameters and characteristic temperatures in the case-based reasoning system.

APPENDIX VI

CASE BASE

Table VI-1 – Case Base

Parameters	Case 1	Case 2	Case 3	Case 4	Case 5	Case 6	Case 7
Name of the Case	UM_GQNBS3	UM_GQ1MBS4_6	UM_GQBB3	UM_GQ1BB4_6	UM_GQ2MBS3	UM_GQ10MBS3	UM_GQ10BB3
Coolrate_factor	CR34;	CR34;	CR34;	CR34;	CR37;	CR41;	CR41;
Modification	unmod;	unmod;	unmod;	unmod;	unmod;	unmod;	unmod;
Casting_section	MBS3_25;	MBS46;	BB3_25;	BB46;	MBS3_25;	MBS3_25;	BB3_25;
Target_modification_level	1;	1;	1;	705.13;	703.58;	688.77;	688.77;
Initial_Sample_Temperature	705.13;	705.13;	705.13;	606.19;	607.61;	610.49;	610.49;
Liquidus_Temperature	606.19;	606.19;	606.19;	595.42;	595.13;	595.38;	595.38;
Liquidus_Undercooling_Temperature	595.42;	595.42;	595.42;	15.4;	15.4;	20;	20;
Liquidus_Undercooling_Time	15.4;	15.4;	15.4;	596.18;	595.93;	595.65;	595.65;
Liquidus_Recalescence_Temperature	596.18;	596.18;	596.18;	596.06;	595.77;	595.39;	595.39;
Coherency_Temperature	596.06;	596.06;	596.06;	30.6;	31.2;	11.68;	11.68;
Coherency_Time	30.6;	30.6;	30.6;	13.24;	21.63;	18.93;	18.93;
a6_alphaDENIDF	13.24;	13.24;	13.24;	582.59;	569.21;	572.6;	572.6;
AlSiNucleation_Temperature	582.59;	582.59;	582.59;	98.2;	94.4;	81.4;	81.4;
AlSiNucleation_Time	98.2;	98.2;	98.2;	-2.02;	-1.63;	-2.46;	-2.46;
deltaT	-2.02;	-2.02;	-2.02;	505.02;	505.47;	506.44;	506.44;
AlCuEutectic_Temperature	505.02;	505.02;	505.02;	322.6;	288.6;	268.8;	268.8;
AlCuEutectic_Time	322.6;	322.6;	322.6;	481.37;	479.78;	479.47;	479.47;
Solidus_Temperature	481.37;	481.37;	481.37;	359.4;	342;	321.2;	321.2;
Solidus_Time	359.4;	359.4;	359.4;				
Test_sample_mass	164.9;	164.9;	164.9;	164.9;	165.5;	171.5;	171.5;
Test_sample_temperature	'OK';	'OK';	'OK';	'OK';	'OK';	'OK';	'OK';
Sample_quality	'OK'	'OK';	'OK'	'OK'	'OK';	'OK';	'OK';
Silicon_morphology	'Unmodified';	'Unmodified';	'Unmodified';	'Unmodified';	'Unmodified';	'Unmodified';	'Unmodified';
AFS_silicon_modification_level	1;	1;	1;	1;	1;	1;	1;
Strontium_content	7;	7;	7;	7;	7;	7;	7;
Hydrogen_level	0.138;	0.138; - mH2/100grAl	0.138;	0.138;	0.138;	0.114;	0.114;
Solidification_range	'OK';	'OK';	'OK';	'OK';	'OK';	'OK';	'OK';
Grain_size	7.5-10'	7.5-10'	'-11';	'-11';	7.5-10';	7.5-10';	7.5-10';
Grain_refinement	'Non Grain Refined Melt'	'Non Grain Refined Melt'	'Non Grain Refined Melt'	'Non Grain Refined Melt'	'Non Grain Refined Melt';	'Non Grain Refined Melt';	'Non Grain Refined Melt';
Cooling_rate_of_casting_section	0.3;	0.2;	0.6;	0.45;	0.3;	0.6;	0.6;
Propensity_to_shrinkage_porosity	'Low';	'Low';	'Low';	'Low';	'Low';	'Low';	'Low';
Area_Percent_Porosity	0.1	0.19;	0.13;	0.06;	0.126;	0.16;	0.13;
Area_Percent_Copper_Based_Phases	1.22;	1.22;	1.22;	1.22;	1.33;	0.32;	1.22;
Maximum_Recommended_TSR_Temperature	496.37;	496.36;	496.37;	496.37;	494.78;	494.47;	494.47;
Matrix_MicroHardness_HV	94.41;	87;	99;	101;	92.1;	98.7;	99;
Percent_Elongation	0.7;	0.5;	0.3;	0.4;	0.5;	0.5;	0.3;
UTS	218.64	214	212;	220;	229.07;	256.3;	212;
TwoPercent_YieldStrength	199.88;	195;	204;	100;	197.87;	244.36;	204;
Brinell_Hardness	96.3;	92.6;	92.6;	92.6;	93;	96;	92.6;
Sample_Microstructure	'unmodified.jpg';	'unmodified.jpg';	'unmodified.jpg';	'unmodified.jpg';	'unmodified.jpg';	'unmodified.jpg';	'unmodified.jpg';
Comments	'High level of hydrogen in the melt'	'High level of hydrogen in the melt'	'High level of hydrogen in the melt'	'High level of hydrogen in the melt'	'High content of hydrogen in the melt';	Melt Quality OK';	Melt Quality OK';
Recommendations	'Verify with Reduced Pressure Test'	'Verify with Reduced Pressure Test'	'Verify results with Reduced Pressure Test'	'Verify results with Reduced Pressure Test'	'Repeat test to confirm results';		
Recommendations	'Verify melt temperature and degassing efficiency'	'Verify melt temperature and degassing efficiency'	'Verify melt temperature and degassing efficiency'	'Verify melt temperature and degassing efficiency'	'Verify results with Reduced Pressure Test';		
Recommendations					'Verify melt temperature and degassing efficiency';		

Table VI-2 – Case Base (continued)

Case 8	Case 9	Parameters	Case 10	Case 11	Case 12	Case 13	Case 14
UM_GQ10MBS4_6	UM_GQ10BB4_6	Name of the Case	UM_GQ13MBS3	UM_GQ15MBS3	UM_LS2MBS3	UM_LS5MBS3	UM_LS7MBS3
CR41;	CR41;	Coolrate_factor	CR33;	CR30;	CR44;	CR41;	CR43;
unmod;	unmod;	Modification	unmod;	unmod;	unmod;	unmod;	unmod;
MBS46;	BB46;	Casting_section	MBS3_25;	MBS3_25;	MBS3_25;	MBS3_25;	MBS3_25;
688.77;	688.77;	Target_modification_level	701.24;	690.75;	678.25;	678.37;	693.54;
610.49;	610.49;	Initial_Sample_Temperature	603.28;	605.22;	608.63;	609.16;	610.;
595.38;	595.38;	Liquidus_Temperature	595.15;	595.99;	594.31;	593.36;	595.21;
20;	20;	Liquidus_Undercooling_Temperature	13.4;	19.5;	19.6;	19.8;	18.8;
595.65;	595.65;	Liquidus_Undercooling_Time	596.46;	596.68;	594.31;	594;	595.42;
595.39;	595.39;	Liquidus_Recalescence_Temperature	596.4;	596.45;	593.38;	593.38;	595.27;
11.68;	11.68;	Coherency_Temperature	34.2;	40.4;	11.11;	12.28;	12.51;
18.93;	18.93;	Coherency_Time	22.6;	34.95;	18.21;	20.5;	18.98;
572.6;	572.6;	als_alphaDENIDF	569.14;	568.43;	570.46;	572.21;	574.06;
81.4;	81.4;	AlSiNucleation_Temperature	102.6;	130.2;	78;	86.8;	76.8;
-2.46;	-2.46;	AlSiNucleation_Time	-0.41;	-3;	-1.3;	-1.1;	-1.87;
506.44;	506.44;	deltaT	504.66;	505.6;	503.75;	503.75;	506.16;
268.8;	268.8;	AlCuEutectic_Temperature	322.6;	365.8;	206.4;	274.8;	261.2;
479.47;	479.47;	AlCuEutectic_Time	481.32;	480.21;	453.92;	472.51;	471.03;
321.2;	321.2;	Solidus_Temperature	375.6;	434.2;	348;	335.6;	321.4;
		Solidus_Time					
171.5;	171.5;	Test_sample_mass	176.8;	180.5;	165.8;	176.6;	170.2;
'OK';	'OK';	Test_sample_temperature	'OK';	'OK';	'Low temperature of the test sample'	'Low temperature of the test sample'	'OK';
'OK';	'OK';	Sample_quality	'OK';	'Large Sample Mass';	'Insufficient preheating time';	'Insufficient preheating time'	'Sample OK'
'Unmodified';	'Unmodified';	Silicon_morphology	'Unmodified';	'Unmodified';	'Unmodified';	'Unmodified';	'Unmodified';
1;	1;	AFS_silicon_modification_level	1;	1;	1;	1;	1;
7;	7;	Strontium_content	7;	7;	7;	7;	7;
0.114;	0.114;	Hydrogen_level	0.147;	unknown;	0.108;	0.123;	0.128;
'OK';	'OK';	Solidification_range	'OK';	'OK';	'Longer temperature solidification range'	'Longer temperature solidification range'	'Longer temperature solidification range'
7.5;	7.5-10';	Grain_size	7.5-10';	7.5-10'	7.5-10'	7.5-10'	7.5-10';
'Non Grain Refined Melt';	'Non Grain Refined Melt';	Grain_refinement	'Non Grain Refined Melt';	'Non Grain Refined Melt';	'Non Grain Refined Melt';	'Non Grain Refined Melt'	'Non Grain Refined Melt'
0.2;	0.45;	Cooling_rate_of_casting_section	0.3;	0.32;	0.3;	0.3;	0.32;
'Low';	'Low';	Propensity_to_shrinkage_porosity	'Low';	'Low';	'Low';	'Low';	'Low';
0.15;	0.1;	Area_Percent_Porosity	0.16;	0.16;	0.20;	0.22;	0.304;
0.32;	1.22;	Area_Percent_Copper_Based_Phases	1.22;	1.22;	2.7;	2.65;	2.85;
494.47;	494.47;	Maximum_Recommended_TSR_Temperature	496.32;	495.21;	468.92;	487.51;	486.03;
102;	104;	Matrix_MicroHardness_HV	92.11;	92.11;	71.67;	73.08;	73.08;
0.4;	0.4;	Percent_Elongation	0.62;	0.62;	0.;	0.;	0.;
215;	245;	UTS	216.72;	216.72;	0.;	0.;	0.;
197;	225;	TwoPercent_YieldStrength	201.65;	201.65;	0.;	0.;	0.;
100;	100;	Brinell_Hardness	99.1;		0.;	0.;	0.;
'unmodified.jpg';	'unmodified.jpg';	Sample_Microstructure	'unmodified.jpg';	99.1;	'lowsolidus.jpg';	'lowsolidus.jpg';	'lowsolidus.jpg';
'Melt Quality OK';	'Melt Quality OK';	Comments	'High content of hydrogen in the melt';	'unmodified.jpg';	'No mechanical properties available'	'No mechanical properties available'	
		Recommendations	'Verify results with Reduced Pressure Test';	'Melt Quality OK'	'Verify the levels of Sr,Na,Zn'	'High levels of Sr,Na,Zn Verify with OES test'	'High levels of Sr,Na,Zn Verify with OES test'
			'Verify melt temperature and degassing efficiency';		'Repeat test paying attention to sample quality';	'Repeat test paying attention to sample quality';	'Monitor the level of trump elements in the melt'
		Recommendations					

Table VI-3 – Case Base (continued)

Case 15	Case 16	Case 17	Case 18	Case 19
M_IMBS3	M_IBB3	M_IMBS4_6	M_IBB4_6	M_2MBS3
CR44;	CR44;	CR44;	CR44;	CR38;
part_mod;	part_mod;	part_mod;	part_mod;	part_mod;
MBS3_25;	BB3_25;	MBS46;	BB46;	MBS3_25;
678.96;	678.96;	678.96;	678.96;	680.73;
608.43;	608.43;	608.43;	608.43;	606.76;
593.82;	593.82;	593.82;	593.82;	593.66;
13.8;	13.8;	13.8;	13.8;	14.8;
595.37;	595.37;	595.37;	595.37;	595.08;
592.58;	592.58;	592.58;	592.58;	593.02;
38.8;	38.8;	38.8;	38.8;	40.6;
24.73;	24.73;	24.73;	24.73;	23.81;
555.24;	555.24;	555.24;	555.24;	554.80;
130.2;	130.2;	130.2;	130.2;	115.8;
10.33;	10.33;	10.33;	10.33;	9.69;
530;	530;	530;	530;	513.74;
205.8;	205.8;	205.8;	205.8;	257.8;
493.14;	493.14;	493.14;	493.14;	493.27;
258.6;	258.6;	258.6;	258.6;	300.6;
168.8;	168.8;	168.8;	168.8;	187.2;
'Low temperature of the test sample'	'Low temperature of the test sample'	'Low temperature of the test sample'	'Low temperature of the test sample'	'OK';
'Insufficient preheating time'	'Insufficient preheating time'	'Insufficient preheating time'	'Insufficient preheating time'	'Large sample mass';
'Partially Modified'	'Partially Modified'	'Partially Modified'	'Partially Modified'	'Partially Modified'
3.5;	3.5;	3;	4;	3.5;
68;	68;	68;	68;	68;
'unknown';	'unknown';	'unknown';	'unknown';	'unknown';
'OK';	'OK';	'OK';	'OK';	'OK';
'-10';	'-10';	'-7.5';	'-10';	7.5-10'
'Non Grain Refined Melt'	'Non Grain Refined Melt'	'Non Grain Refined Melt'	'Non Grain Refined Melt'	'Non Grain Refined Melt'
0.3;	0.6;	0.2;	0.45;	0.3;
'High';	'High';	'High';	'High';	'High';
0.54;	0.54;	0.36;	0.29;	0.52;
1.22;	1.22;	1.22;	1.22;	1.22;
508.4;	508.14;	508.14;	508.14;	508.27;
103;	103;	93;	103;	98
10;	10;	0.4;	0.6;	10;
236;	236;	182;	235;	191;
210;	210;	0;	223;	181;
104;	104;	100;	100;	98.6;
'part_mod.jpg';	'part_mod.jpg';	'part_mod.jpg';	'part_mod.jpg';	'part_mod.jpg';
'Melt quality OK';	'Melt quality OK'	'Melt quality OK';	'Melt quality OK';	'Melt quality OK';
'Monitor closely the temperature of the melt'	'Monitor closely the temperature of the melt'	'Monitor closely the temperature of the melt'	'Monitor closely the temperature of the melt'	'Monitor closely the temperature of the melt';
'Monitor the hydrogen level and metal cleanliness'	'Monitor the hydrogen level and metal cleanliness'	'Monitor the hydrogen level and metal cleanliness'	'Monitor the hydrogen level and metal cleanliness'	'Monitor the hydrogen level and metal cleanliness'

APPENDIX VII

EXAMPLE OF THE VALIDATION PROCEDURE (Retrieval Test)

Table VII-1 – Examples of Cases Successfully Retrieved and Retrieved with Error During the Adaptation Test.

The input parameters are included in Appendix VI.

	SUCCESSFULLY RETRIEVED		
	Case 3		
Solution Parameter	**Appraised Value**	**Real Value**	**RE %**
Sample Mass	164.9	176.44	6.54
Sample Temperature	ok	ok	0.00
Sample Quality	ok	ok	0.00
Silicon Morphology	unmod	unmod	0.00
AFS Si Modification Level	1	1.0	3.09
Sr Content	7	7.33	4.50
H2 Level	0.138	0.114	21.05
Solidification Range	ok	ok	0
Grain Size	ok	not ok	100
Grain Refinement	ok	ok	0
Cooling Rate Casting	0.6	0.6	0
Propensity to Shrinkage	low	low	0
Area % Porosity	0.13	0.13	0
Area % Cu Based Phases	1.22	1.22	0
Maximum TSR Temperature	496.37	496.37	0
Vickers Hardness	99	99	0
% Elongation	0.3	0.3	0
Ultimate Tensile Strength	212	212	0
Yield Strength	204	204	0

RETRIEVED WITH ERROR		
Case 8		
Appraised Value	**Real Value**	**RE %**
171.52	165.3	3.76
ok	ok	0.00
ok	ok	0.00
unmod	unmod	0.00
1	1.0	1.01
7	8.14	14.00
0.114	0.138	17.39
ok	ok	0
ok	ok	100
ok	ok	0
0.2	0.2	0
low	low	0
0.15	0.19	21.05
0.32	1.22	73.77
494.47	494.47	0
102	87	17.24
0.4	0.5	0
215	214	0
197	195	0

Table VII-2 – Examples of Cases Successfully Retrieved and Retrieved with Error During the Adaptation Test (continued)

	SUCCESSFULLY RETRIEVED		
	Case 3		
Solution Parameter	**Appraised Value**	**Real Value**	**RE %**
Brinell Hardness	92.6	92.6	0
Microstructure	unmod	unmod	0
Comments	ok	not ok	100
Recommendations 1	ok	ok	100
Recommendations 2	ok	ok	100
Total RE =	**435.19**		
Total Possible RE =	**2400**		
Overall RE =	**0.18**		
RAC =	**20%**		
Success=	**ok**		

RETRIEVED WITH ERROR		
Case 8		
Appraised Value	**Real Value**	**RE %**
100	92.6	0
unmod	unmod	0
ok	high h	100
ok	-	100
ok	-	100
548.23		
2400		
0.23		
20%		
not ok		

RE = Relative Error

RAC = Result Acceptability Criteria

VITA AUCTORIS

Name:	Graciela Pelayo Chagoya
Place of Birth:	Mexico City, Mexico
Year of Birth:	1975
Education:	Universidad Autonoma Metropolitana
	Mexico City, Mexico
	1992-1996
	B. Sc. in Industrial Engineering